Naval Surface Warfare Center
Carderock Division
West Bethesda, MD 20817-5700

NSWCCD-65-TR–2001/04 January 2001

Survivability, Structures, and Materials Directorate

Technical Report

Guidelines for the Design of Advanced Double Hull Vessels

by

Jerome P. Sikora

Edward A. Devine

20030109 173

DEPARTMENT OF THE NAVY

NAVAL SURFACE WARFARE CENTER, CARDEROCK DIVISION
9500 MACARTHUR BOULEVARD
WEST BETHESDA MD 20817-5700

<div align="right">

9110
Ser 65-83
7 Aug 02

</div>

From: Commander, Naval Surface Warfare Center, Carderock Division
To: Chief of Naval Research (ONR 334)

Subj: ADVANCED DOUBLE HULL PROGRAM

Ref: (a) Advanced Double Hull Task of the FY97 BA2 Surface Ship Hull, Mechanical and Electrical Technology, Program Element 0602121N, Task SV5

Encl: (1) NSWCCD-65-TR–2001/04, *Guidelines for the Design of Advanced Double Hull Vessels*

1. Reference (a) requested the Naval Surface Warfare Center, Carderock Division (NSWCCD) to perform a major research and development effort leading to practical application of advanced double hull structural design concepts for naval combatants, auxiliaries and commercial tank vessels. Enclosure (1) summarizes all work subsequently performed and presents design guidelines for an alternative concept with only longitudinal, unidirectional framing.

2. Comments or questions may be referred to Mr. Jerome P. Sikora, Code 651; telephone (301) 227-1757; e-mail, SikoraJP@nswccd.navy.mil.

J. E. BEACH
By direction

Copy to:

COMNAVSEASYSCOM WASHINGTON DC
[SEA 05D, SEA 05M, SEA 05P, SEA 05P1, SEA 05P4, SEA 05R]

CNR ARLINGTON VA [ONR 334 (Barsoum, Gagorik)]

DTIC FORT BELVOIR VA

NAVSURFWARCEN CARDEROCKDIV
BETHESDA MD [Codes 3442 (TIC), 60 (w/o encl), 61, 613, 613 (LeBegue), 615, 62, 65, 65R (2), 651 (20 copies), 651 (Devine (10 copies), Rodd), 652, 653, 653 (Kihl), 654, 654 (Knight, Melton (15 copies)), 655, 66, 664]

Naval Surface Warfare Center
Carderock Division
West Bethesda, MD 20817-5700

Guidelines for the Design of Advanced Double Hull Vessels

by

Jerome P. Sikora

Edward A. Devine

Enclosure (1)

REPORT DOCUMENTATION PAGE

Form Approved
OMB No. 0704-0188

1. REPORT DATE (DD-MM-YYYY)	2. REPORT TYPE	3. DATES COVERED (From - To)
29-Jan-2001	Final	-

4. TITLE AND SUBTITLE	5a. CONTRACT NUMBER
Guidelines for the Design of Advanced Double Hull Vessels	5b. GRANT NUMBER
	5c. PROGRAM ELEMENT NUMBER 0602121N

6. AUTHOR(S)	5d. PROJECT NUMBER
Jerome P. Sikora, Edward A. Devine	5e. TASK NUMBER SV5
	5f. WORK UNIT NUMBER

7. PERFORMING ORGANIZATION NAME(S) AND ADDRESS(ES) AND ADDRESS(ES)	8. PERFORMING ORGANIZATION REPORT NUMBER
Naval Surface Warfare Center Carderock Division 9500 Macarthur Boulevard West Bethesda, MD 20817-5700	NSWCCD-65-TR-2001/04

9. SPONSORING / MONITORING AGENCY NAME(S) AND ADDRESS(ES)	10. SPONSOR/MONITOR'S ACRONYM(S)
Attn ONR 334 Chief of Naval Research Ballston Centre Tower One 800 North Quincy Street Arlington, VA 22217-5660	11. SPONSOR/MONITOR'S REPORT NUMBER(S)

12. DISTRIBUTION / AVAILABILITY STATEMENT
Approved for public release; distribution is unlimited.

13. SUPPLEMENTARY NOTES

14. ABSTRACT
This report summarizes a major research and development effort and presents guidelines for design of advanced double hull (ADH) naval combatants, auxiliaries and commercial tank vessels. The program was undertaken to improve upon conventional, double hull tanker structure typically consisting of grillage of longitudinal and transverse framing. The ADH framing system is an alternative concept with only longitudinal, unidirectional framing. It embodies an inner hull and an outer hull, which are connected by longitudinal floors or web girders forming a cellular structure similar to a corrugated box. This allows elimination of conventional transverse frames and longitudinal stiffeners on the shell plating. The structural behavior of the ADH is significantly different from that of conventionally framed grillage structure requiring different design methods. The advantages anticipated for this concept are simplification of structure, improved structural resistance in case of collision or grounding, greater resistance to fatigue failure, improved survivability from weapons and reduced construction and maintenance costs.

15. SUBJECT TERMS
ship structures, advanced double hull

16. SECURITY CLASSIFICATION OF:			17. LIMITATION OF ABSTRACT	18. NUMBER OF PAGES	19a. NAME OF RESPONSIBLE PERSON Mr. Jerome P. Sikora
a. REPORT UNCLASSIFIED	b. ABSTRACT UNCLASSIFIED	c. THIS PAGE UNCLASSIFIED	SAR	94	19b. TELEPHONE NUMBER (include area code) 301/227-1757

i/ii

Standard Form 298 (Rev. 8-98)
Prescribed by ANSI Std. Z39.18

Contents

Page

Contents

Contents

Contents

Figures

Tables

Administrative Information

Acknowledgements

1.0 Introduction

Under sponsorship of the Office of Naval Research, the Naval Surface Warfare Center, Carderock Division (NSWCCD), formerly the David Taylor Research Center, conducted a major research and development effort leading to practical application of advanced double hull structural design concepts to naval combatants, auxiliaries, and commercial tank vessels. The Advanced Double Hull (ADH) Technology Project was designated a Congressional Interest Project and funds were appropriated for FY-92 and FY-93, with the period of performance extended through FY-94. Additional funds were allocated in FY-96 and extended through FY-97.

The Oil Pollution Act of 1990 (OPA '90) requires all new construction tanker and product carriers to have double hull construction. Conventional double hull tankers in special product service have been in operation for many years before the enactment of OPA '90. Specific applications included hazardous cargo carriers, chemical product carriers, and low-temperature LNG and LPG carriers. The double hull arrangement provides protection to cargo containment and the environment in the event of casualty and minimizes cargo tank cleaning by having segregated ballast tanks. OPA '90 provided the incentive for this program to develop better, more affordable casualty protection for double hull commercial ships.

1.1 ADH Concept

Conventional longitudinally-framed, single-hull structure consists of a complex grillage of longitudinal framing, widely spaced transverse web frames, and longitudinal and transverse bulkheads providing cargo and watertight subdivision. Conventionally-framed, double hull tanker structure includes a similar grillage of longitudinal and transverse framing. The ADH framing system which is the principal subject of the research program is an alternative concept with only longitudinal, unidirectional framing. The ADH concept embodies an inner hull and an outer hull which are connected by longitudinal floors or web girders forming a cellular structure similar to the panels of a corrugated cardboard box. The inherent strength of the cellular structure allows the elimination of conventional transverse frames and longitudinal stiffeners on the shell plating. This allows the interior of the ship to be smooth and clean. A conventionally-framed, single hull, and an equivalent advanced double hull configuration of a notional naval combatant are compared in Figure 1. The two midship sections of a 32,000 deadweight (DWT) double hull product tanker, the conventional double hull *Paul Buck*-class and an ADH design, are shown in Figure 2.

The structural behavior of the ADH cellular construction is significantly different from that of conventionally framed grillage structure. In a conventional ship, the pressure loads from both the sea and cargo act on the shell plating and are then transmitted partly to the transverse frames and partly to the longitudinal stiffeners. These members then transmit the loads to the transverse

1

and longitudinal bulkheads. In the no-frame, double hull configuration, the lateral loads on the shell plating are transmitted via bending to the longitudinal web members, and then to the transverse bulkheads through shear. Under primary loading, that is, hull girder bending, the plate stiffener collapse behavior of conventional framing is replaced by cellular column collapse behavior of the ADH. This different structural behavior must be accounted for in the design methods for ADH structures. Since this is a new concept, there is little experience with such design methods. (Okamoto 1985) developed some preliminary structural criteria for an ADH product oil carrier.

Some of the advantages anticipated for the ADH concept are:

- simplification of structure with easier fabrication,
- improved structural resistance in case of collision or grounding,
- greater resistance to fatigue failure,
- improved survivability from weapons,
- reduced construction costs for the installation of foundations, insulation, and distributed systems, and
- reduced maintenance costs.

These advantages are quantified in this report. A potential problem introduced by this construction is corrosion within the enclosed cells, and is also addressed herein.

Single Hull **Notional ADH**
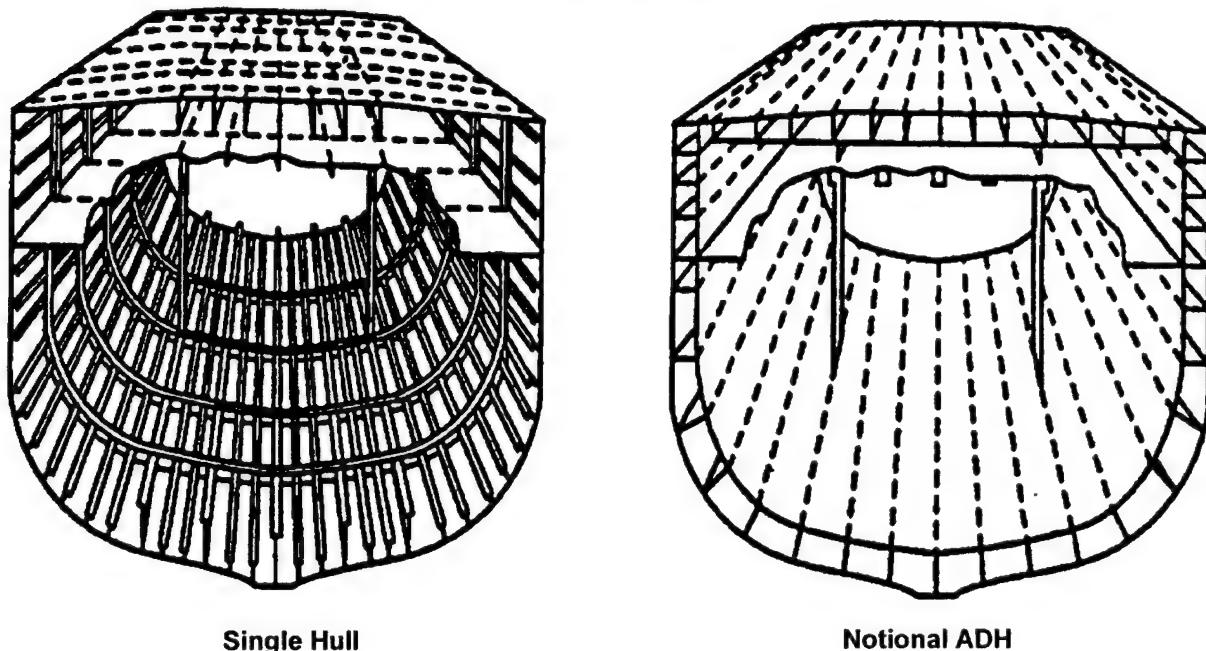
Figure 1. Single Hull and Notional ADH Combatants

Conventional Double Hull *Paul Buck*   **ADH Variant**
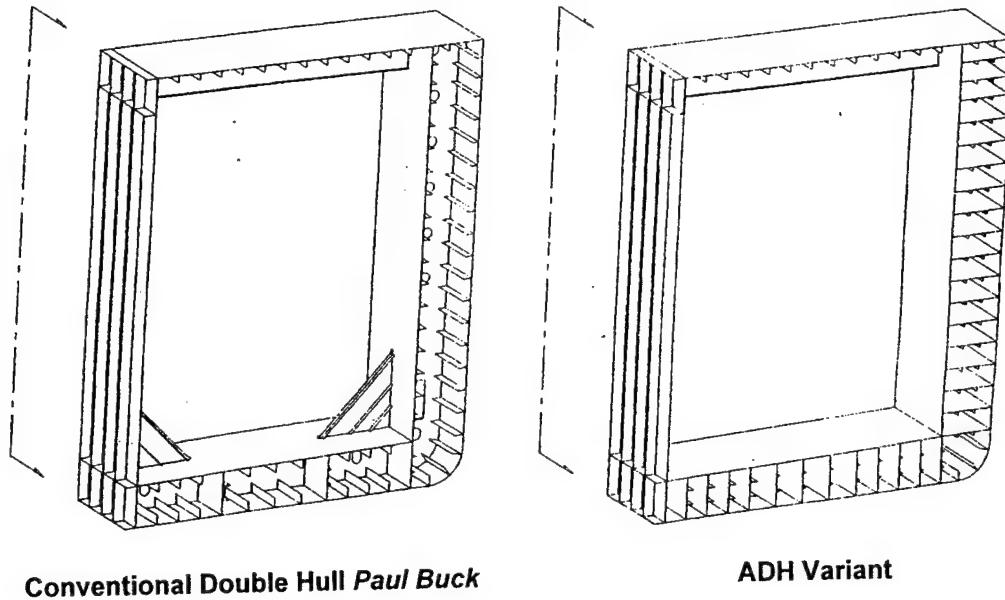
Figure 2. Conventional and ADH T-5 Product Tanker Designs

1.2 Research Program

The ADH program consists of eighteen tasks in the general areas of structural integrity, affordability and survivability. These are shown in the task summary, Table 1. The structural integrity area investigated the strength and stress behavior to determine if there were any critical weaknesses. The affordability area investigated the effect of the ADH concept on acquisition and life cycle costs for both Navy and commercial ships. The survivability area investigated the benefits derived from the ADH cell spaces from combat loads, damage stability, and damage control. This research program has been reported by Melton (1994) and Sikora (1995).

The program included major expenditures for conducting structural model tests and correlating analytical studies. A number of large-scale tests have been conducted under this program: Major tests completed to date include collapse behavior of eleven small-scale and five large-scale column models loaded in axial compression to determine post-buckled residual strength. Two ship cross-section models were tested to collapse under static bending and one ship model was tested to failure from whipping-induced bending from an underwater explosion. Holing tests of several cellular structures were conducted under air blast and underwater explosions. Stranding tests of three, one-fourth scale tanker double bottom models with conventional framing and advanced unidirectional framing systems have also been completed. Nine large-scale grounding tests of double bottom structures have been conducted at a specially constructed test facility. Results of these tests have been published in reports to the ONR sponsor, at an ADH technical symposium sponsored by this program, and before numerous professional societies.

Table 1. Advanced Double Hull Technology Project Summary

Structural Integrity:	Section
Collapse behavior	2
Fatigue life of cellular structures	3
Stress behavior	2
Foundation concepts	4
Grounding response	5
Internal deck options	2
Affordability:	**Section**
Automated fabrication	6
Corrosion protection	8
Outfitting of distributive systems	7
Hydrodynamic performance of new design concepts	N/I
Design integration	N/I
Inspection, maintenance and repair	9.1
Survivability:	**Section**
Resistance to underwater explosion holing damage	See Sikora (2001)
Resistance to underwater explosion whipping damage	See Sikora (2001)
Acoustic signature control	9.4
Damage control	9.2
Equipment shock response	9.3
Resistance to air explosions	See Sikora (2001)

N/I = Not included in this report

1.3 Objective

The objective of this report is to provide succinct design guidelines for the structural integrity and affordability areas. These guidelines were developed from extensive research conducted over many years but are presented herein as simple rules with no effort to justify them. A companion document (Sikora 2001) summarizes their technical basis and presents the supporting test results, analyses, plots, figures, and so forth, as well as a complete bibliography. Guidelines for the survivability area are published in a separate document.

1.4 Contents

This report follows the general project outline presented in Table 1. Guidelines for the structural integrity areas are presented first: (a) structural design rules in Section 2, (b) fatigue methodology in Section 3, (c) foundation design in Section 4, and (d) tanker grounding rules in Section 5. Affordability issues, both construction and lifecycle, are presented next: (a) joining and welding methods in Section 6, (b) outfitting of distributive systems in Section 7, and (c) corrosion control in Section 8. There are no rules for some of the other technical areas at this time: (a) inspection, maintenance and repair, (b) damage control, (c) equipment shock response, and (d) acoustic and infrared signature control.   These topics are briefly discussed in Section 9. In addition, a list of key references of research studies is included to provide guidance.

2.0   Structural Design

2.1 Background

Structural analysis is based on an assessment of the strength and stability adequacy of the structural components when the ship is subjected to wave, buoyancy, deck flooding, wave impact or underwater shock loads. Strength and stability are based on combined tensile, compressive and shear stresses develop in the hull components due to these combined loads. (Hughes 1988; Nappi 1985) provide criteria for the design of structural components.

The traditional component-oriented ship design process is gradually being replaced by design methodology based on computerized numerical analyses for loads and structural responses. Numerical analysis methods such as finite element analysis (FEA) simultaneously evaluate each interacting structural component as it contributes to the overall hull response. The numerical solution generally will be less conservative than the traditional component-based solution, although this level of conservatism may be difficult to assess since it cannot be easily checked manually. Numerical analysis permits evaluations that would be difficult or impossible using traditional procedures. These include complex loading, lateral effects, plate curvature, hull curvature, and non-linear response.

This manually oriented design approach is particularly well suited to preliminary and feasibility design studies where expediency precludes a more involved design based on numerical methods of analysis. It is noted that traditional component-based designs may differ significantly from designs based on numerical analysis. This may be due to several factors including the inability of the simplified traditional methods to account for complex structural behavior. As a general guidance, a correctly performed numerical design procedure is recommended as an acceptable approach that should be given precedence over procedures using traditional methods.

2.2 Rules for the Design of Unidirectional Ship Structures

2.2.1 Assumptions with Respect to Structural Behavior

The method used for preliminary design of the advanced double hull treats a longitudinal web and the associated inner and outer shell plate as an I-beam element (Michaelson and Roseman 1994), as shown in Figure 3. This I-beam element is loaded axially by primary hull girder bending, and in secondary bending between transverse bulkhead supports by hydrostatic seaway loads, live loads and tank loads. These loads combine to stress the inner shell, outer shell and the adjoining web.

A method for calculating the design bending moments is presented in Section 3 of these guidelines. Following traditional U.S. Navy design philosophy, the stress distribution from primary bending is assumed to taper to one half of the stress of the extreme fiber of the hull girder to the neutral axis, resulting in the "K" curves typical in U.S. Navy ship design practice (Naval Sea Systems Command 1976). These are calculated from the design moments and the section properties of the ship as shown in Figure 4. The recommended approach is to use the actual lateral bending moments in conjunction with the vertical bending moments to calculate the corresponding section properties in lieu of the "K" curves.

For preliminary design, the I-beam elements are assumed to behave as beams with fixed end supports at the transverse bulkheads. This is based on the assumption that the double hull will be continuous both forward and aft of the element being designed and that balancing loads will be experienced by the forward and aft elements which will result in behavior similar to that of a fixed element. The only exception to this assumption is with global buckling considerations for the double hull element where it is assumed that the element will behave as a simply supported beam with bulkheads acting as pinned supports. This provides a conservative, worst-case scenario.

In some cases, this level of conservatism may be excessive. To account for some support from adjacent shell and end structures, some degree of fixity can be applied to the ends of the double hull elements. An appropriate level of fixity can be developed based on numerical or analytical methods. See Appendix A of Sikora (2001).

Secondary pressures generally bend the I-beam element inward, although with some ships, such as tankers, an internal cargo load may act in an outward direction. These local bending stresses combine with the hull girder stresses, resulting in a combination of bending stresses, axial stresses, and shear stresses in the inner and outer shell, and web plating.

The magnitude of the secondary load which the I-beam element supports is a function of the longitudinal web spacing, the element span between transverse bulkheads and the hydrostatic pressure as shown in Figure 5.

The effective section of the I-beam element composed of inner and outer hull and longitudinal web components is summed from the effective material of these components, as shown in Figure 3. As a result of hydrostatic pressure, this effective section is assumed to bend as a fixed-fixed beam between transverse bulkheads. Resultant stresses at the inner shell and outer shell are computed by the summation of secondary bending stresses plus the primary bending stresses.

For preliminary design, stresses are checked for adequacy in both hog and sag bending at the four locations identified for the inner and outer hull at both mid-span and ends of the double-hull element.

$d = s \cdot \cos(\theta)$

$t_e = t_w / \cos(\theta)$

Development of design model for advanced double hull element

$b_1 = (b_a + b_b) / 2$

$b_3 = (b_c + b_d) / 2$

$t_1 = (t_a + t_b) / 2$

$t_3 = (t_c + t_d) / 2$

Design model of double hull element with averaged plate panel span widths
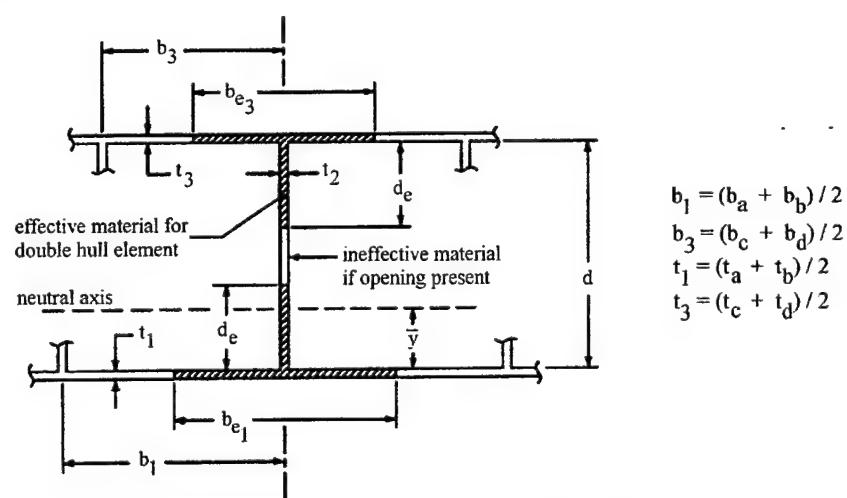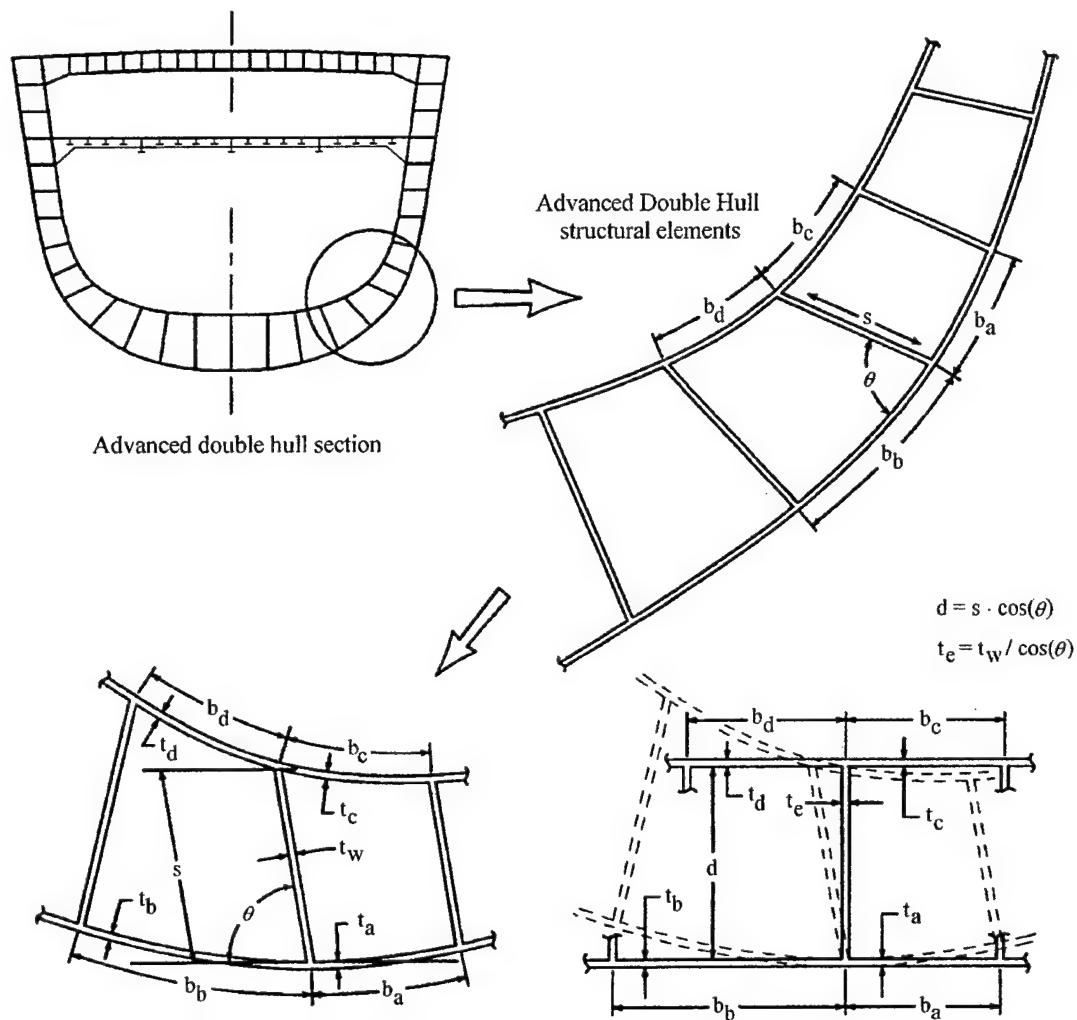
Figure 3.   Development of Secondary ADH I-beam Design Element

7

Hogging Condition   Sagging Condition

trochoidal wave with
height = $1.1 \sqrt{L}$

tension   compression

compression   tension

Hogging Response   Sagging Response

tension at deck   weather deck   compression at deck

f_{TD} midship section f_{CD}

neutral axis

f_{CK} ADH f_{TK}
                                        structure
compression at keel   keel   tension at keel

Actual Longitudinal Primary Bending Stresses

Tensile Stresses   Compressive Stresses

f_{TD} f_{TD} f_{CD} f_{CD}

f_{TNA} f_{CNA}

f_{TK} f_{TK} f_{CK} f_{CK}

ADH structure   internal structure   ADH structure   internal structure

f_{TNA} = greater of $f_{TD}/2$ or $f_{TK}/2$ f_{CNA} = greater of $f_{CD}/2$ or $f_{CK}/2$

Figure 4. Primary Longitudinal Design Stress

8
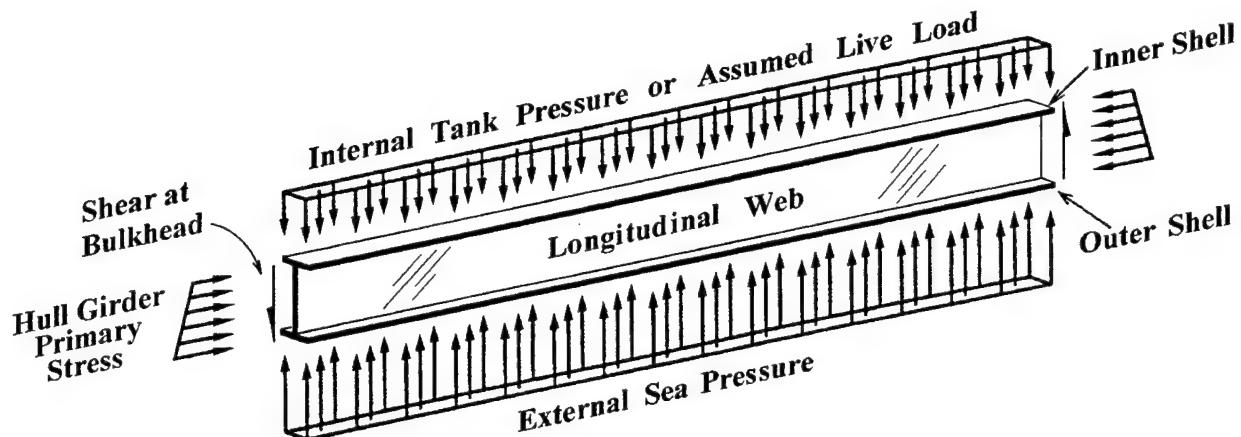
Figure 5. Secondary Pressures on Double Hull I-beam Element

Advanced double hull elements will always have two or more adjacent connected panels welded together. Each connecting element must be evaluated with respect to its slenderness, b/t. If the plate slenderness for any adjacent connecting panel has a b/t that varies by more than 25 percent from the panel being evaluated, the compressive buckling strength, F_{cr}, is defined for the panel being evaluated using $k = 4.0$ and the simple average of F_{cr} is calculated for that panel and all panels attached to it. This will have the effect of strengthening the slender panels and reducing the buckling strength of the less slender (usually thicker) panels.

2.2.2 Structural Design Procedures

The design process for the advanced double hull is an extension of traditional U.S. Navy design procedures (Melton et al. 1994; Nappi 1985; Naval Sea Systems Command 1976). This process typically starts with an assumed section based on typical configuration, plating thicknesses and material selections, and proceeds through several iterations, which consist of checking each I-beam element for compliance with a set of adequacy equations. If the plate fails, it is incrementally thickened until it passes all criteria. When the plate is satisfactory, it is examined for excessive thickness and reduced, if necessary. Changing the plating thickness results in a change in the hull girder section properties, which affects the primary stresses that are distributed within the structure. The re-calculation of primary stresses can be done after each double hull element is designed or at discrete points in the design process. This is a practical consideration based on the degree of automation with the process, which is certainly enhanced through the use of computer programs or spreadsheets.

2.2.2.1 Itemized Procedural Summary

    a. Identify structural configuration:

        1) define section geometry; and

        2) identify double hull elements.

    b. Determine primary stresses and normal loads:

        1) if beginning of design cycle, assume primary stresses or assume structural scantlings and solve for primary stresses;

2) for secondary or a subsequent step in design cycle, calculate overall section properties and bending stress distribution based on hog and sag moments;

3) perform longitudinal strength checks; and

4) for the distribution of primary stresses through the cross-section: When vertical primary stress distributions are only desired, use "K" curve distribution for the inner and outer shells. When vertical and lateral primary stresses are to be evaluated, combine the actual vertical and lateral stresses to develop the design primary stress distribution.

c. Select trial plates (and possibly stiffener for web) for inner and outer shell and web components:

1) identify if web is longitudinally stiffened; and

2) check minimum plate thickness requirement based on normal loads.

d. If web plate is stiffened, determine section properties for combined plate-stiffener.

e. Determine section properties for double-hull element composed of inner and outer hull and longitudinal web panels.

f. Determine secondary bending moments and shear forces for double-hull element.

g. Determine secondary bending and shear stresses at critical locations for double-hull element.

Perform the following steps for each inner or outer shell or web component of the ADH element:

h. Determine following:

1) effective width of plating;

2) plate width factor, β; and

3) buckling factor, C_k.

i. If stiffened web, determine secondary bending moments and shear stresses for stiffened-plate.

j. Check for critical buckling of plate panel in compression and shear. Check averaging requirement (Section 2.2.2.4) if difference in thickness between adjacent plate panels exceeds 25 percent.

k. Check for ultimate compressive strength of plate panel.

l. Perform tension check.

m. If stiffened web, perform following checks:

1) combined bending and column stresses (bending/column interaction) for combined plate-stiffener; and

2) lateral stability check for stiffener and determine required spacing and size of ILS according to Design Data Sheet DDS 100-4 (Naval Ship Engineering Center 1979).

n. For overall double-hull element, check for combined bending and column stresses (bending/compression interaction).

2.2.2.2 Longitudinal Strength Checks

Longitudinal strength checks and procedures for the advanced double hull are similar to those developed for conventional ship structures (Naval Sea Systems Command 1976). These include guidelines for establishing material effectiveness based on openings and discontinuous structures, design limitations for primary stresses and minimum primary bending stress distributions across the hull section ("K" curves).

2.2.2.2.1 Criteria for Longitudinal Material Effectiveness

For calculation of primary longitudinal hull section properties, effective material must be longitudinally continuous in accordance with guidelines presented in Figure 6. As can be seen, ineffective "shadow" regions are defined based on a 4:1 slope transition from the point of discontinuity. Although the shadow regions are not included in the section property calculation, it is presumed that they still experience the full primary longitudinal bending stress state (during bending, plane sections are assumed to remain plane), which must be accounted for during design.

2.2.2.2.2 Limitations for Design Primary Stresses

Design primary bending stresses are developed based on one of several accepted and empirical methods including hydrostatic balance in a specified wave form, probabilistic prediction for a specified operational environment and ship lifespan, and direct measurement based on model or full-scale tests. Design primary bending stresses will include compression and tension due to hull flexural hog and sag response. Regardless of the method used for its development, each component of design primary bending stress must be adjusted to include a future growth margin stress as shown in the following:

$$f_{1D} = f_{1C} + M_S \qquad (2.01)$$

where f_{1C} =   calculated primary stress

M_S =   margin stress, defined as:

=   1.0 tsi (2240 psi) for combatant ships,

=   0.5 tsi (1120 psi) for other ships.

Design primary shear stress, f_{1SD}, is based on the following guidelines:

$$f_{1SD} = 1.1 \times f_{1SC} \qquad (2.02)$$

where f_{1SC} =   calculated primary shear stress

These design primary stresses are to be limited as follows:

		(2.03)
for ordinary steel (OS):	f_{1D} or $f_{1SD} \leq$ 8.5 tsi (19,040 psi)	
for high-strength steel (HSS):	f_{1D} or $f_{1SD} \leq$ 9.5 tsi (21,280 psi)	
for HY-80 or HSLA-80:	f_{1D} or $f_{1SD} \leq$ 10.5 tsi (23,520 psi)	
for aluminum alloys:	f_{1D} or $f_{1SD} \leq$ 4.5 tsi (10,080 psi)	

"Shadow" or inef-
fective Area

12 x 4 x 22# I-T

6"X 4"X 15" I-T   25.5#

BHD BELOW

HATCH

4
1

SEE DETAIL "A"

6"X 4"X 15# I-T

25.5# Plate

FWD
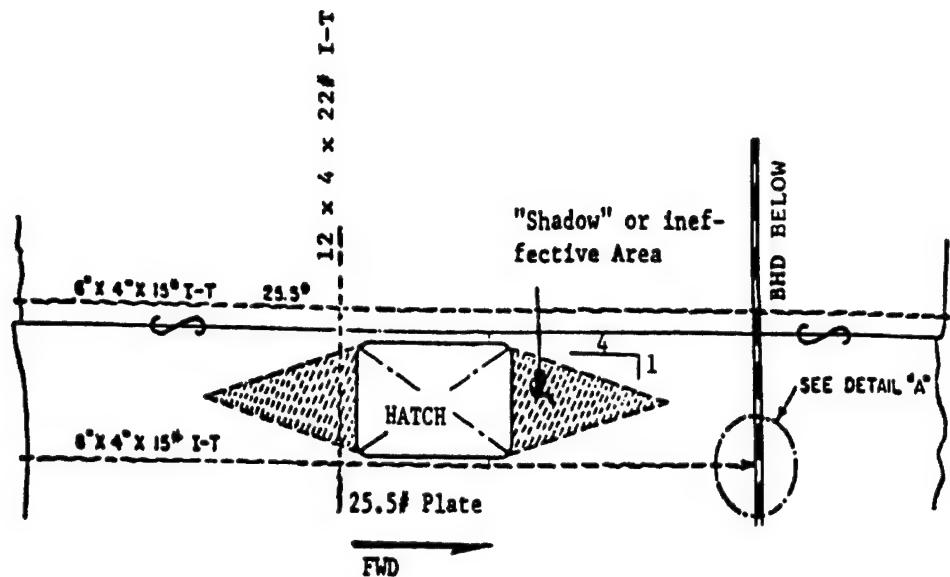
PLAN VIEW OF DECK
Showing Ineffective Material
In Way of Opening

DK

6"X 4"X 15° I-T   NOT
EFFECTIVE

BHD

DETAIL "A"

FWD

BHD

BHD

SECOND DECK AT ₡

SECOND DECK

6"X 4"X 19°I-T

SLOPE
1 TO 4

EFFECTIVE
PLATING

6"X 4"X 10° I-T

OPEN BAY
(NO LONG.
BHD)

10.2°

INEFFECTIVE
PLATING

OPEN BAY
(NO BULKHEAD)

FIRST PLATFORM (See Note)

FIRST PLATFORM INEFFECTIVE AT ₡ FRS. 35½ - 4½

16"X 8½"X 21°I-T

EFFECTIVE MATERIAL IN
SHORT LONGITUDINAL
BULKHEAD

NOTE:
    BULKHEAD CANNOT PULL FROM
INEFFECTIVE PORTION OF FIRST
PLATFORM.

Figure 6. Criteria for Longitudinal Effectiveness

2.2.2.2.3 *Design Primary Stress Distribution Across Section*

The design primary stress distribution applied for design should preferably be the algebraic sum of the actual primary vertical, lateral and torsional primary stresses without modification or subsequent factoring.

However, as the lateral and torsional stress distributions will not normally be available to the designer at the preliminary design stage, the traditional method is to design for just the vertical bending moments due to wave-induced and stillwater hydrostatic loads. This will result in maximum bending stresses at the extreme hull fibers diminishing to zero at the neutral axis. A factoring approach is then applied to the shell structure primary stresses to approximately account for the lateral and torsional stresses, which results in the primary stress distribution shown in Figure 4. As can be seen, rather than a zero stress state at the neutral axis, a primary stress equal to half the maximum-fiber stress is established at the neutral axis location with a linear distribution varying from the neutral axis to the extreme fiber. Stresses based on this so-called "K" curve are applied to the inner and outer shell plating, double hull longitudinal webs, and any attached longitudinal stiffeners and girders. All other longitudinal structures, including the decks and longitudinal bulkheads, can be designed without this "K" curve limitation.

2.2.2.3 Minimum Plate Thickness Check
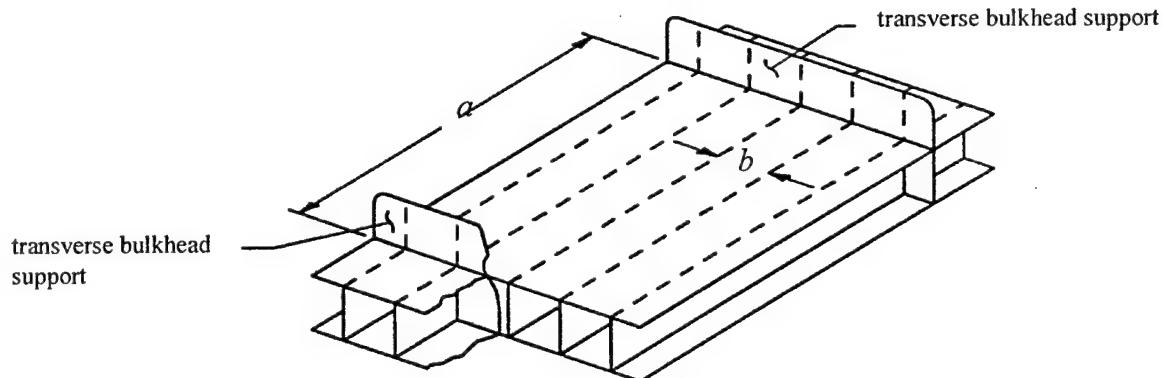
Figure 7. Plate Panel Characteristics

$$t_{min} = \frac{bk\sqrt{H}}{c} \qquad (2.04)$$

where t_{min} = minimum plate thickness, inches,

b = plating span, inches,

H = Equivalent uniform plate load, head of seawater, ft,

c = "Pseudo-stress" coefficient, based on material and allowable permanent set; taken from Table 2,

k = plate shape factor, based on aspect ratio, $\alpha = b/a$ or a/b, whichever is less

  = 1.0 for $\alpha < 0.5$ (2.05)

  = $0.450 + 2.684\alpha - 4.000\alpha^2 + 1.667\alpha^3$ for $0.5 \leq \alpha \leq 0.7$,

$$= \quad 2.131 - 3.685\alpha + 4.001\alpha^2 - 1.668\alpha^3 \quad \text{for } \alpha > 0.7$$

and, $\quad a \quad = \quad$ plating length, inches.

Typically, the plate thickness derived using this procedure is a lower bound. Other design requirements, presented in subsequent sections, will likely increase thickness requirements.

Table 2. Pseudo-Stress Coefficients

Material	c-Factor for Elastic Response	c-Factor for Elastic-Plastic Response	c-Factor for Plastic Response
OS	350	550	700
HSS	400	630	800
HSLA-80	500	750	900
HY-80	500	750	900
HY-100	550	800	1000
HY-130	600	850	1100
AL5086	250	400	500
AL5456	300	470	600

The "Elastic" c-factor is generally intended for structures normally subjected to live loads, such as decks, platforms, topside structures and adjacent tank structure. The "Elastic-plastic" c-factor is generally intended for those structures primarily subjected to hydrostatic and environmental loads, such as lower shell plating and tanks; the "Plastic" c-factor is generally intended for flooding and damage loads.

2.2.2.4 Check for Critical Buckling of Plate Panel (combined compression, bending and shear)

As shown in Figure 8, there are four states of in-plane stress, which may impact the stability of an advanced double hull structural element, and these include longitudinal compression, transverse compression, shear and longitudinal bending. Advanced double hull panel elements can be identified as either shell elements or web elements and each of these types will have three significant stress states to consider. Significant magnitudes of the four stress states will not generally occur simultaneously at significant magnitudes. The following summary of significant stress states for design are considered for the two plate panel types:
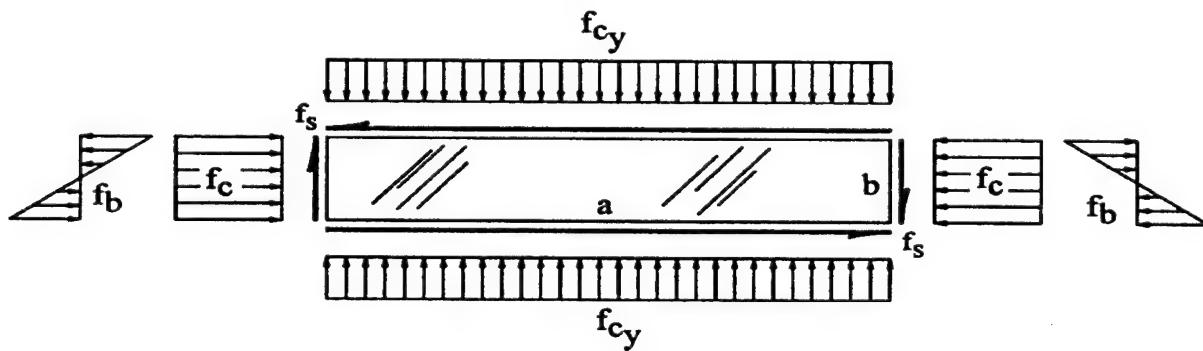
Figure 8. Double Hull Plate Element In-plane Stresses

1) ***Shell elements (inner or outer shell)***. These panels may have significant in-plane biaxial (longitudinal and transverse) stress in combination with in-plane shear stress. In-plane bending will generally be low and will result from differences in primary bending, mainly for vertically-oriented side-shell elements. In-plane shear, due to primary hull girder bending, may be significant at the neutral axis of the cross-section.

2) ***Longitudinal web elements***. These panels may have significant longitudinal compressive stress in combination with significant in-plane bending resulting from secondary loads in conjunction with, to a lesser extent, a bending component resulting from differences in primary bending between the top and bottom of the web element. In-plane shear stress may be significant, again primarily resulting from secondary loadings. Transverse in-plane compression will generally not be significant, although it may be important if the web is continuous with a deck or platform.

A reliable, general interaction equation for combining biaxial bending and shear in-plane stresses was not identified. However, it is recognized that a design situation involving the components of the double hull beam element where all four stress components occur simultaneously in significant magnitude is unlikely to exist. Therefore, design of these double hull elements shall be based on the evaluation of the following two interaction equations, one combining transverse compression with in-plane shear and the other combining longitudinal compression with in-plane bending and shear. The procedure is to assess the critical interaction equation, which will generally be that which results in the greater sum. Acceptability requires that both equations satisfy the requirement that the sum stress ratio term not exceed 1.0.

$$\frac{f_c}{F_{cr}} + \left(\frac{f_{cy}}{F_{cry}}\right)^2 + \left(\frac{f_s}{F_{crs}}\right)^2 \leq 1.0 \qquad (2.06a)$$

$$\frac{f_c}{F_{cr}} + \left(\frac{f_b}{F_{crb}}\right)^2 + \left(\frac{f_s}{F_{crs}}\right)^2 \leq 1.0 \qquad (2.06b)$$

where f_c =   uniform longitudinal compressive stress in plate. Depending on the orientation of the double hull element, this will be the resultant of a primary stress component and a secondary stress component.

f_{cy} =   uniform transverse in-plane compressive stress in plate panel. This is the stress acting along the long panel edges. In lieu of deriving these stresses using numerical or other means, these stresses are approximated through static balance of hydrostatic and dead weight loads.

f_b =   in-plane bending stress in the plate panel resulting from either secondary bending, primary bending or a combination of primary and secondary bending. Secondary bending stress is generally significant for the longitudinal web. Primary bending stress can be expressed as the sum of uniform axial stress and bending stress components when there is variation in primary stress across the width of the plate panel, as with side shell plating.

f_s =   in-plane shear stress in plate. Depending on the orientation of the double hull element, this will be the resultant of a primary stress component and a secondary stress component. Note that for midship section design, the

primary shear stress component is normally of small magnitude and is generally neglected.

F_{cr} = critical compressive longitudinal buckling strength $F_{cr} = F_{cr_e}$ for $F_{cr_e} < F_L$.

$$F_{cr} = \frac{F_{cr_e}^2 F_y}{F_{cr_e}^2 + F_L\left(F_y - F_L\right)} \quad \text{for } F_{cr_e} \geq F_L \tag{2.07}$$

where F_{cre} = elastic critical compressive longitudinal buckling strength

$$F_{cr_e} = \frac{Ck_c E}{\left(\dfrac{b}{t}\right)^2} \tag{2.08}$$

F_y = yield strength,

F_L = proportional stress, specified as a material property,

E = elastic modulus,

b = plate span,

t = plate thickness,

$$C = \frac{\pi^2}{12\left(1 - v^2\right)} \tag{2.09}$$

v = Poisson's ratio = 0.3, for steel

k_c = plate factor for longitudinal compressive strength, assuming simply-supported plate boundary conditions.

$$k_c = 4.0 \tag{2.10}$$

F_{cry} = critical compressive transverse buckling strength

$$F_{cry} = F_{cry_e} \text{ for } F_{cry_e} < F_L \tag{2.11}$$

$$F_{cry} = \frac{F_{cry_e}^2 F_y}{F_{cry_e}^2 + F_L\left(F_y - F_L\right)} \quad \text{for } F_{cry_e} \geq F_L$$

where F_{cry_e} = elastic critical compressive transverse buckling strength

$$F_{cry_e} = \frac{Ck_y E}{\left(\dfrac{b}{t}\right)^2} \tag{2.12}$$

k_y = plate factor for transverse compressive strength, assuming simply-supported plate boundary conditions.

$$k_y = (a/b + b/a)^2 \tag{2.13}$$

a = length of plate panel

F_{crb} = Critical in-plane bending buckling strength

$$F_{crb} = F_{crb_e} \quad \text{for} \quad F_{crb_e} < F_L \tag{2.14}$$

$$F_{crb} = \frac{F_{crb_e}^2 F_y}{F_{crb_e}^2 + F_L(F_y - F_L)} \quad \text{for} \quad F_{crb_e} \geq F_L$$

where F_{crb_e} = Elastic critical in-plane bending buckling strength

$$F_{crb_e} = \frac{C k_b E}{\left(\dfrac{b}{t}\right)^2} \tag{2.15}$$

k_b = plate factor for in-plane bending buckling strength, assuming simply-supported plate boundary conditions.

$$k_b = 24 \quad \text{for } a \geq 0.6667\, b \tag{2.16}$$

$$k_b = 24 + 73\,(0.6667 - a/b)^2 \quad \text{for } a < 0.6667\, b$$

F_{crs} = critical in-plane shear buckling strength

$$F_{crs} = F_{crs_e} \quad \text{for } F_{crs_e} < F_{SL} \tag{2.17}$$

$$F_{crs} = \frac{F_{crs_e}^2 F_{sy}}{F_{crs_e}^2 + F_{SL}(F_{sy} - F_{SL})} \quad \text{for } F_{crs_e} \geq F_{SL}$$

where F_{crs_e} = elastic critical in-plane shear buckling strength

$$F_{crs_e} = \frac{C k_s E}{\left(\dfrac{b}{t}\right)^2} \tag{2.18}$$

k_s = plate factor for in-plane shear buckling strength, assuming simply-supported plate boundary conditions.

$$k_s = 5.34 + 4.0 / (a/b)^2 \quad \text{for } a \geq b \tag{2.19}$$

$$k_s = 5.34 + 4.0 / (b/a)^2 \quad \text{for } a \leq b$$

F_{sy} = shear yield strength $= F_y / \sqrt{3}$

F_{SL} = shear proportional limit $= F_L / \sqrt{3}$

17

2.2.2.5 Check for Ultimate Strength of Plate Panel in Axial Compression

The following interaction equation is to be used for the ultimate strength of plate panels in axial compression. Sikora (2001) shows the derivation of equation (2.20).

$$\frac{f_c + f_{b\,ave}}{F_u} + \left(\frac{f_{cy}}{0.8F_{uy}}\right)^2 + \left(\frac{f_s}{0.8F_{us}}\right)^2 \leq 1.0 \tag{2.20}$$

where f_c, f_{cy}, f_s are defined in the buckling check, previously performed in Section 2.2.2.4, and $f_{b\,ave}$, F_u, F_{uy}, and F_{us} are subsequently defined.

2.2.2.5.1 Longitudinal In-plane Compressive Ultimate Strength (long panel)

The following expression predicts ultimate strength of an advanced double hull plate panel load on the transverse, or shorter edge. This expression is based on a reduced effective sectional area of plating exceeding yield stress, and has been factored to account for residual weld stresses.

$$F_u = F_y\left[\left(\frac{2.25}{\beta} - \frac{1.25}{\beta^2}\right)R_r\right] \quad \text{for } \beta \geq 1.25 \tag{2.21}$$

$$F_u = F_y R_r \quad \text{for } \beta < 1.25$$

$$\text{where} \quad \beta = \frac{b}{t}\sqrt{\frac{F_y}{E}} \tag{2.22}$$

R_r = Strength reduction ratio due to weld residual stresses

$$R_r = 1 - \left(\frac{f_r}{F_y}\frac{E_t}{E}\frac{\beta^2}{2.25\beta - 1.25}\right) \quad \text{for } \beta \geq 1.25 \tag{2.23}$$

$$R_r = F_y R_r \quad \text{for } \beta < 1.25$$

$$\text{If } R_r > 0.8, R_r = 0.8 \tag{2.24}$$

where $\dfrac{f_r}{F_y}$ = ratio of residual compressive stress at middle of plate panel to compressive yield strength

$$= \frac{2\eta}{b/t - 2\eta} \tag{2.25}$$

where η = tension block width factor, which is a function of the weld characteristics and typically ranges from 3.0 to 4.5, as shown in Figure 9. η is an empirically-derived term based on material, weld process and weld quality. η will tend to

18

increase with increasing material yield stress. For concept designs, $\eta = 4.5$ is recommended.

$\dfrac{E_t}{E}$ = ratio of the structural tangent modulus in compression to the elastic stiffness modulus. This tangent modulus term applies a reduction based on inelastic material properties by approximating the material stress-strain curve above the proportional limit as a parabola.

$$= \left(\frac{C_k \beta^2}{C_k^{\,2} + p_r(1 - p_r)\beta^4} \right)^2 \quad \text{for } \beta \le \sqrt{\frac{C_k}{p_r}} \tag{2.26}$$

$$= 1.0 \quad \text{for } \beta > \sqrt{\frac{C_k}{p_r}}$$

where C_k = Ck_c, C as defined in Equation (2.09) and k_c as defined in Equation (2.10).
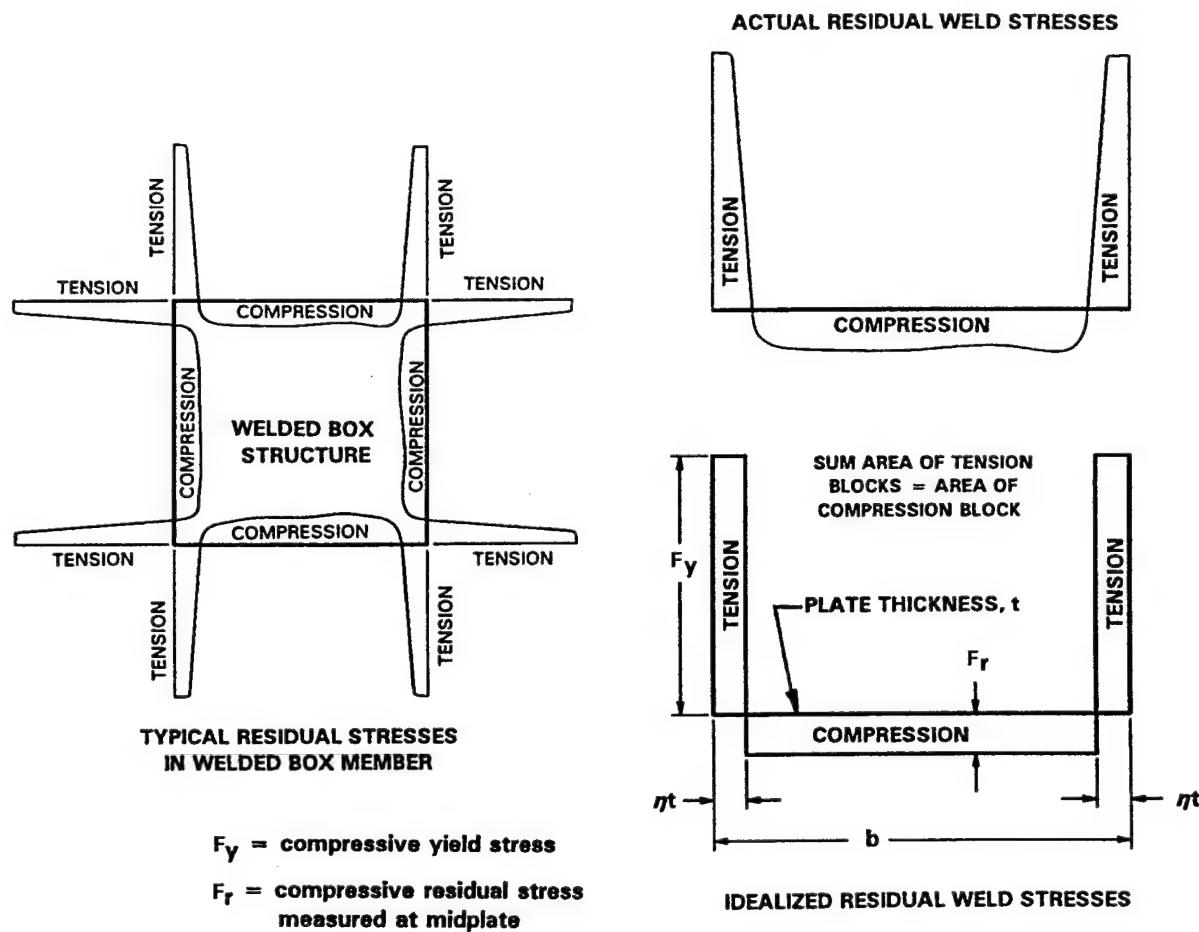
Figure 9. Derivation of η Factor for Weld Residual Stresses

These equations can be simplified as he following expressions which apply to steels typically used in ship construction:

$$\frac{E_t}{E} = \left(\frac{3.62\beta^2}{13.1 + p_r(1 - p_r)\beta^4}\right)^2 \quad \text{for } \beta \le \frac{1.9}{\sqrt{p_r}} \tag{2.27}$$

$$\frac{E_t}{E} = 1.0 \quad \text{for } \beta > \frac{1.9}{\sqrt{p_r}}$$

where p_r =   ratio of the structural proportional strength to the compressive yield stress for the material

$$= (F_L - f_r)/F_y \tag{2.28}$$

$$\approx 0.5 \text{ for welded ship steels}$$

where F_L =   material proportional stress,

         f_r =   compressive residual stress at middle of plate,

         F_y =   compressive yield stress.

2.2.2.5.2 Transverse In-plane Compressive Ultimate Strength (wide panel)

The following expression predicts ultimate strength of a plate panel loaded on the longitudinal, or longer edge. This wide-plate expression is based on an assumption of an effective width of plating stressed to yield at the edges and a wide middle region along the long edge where the plate remains stressed at the elastic buckling stress. In this simplified model, no accounting of weld residual stresses has been included.

$$F_{u_y} = F_y\left[\frac{0.9}{\beta^2} + \frac{1.9}{\alpha\beta}\left(1 - \frac{0.9}{\beta^2}\right)\right] \tag{2.29}$$

where $\alpha =$ plate panel aspect ratio $= a / b$

        $a =$ plate panel length in the longitudinal direction

2.2.2.5.3 In-plane Ultimate Shear Strength

An in-plane, shear ultimate strength equation is not readily available. However, an estimate of the shear ultimate strength is obtained by combining the shear buckling strength and the post-tension shear field strength, and this is summarized in the following equations. This approach is inherently conservative because the maximum secondary stress is used, although it is only maximized at the forward and aft ends of the panel and is zeroed in the mid-panel region.

$$F_{u_s} = (F_{crs} + F_{tfs}) \tag{2.30}$$

where F_{crs} =   critical shear buckling strength, calculated previously,

        F_{tfs} =   tension field shear strength,

$$= \frac{f_t}{2\sqrt{1 + \left(a/b\right)^2}} \tag{2.31}$$

$$\text{where} \quad f_t = \left(1 - \frac{F_{crs}}{F_{sy}}\right)F_y \tag{2.32}$$

$$F_{sy} = \text{shear yield strength} = F_y / \sqrt{3} \tag{2.33}$$

If the aspect ratio (a/b) is greater than 3, then post-tension field strength will not develop. Therefore, for ADH structure, where $a/b \gg 3$, post-tension failure will not develop and shear strength is based on shear buckling.

2.2.2.5.4 In-plane Ultimate Bending Strength

The following expression calculates the ultimate bending strength under in-plane loading. The procedure is based on determining the total compressive force component from the in-plane bending stress distribution for the plate panel and averaging this compressive stress over the entire transverse cross-sectional area of the plate.

$f_{b\,ave}$ = average equivalent uniform stress component of in-plane bending stress

$$f_{b\,ave} = \frac{f_{bc} - f_{bt}}{2} + \frac{f_{bc} + f_{bt}}{8} \tag{2.34}$$

where f_{bc} is the maximum component of in-plane bending compressive stress,

f_{bt} is the maximum component of in-plane bending tensile stress,

These stresses are defined as positive in magnitude, if $f_{b\,ave} < 0.0$, $f_{b\,ave} = 0.0$.

2.2.2.6 Check for Tensile Stresses

A check is performed to evaluate the resultant tensile stress resulting from combined primary and secondary bending. Secondary bending of the double hull element results in tensile stresses in the inner hull at midspan and outer hull at the transverse bulkhead support and in the web at midspan and support locations. In addition, if the web is stiffened, there is an additional secondary bending moment that may exist if the web is subjected to tank loads. The following equations are applied:

$$\frac{f_t + f_{bt}}{F_B} \le 1.0 \tag{2.35}$$

where $f_t =$ primary tensile stress due to hog-sag bending;

$f_{b_t} =$ tensile stress due to secondary bending within double hull element. For stiffened web taking tank load, this will also include secondary bending for stiffened web plate;

$F_B =$ allowable working strength, which is provided as a material property or derived from the following equation:

$$F_B = 0.5\left(\frac{F_y}{1.25} + \frac{F_{ult}}{2.15}\right) \tag{2.36}$$

where $F_y =$ material yield strength,

       $F_{ult} =$ material ultimate tensile strength.

2.2.2.7 Check for Combined Bending and Column Stresses

This check evaluates the global buckling strength of the double hull element composed of inner and outer shell and web elements in combination with the maximum compressive secondary bending stress. This secondary stress is maximized at several possible locations, including the outer hull panel at mid-span and the inner hull panel at the ends where it is welded to the transverse bulkheads.

$$\frac{f_{b\,max}}{F_B} + \frac{f_c}{K_s F_c} \leq 1.0 \tag{2.37}$$

where $f_{b\,max} =$ maximum component of secondary bending compressive stress in either inner or outer hull plate panel. Critical locations are inner hull at transverse bulkhead support and outer hull at middle of plate panel;

    $f_c =$ maximum compressive primary stress acting on double hull element due to hog-sag bending;

    $F_B =$ allowable working strength, which is provided as a material property or derived, as previously done with tension check;

    $K_s =$ slenderness coefficient;

$$= 0.67 \text{ for } L/r \geq 60 \tag{2.38}$$

$$= 0.80 \text{ for } L/r < 60$$

where $L/r =$ slenderness ratio,

    $L =$ column length, which is taken as the distance between transverse bulkheads for the double hull element;

    $r =$ radius of gyration for effective material of the double hull element composed of inner and outer hull and longitudinal web panels;

$$r = \sqrt{\frac{I_{eff}}{A_{eff}}} \tag{2.39}$$

22

where $\quad I_{\text{eff}} = \quad$ moment of inertia for effective material of double hull element,

$\qquad A_{\text{eff}} = \quad$ cross-sectional area of effective material of double hull element,

$\qquad F_c \quad = \quad$ column strength for section based on effective material of the double hull element composed of inner and outer hull and web plate panels,

$$
\begin{aligned}
&= F_y && \text{for } C < 1.4 \\
&= F_y (1.235 - 0.168C) && \text{for } 1.4 \le C \le 4.8 && (2.40) \\
&= F_y (\pi^2 / C^2) && \text{for } C > 4.8
\end{aligned}
$$

$$
\text{where} \quad C = K_c \frac{L}{r} \sqrt{\frac{F_y}{E}} \qquad\qquad (2.41)
$$

$\qquad K_c \quad = \quad$ column end fixity coefficient,

$\qquad\qquad = \quad$ 1.0 for pinned-end column (recommended for design of double hull),

$\qquad\qquad = \quad$ 0.5 for fixed-end column.

2.2.2.8 Design of Stiffened Longitudinal Web Frames

Longitudinal stiffeners on the double hull web frames reduce the effective plating span by partitioning the full web span into two or more narrower spans, thus greatly reducing the plating thickness requirement. Therefore, the stiffeners and the associated effective width of plating to which they are welded must be sufficient to develop and maintain a line of support extending along the full length of the web plate panel. In most cases, the stiffened web element experiences only primary stresses and possibly secondary stresses due to the secondary bending of the double hull element composed of inner and outer hull and web plate panels. The stiffened web member will not generally be subjected to normal loads unless the longitudinal web is watertight and functions as a tank boundary subjected to tank loads. In this case, design of the stiffened web member largely follows the guidelines of Design Data Sheet DDS 100-4 (Naval Ship Engineering Center 1979). Figure 10 presents the parameters for stiffened longitudinal members.

One weight reducing option is to employ transverse breakers to reduce buckling of the web plates. Another option is to use one or more longitudinal stiffeners. In most cases, where normal loads are not experienced, the stiffened plate will experience only axial loads and the following procedures are applied.
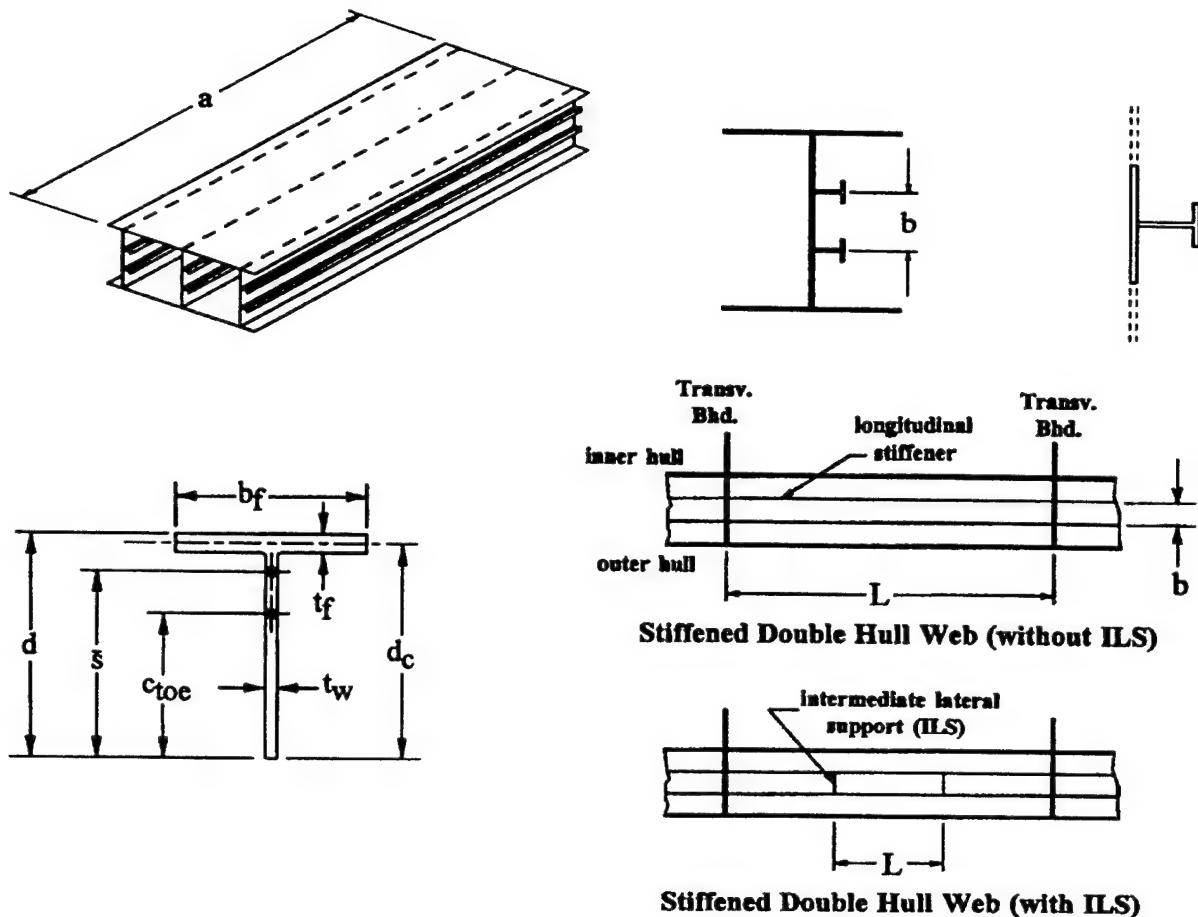
Figure 10. Notation for Longitudinally Stiffened Members

2.2.2.8.1 Recommended Procedure for the Design of Longitudinally-stiffened Advanced Double Hull Plate Webs in the Absence of Significant Normal Loads

Advanced double hull longitudinal webs differ from typical ship plate structures in the nature of the structural loading to which they are subjected and designed. Because they are typically characterized by openings to permit access or transfer of fluids between adjacent ADH cells, there will typically be no significant level of normal loading, although the full magnitude of primary axial stress can be expected. Hence, the traditional methods of stiffened-plate design, which are based on secondary bending response of the stiffened-plate element in combination with primary axial stress, will be inadequate for these members. As with the design of other ship plate-structure elements, there will be a strong desire to incorporate one, or more, longitudinal stiffeners on the web as an efficient means of minimizing weight of the resulting structure. However, for the ADH webs, the primary purpose of these stiffeners is to subdivide the web plate panel into narrower sub-panels to permit greatly reduced plating thicknesses. Although the resulting stiffened web panels are not expected to sustain significant normal loads, both plate and stiffeners will be subjected to the full magnitude of primary bending stress. Hence, these elements will be designed based on local buckling considerations.

Bleich (1952) provides a convenient closed-form solution for the buckling design of the longitudinal webs. This solution accounts for the web as a stiffened, subdivided-plate supported

on all sides rather than as a column composed of a stiffened-plate as has been the traditional U.S. design approach. This formulation, as presented by Bleich, develops a stiffener sufficient to support the web plate panel to the elastic buckling load along a line of support described by the sides of the web and joint with each of the stiffeners. This formulation requires a degree of fixity sufficient to provide for the plate panel to elastically buckle in a pattern consistent with the traditional differential equations that govern the behavior of buckling plates. Two conditions are covered by the Bleich expressions, and these include a single, centerline stiffener and two stiffeners spaced equidistant.

$$I_{req} = \frac{b_{eff}t_{min}^{3}}{12(1-v^2)n_s}\gamma_{max} \qquad (2.42)$$

where I_{req} =   minimum required moment of inertia for combined plate and stiffener. The calculation of I_{req} is based on the combined area of a single stiffener and the effective area of plating to which it is welded. The effective plate area will be the product of the actual plate thickness of the web, t, and the effective breadth of the plate, b_{eff}, which is developed as follows:

b_{eff} =   lesser of the following two expressions:

$$b_{eff} = \frac{b}{(n_s+1)} \qquad b_{eff} = 2t\sqrt{\frac{E}{F_y}} \qquad (2.43)$$

F_y =   yield stress for the plate material

γ_{max} = $24.35 + 110.4\delta + 129.9\delta^2$ if one stiffener supporting web,   (2.44)

γ_{max} = $96 + 610\delta + 975\delta^2$ if two stiffeners supporting web

δ =   stiffener/plate area ratio for entire stiffened web, $\delta = \dfrac{n_s A_t}{bt_{min}}$

n_s =   number of evenly-spaced web stiffeners,

A_t =   cross-sectional area of a single stiffener,

B =   web span, inner to outer shell,

t_{min} =   minimum plate thickness, based on buckling strength considerations, geometric, loading and material characteristics of the web provided as follows:

$$t_{min} = \sqrt{\frac{12(1-v^2)F_c b^2}{k_w \pi^2 E\sqrt{\tau}(n_s+1)^2}} \qquad (2.45)$$

where v =   Poisson's ratio for material; typically = 0.3 for steel;

F_c =   design stress;

k_w =   plate factor; k_w = 4.0 for simply-supported plate assumed in this model;

E =   elastic modulus;

25

E_t =   tangent modulus - slope of the stress-strain curve at a given stress state above the proportional stress; typically less than elastic modulus, E, in magnitude;

τ =   ratio - tangent modulus, E_t, divided by elastic modulus, E; τ will be typically be 1.0 for double hull web applications where the design stress, F_c, reflects an elastic stress well below the proportional stress. However, for some applications, F_c may exceed the proportional stress and τ will be less than 1.0.

For those stiffened webs which must be designed to sustain normal loads in addition to axial loads, as will be the case for longitudinal webs that must function as tank boundaries, it will be necessary to apply traditional stiffened plate design procedures. See 2.2.2.8.4. The procedure is similar to that applied to decks, sideshell and other stiffened-plate structure supporting significant normal loads, such as hydrostatic loading, as has been previously described.

2.2.2.8.2 Requirements for stiffener dimensions

The ratio of the width of the stiffener flange (b_f) to twice the thickness of the flange (t_f) ($\frac{b_f}{2t_f}$) shall not exceed 15.

2.2.2.8.3 Lateral stability (torsional buckling) check for stiffener

If the lateral stability check fails, options include increasing the size of the stiffener and providing intermediate lateral supports (ILS) or transverse frames spanning the width of the longitudinal web, which reduces the effective stiffener length. The following guideline specifies the required number of ILS to satisfy the lateral stability check:

$$\frac{L}{L_s} \le 1.0 \tag{2.46}$$

where L =   laterally-unsupported length of stiffener,

        L_s =   maximum length of a stable stiffener,

$$L_s \doteq K_f^{\cdot} \pi \sqrt{\frac{E\left(I_z \bar{s}^2 + \Gamma\right)}{I_p F_y - GJ}} \tag{2.47}$$

where K_f =   Stiffener end fixity coefficient,

              =   1.0 for pinned ends,

              =   2.0 for fixed ends,

              =   1.414 for intermediate fixity (recommended for design),

    G =   shear modulus, which is provided as a material property or derived using the following equation:

$$G = \frac{E}{2(1+v)} \tag{2.48}$$

I_z =   moment of inertia about the tee web plane,

$$I_z = \frac{t_f b_f{}^3 + d t_w{}^3}{12} \tag{2.49}$$

$\bar{s}$ =   height of shear center above toe of tee,

$$\bar{s} = \frac{d + (d + t_f)\big/\left[1 + (d/t_f)(t_w/b_f)^3\right]}{2} \tag{2.50}$$

Γ =   longitudinal warping constant,

$$\Gamma = \frac{t_w{}^3 d^3 + \left(t_f{}^3 b_f{}^3\right)\big/4}{36} \tag{2.51}$$

J =   St. Venant Torsion Constant,

$$J = \frac{d t_w{}^3 + b_f t_f{}^3}{3} \tag{2.52}$$

I_t =   vertical moment of inertia about stiffener toe (stiffener only)

$$I_t = \frac{t_w d^3}{3} + b_f t_f \left(d_c{}^2 + \frac{t_f{}^2}{12}\right) \tag{2.53}$$

I_p =   polar moment of inertia about toe of stiffener,

$$I_p = I_t + I_z \tag{2.54}$$

d_c =   depth of stiffener to mid-thickness of flange.

The required number of ILS to satisfy the lateral stability check is therefore:

$$\text{if } L < L_s, \qquad\qquad \text{number of ILS} = 0 \tag{2.55}$$

$$\text{if } L_s < L < 1.75\,L_s, \qquad\qquad \text{number of ILS} = 1$$

$$\text{if } 1.75\,L_s < L < 2.50\,L_s, \qquad\qquad \text{number of ILS} = 2$$

$$\text{if } 2.50\,L_s < L < 3.00\,L_s, \qquad\qquad \text{number of ILS} = 3$$

$$\text{if } L > 3.00\,L_s, \qquad\qquad \text{number of ILS} = \text{integer}\left(\frac{L}{0.75 L_s} + 1\right)$$

Details for dimensioning of ILS should follow the guidance outlined in DDS 100-4 (Naval Ship Engineering Center 1979).

2.2.2.8.4 Stiffened Double Hull Webs Subjected to Lateral Loads (tank loads)

If webs are subjected to normal loads, such as tank loads, then, in addition to the previously described design checks, additional checks must be made to account for the stresses relating to secondary bending of the plate-stiffener web component. In this case, these stresses are added to the previously defined advanced double hull secondary bending stresses and the primary bending stresses. As with the double hull element, secondary stresses must be evaluated at the four locations defined by the mid-span and ends of the stiffened plate element at both the plate and the flange positions. It is assumed that normal loads will be applied from the unstiffened side of the plate panel such that the plate would be in compression and the stiffener in tension at midspan. Reverse loads can be evaluated (stiffener in bending compression at midspan) but this requires additional buckling considerations for the stiffener that are not provided within these guidelines or DDS 100-4. The design length for the stiffened-plate web element will be the same as the design length for the double hull element unless transverse framing which spans the full width of the web is used. The plating span, b, is the span between adjacent stiffeners and not the full width of the web plating. In general, the procedure for design of the stiffened webs follows procedures outlined in DDS 100-4. The following guidance is provided.

2.2.2.8.4.1 MINIMUM PLATE THICKNESS CHECK (SEE SECTION 2.2.2.3)

The plating span, b, is the spacing between the stiffeners. Otherwise, the procedure follows as previously described in Section 2.2.2.3.

2.2.2.8.4.2 CHECK FOR CRITICAL BUCKLING OF PLATE PANEL (SEE SECTION 2.2.2.4)

An additional secondary, uniform longitudinal in-plane compressive stress must be defined and added to the primary compression and secondary compression due to bending of the double hull element composed of inner and outer hull and web panels. The plating span is the spacing between adjacent stiffeners and not the full width of web plating. Otherwise, the procedure follows that previously described in Section 2.2.2.4 for the double hull element.

2.2.2.8.4.3 CHECK FOR ULTIMATE STRENGTH OF PLATE PANEL (SEE SECTION 2.2.2.5)

The additional secondary, uniform longitudinal in-plane compressive stress described in the previous paragraph is added to the primary compression and secondary compression due to bending of the double hull element in the same way as for the buckling check. The plating span is the spacing between adjacent stiffeners and not full width of web plating. Otherwise, the procedure follows that previously described in Section 2.2.2.5 for the double hull element.

2.2.2.8.4.4 CHECK FOR TENSILE STRESSES (SEE SECTION 2.2.2.6)

An additional secondary tension is defined due to the normal loading of the plate-stiffener element, and this is added to the secondary tension already defined for the double hull element. Midspan and edge tension stresses must be considered to determine the maximum bending stress. Otherwise, the procedure follows as previously described in Section 2.2.2.6.

2.2.2.8.4.5 CHECK FOR COMBINED BENDING AND COLUMN STRESSES (SEE SECTION 2.2.2.7)

The procedure is similar to that described in Section 2.2.2.7, except that the secondary bending stress is based on the tank load on the plate-stiffener element and the L/r term is defined for the stiffened plate and not the double hull element. This check is done in addition to that for the double hull element.

2.2.2.8.4.6 SHEAR CHECK

$$\frac{f_{sa}}{0.60F_B} \leq 1.0 \tag{2.56}$$

where f_{sa} = average shear stress acting through web of stiffener at end support due to normal load on web,

F_B = allowable working strength, see Section 2.2.2.6

2.2.2.8.5 Cross-sectional properties of plate and combined tee and plate

Definitions of the cross-sectional properties of a typical combined tee and plate are shown in Figure 11.
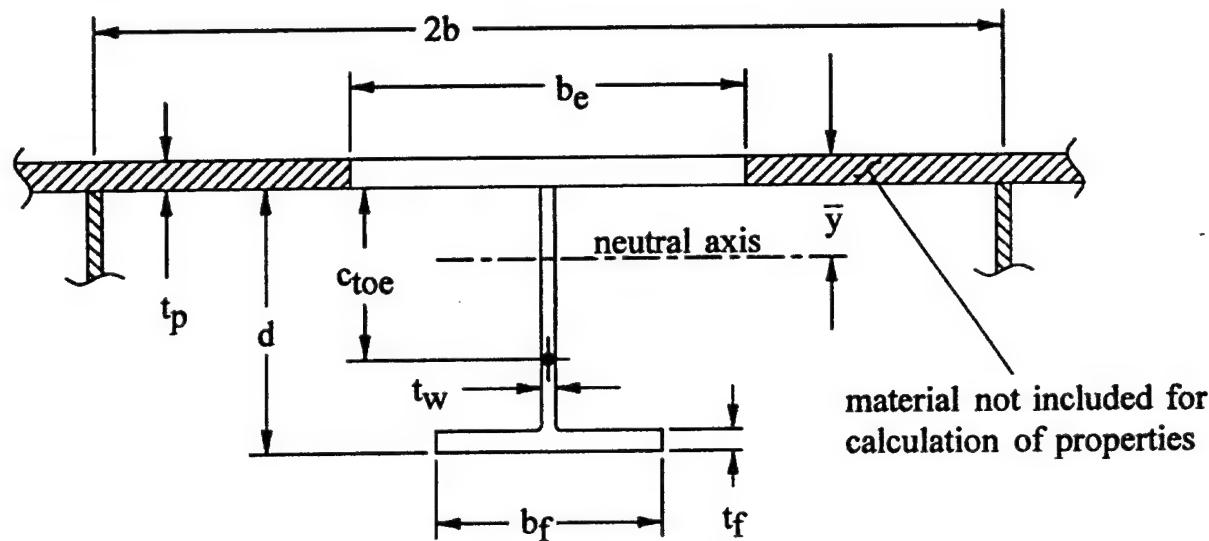
Figure 11. Characteristic Dimensions for T-Stiffened Panels

Effective breadth of plating, b_e:

b_e = taken as the least of the following three equations:

$$b_e = 2t_p \sqrt{\frac{E}{F_y}} \quad \text{where } F_y = \text{yield strength, } E = \text{stiffness modulus}$$

$$b_e = b \tag{2.57}$$

$$b_e = L/3$$

Neutral axis, $\bar{y}$ = distance between the outside of the plate and the neutral axis of the combined plate and stiffener:

$$\bar{y} = \frac{\sum y_i A_i}{\sum A_i} \tag{2.58}$$

$$\bar{y} = \frac{b_e t_p \left(t_p/2\right) + t_w \left(d - t_f\right)\left[\left(d - t_f\right)/2 + t_p\right] + b_f t_f \left(d - t_f/2 + t_p\right)}{b_e t_p + t_w \left(d - t_f\right) + b_f t_f}$$

Moment of inertia for combined plate and tee, I:

$$I = \sum \frac{bh^3}{12} + \sum Ad^2 \tag{2.59}$$

$$I = \frac{b_e t_p^{\,3}}{12} + b_e t_p \left(\bar{y} - t_p/2\right)^2 + I_{tee} + A_{tee}\left(C_{toe} + t_p - \bar{y}\right)^2$$

where I_{tee} = moment of inertia for tee, alone,

A_{tee} = cross-sectional area for tee, alone,

C_{toe} = height of center-of-gravity for tee, alone,

I_{tee}, A_{tee}, and C_{toe} are tabulated in standard tee catalogs or derived.

Elastic section moduli, S_p and S_f:

$$\text{Section modulus for plate, } S_p = \frac{I}{\bar{y}} \tag{2.60}$$

$$\text{Section modulus for stiffener flange, } S_f = I/\left(d + t_p - \bar{y}\right) \tag{2.61}$$

Total cross-sectional area, A_{tot}:

$$A_{tot} = bt_p + A_{tee} \tag{2.62}$$

Effective cross-sectional area, A_{eff}:

$$A_{eff} = b_e t_p + A_{tee} \tag{2.63}$$

Shear area, A_s:

$$A_s = \left(d + t_p\right)t_w \tag{2.64}$$

Radius of gyration, r:

$$r = \sqrt{\frac{I}{A_{eff}}} \tag{2.65}$$

2.2.2.9 Transverse Bulkhead Design

A fundamental assumption of the behavior of the advanced double hull is that the double hull element, with transverse frames eliminated, is entirely supported by the transverse bulkheads. This contrasts with a conventional hull structure where transverse frames support the shell and deck structures at regular intervals. As a result, the bulkhead will be required to support the large shear forces that are transmitted by the double hull longitudinal webs. This contrasts with the conventional hull structure where the bulkheads were predominantly designed to withstand secondary loads.

Because of the large shear forces transmitted by the longitudinal webs into the bulkheads, it will be necessary to maintain lines of support to transfer the shear forces of the longitudinal webs into the bulkhead in a manner which assures an efficient distribution of forces throughout the bulkhead. This requires that the webs align with stiffeners in the bulkheads, as shown in Figure 12, to maintain the lines of support for distribution of the double hull forces into the bulkhead. This contrasts with the conventional bulkhead, which is primarily vertically stiffened. To prevent stress concentration problems, brackets may be required for the transition from the webs into the bulkhead frame. The overall impact of these requirements will be that the bulkhead for the advanced double hull design may be a heavier structure than that of the transverse bulkhead for the conventional hull.

Design of the bulkhead should follow NAVSEA guidance (Naval Sea Systems Command 1976). Forces and design stresses will be based on conventional service and damage head loads.

A weight-efficient alternative design concept for long compartments is the deep frame or partial transverse bulkhead. These structures provide sufficient transverse strength to support the longitudinal cellular structure while preserving a large volume within the compartment. The downside is small increase in producibility costs. Whether conventional transverse bulkheads or deep frame/partial bulkheads are selected, it is recommended that numerical modeling be performed to verify elimination of either grillage structure or brackets for the transition from the double hull longitudinal webs into the bulkhead structure.

2.2.2.10 Double Hull End Transitions

Figure 13 and Figure 14 show a typical end transition for an advanced double hull. This assures a smooth and uniform transition of each of the double hull elements defined by inner and outer hull and web panels into longitudinal stringers, girders, decks, longitudinal bulkheads, or longitudinal web frames within a conventional double bottom structure.

Although the double hull will end or begin at a transverse bulkhead, it is preferable to continue the double hull a short distance beyond the bulkhead. This will reduce stress and provide for the inner flange of an effective ring frame structure comprising the transverse bulkhead margin plate for support of the double hull. The transition should extend far enough to permit a taper with approximately a 4:1 slope to minimize stress concentration effects (Ford, Grassman, and Michaelson 1994).

Numerical modeling is recommended to determine the most appropriate configuration for this transition. Otherwise, it is recommended that methods be applied for preliminary design of these transition structures that are consistent with both DDS 100-4 (Naval Ship Engineering Center 1979) and the NAVSEA design manual (Naval Sea Systems Command 1976).
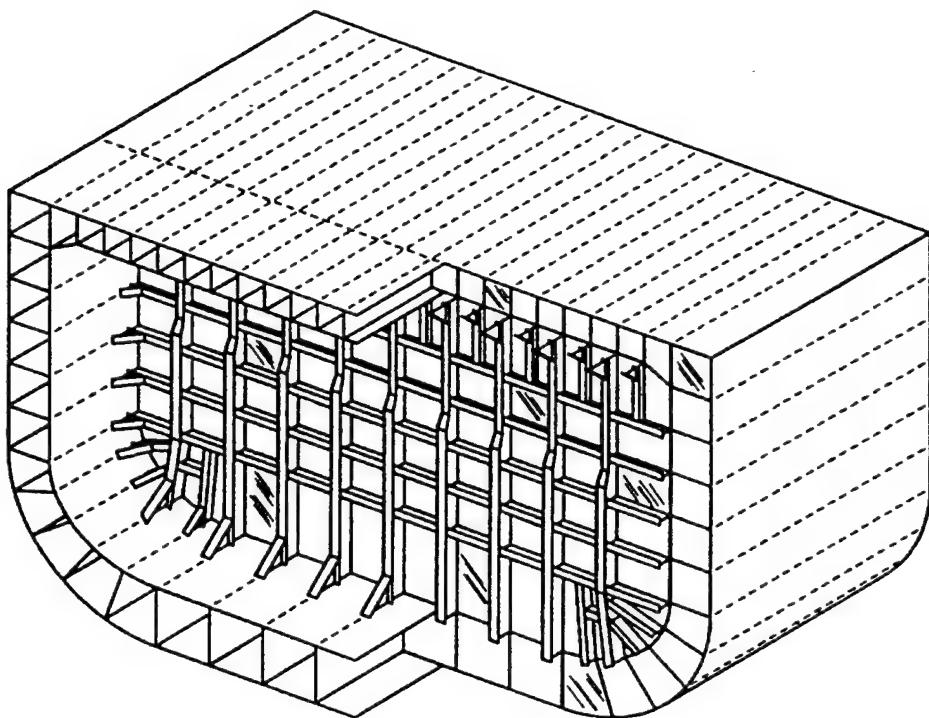
Figure 12. Advanced Double Hull Transverse Bulkhead Design Configuration
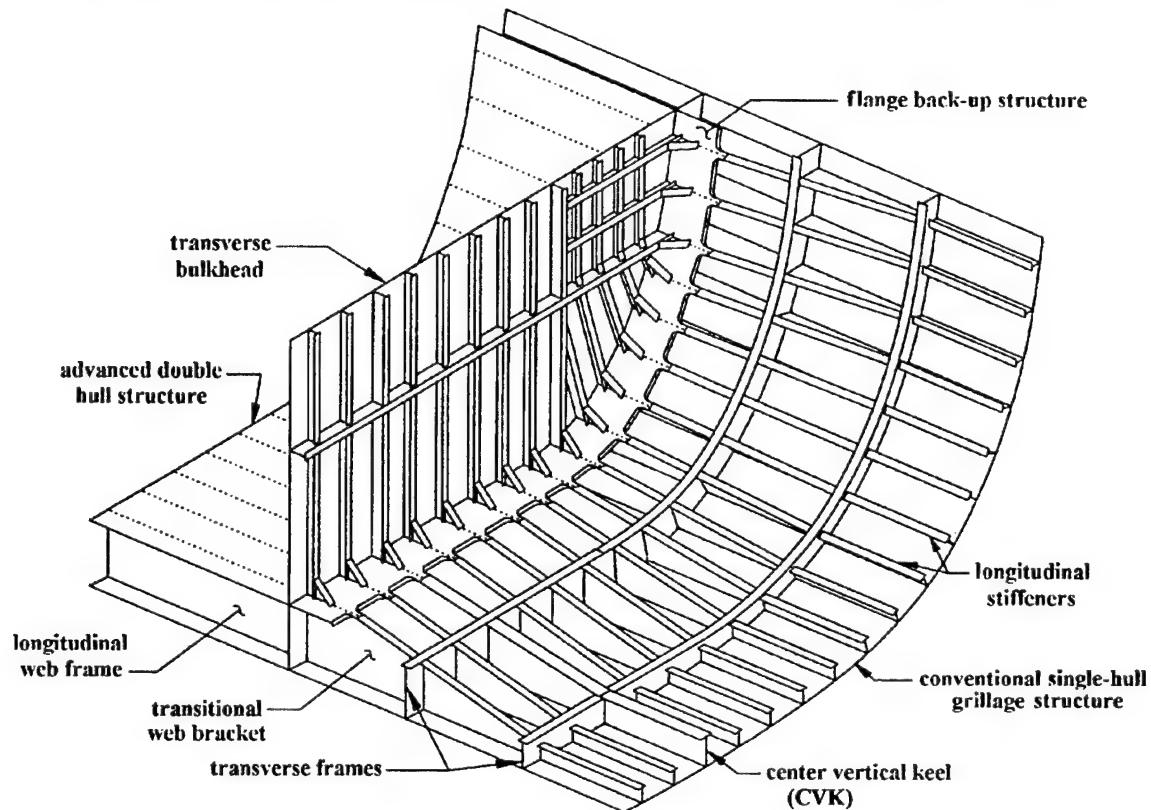
Figure 13. Typical Double Hull End Transition
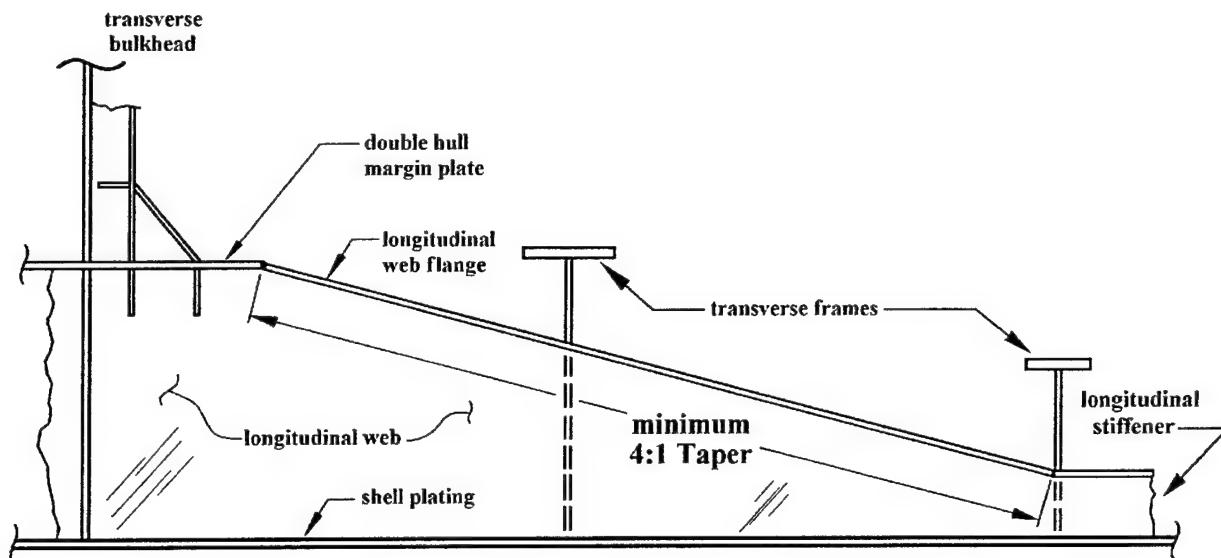
Figure 14. Taper in Longitudinal Web at Double Hull/Single Hull Transition

2.2.2.11 Openings and Access

The double hull structure will characteristically require access and penetration openings in the longitudinal web frames and the shell (primarily inner shell) plating, and these openings will strongly affect the behavior of the elements (Bruchman and Atwell 1991). These openings will cause significant areas of ineffective structure and will create stress concentrations in the structure adjacent to the openings. These openings will require reinforcement through the use of reinforcing rings (coamings), insert plates, or a combination of such reinforcements.

In general, double hull openings can be classed as either longitudinal web openings or shell openings. Shell openings will principally be within the inner shell to minimize degradation of hull strength and watertight integrity. Web openings are strongly affected by primary bending stress, secondary shear stress and, to a lesser extent, secondary bending stress.

Shell openings will reduce or eliminate structure that is effective flange material of the double hull structural element. Hence, the position and orientation of the openings must be carefully selected to minimize adverse effects. In general, shell openings should be positioned along panel centerlines and longitudinal continuity should be retained to the greatest extent possible.

Longitudinally, openings should be positioned away from either the middle or ends of the double hull web elements, where secondary stresses are maximized. Ideally, openings should be situated between one-fifth and one third of the longitudinal web span where the secondary bending moment is minimized and the shear is significantly reduced. Openings within 1/8 span length of either transverse bulkhead support location should be avoided. Adjacent openings in attached web and shell elements should be longitudinally staggered. This will minimize interactions that would weaken the double hull element secondary sectional properties and will reduce possible stress concentration affects. Openings should be staggered for adjacent webs such that they occur alternately on opposite ends of the double hull span between bulkhead supports to minimize undesirable reductions in overall sectional stiffness.

2.2.2.11.1 Criteria for Reinforcement of Openings in Advanced Double Hull Structure

2.2.2.11.1.1 GENERAL REQUIREMENTS AND PROCEDURES

Fatigue cracking, local yielding, and plate instability are the three principal failure modes which must be evaluated for openings in plating.

Strength analysis is required for all advanced double hull structures, and fatigue analysis is required for all structures subjected to significant cycle stresses, such as longitudinal structures subjected to primary (hog-sag) bending. Fatigue analysis procedures are addressed in Section 3.

Reinforcing rings, used individually or in combination with insert plating, are generally required for all double hull openings with a clear opening 5 inches (125 mm) or greater in size as a means of assuring edge stability and reducing stress concentrations. An explicit stability check is required for openings lacking reinforcing rings, and additional reinforcement may be necessary.

The design procedure requires evaluation of localized stresses associated with the opening. Openings are classified as either simple or complex. Localized stresses associated with a simple opening may be assessed using closed-form solutions for stress-concentration factors (SCFs) based on the geometric characteristics of the opening and its associated reinforcements. For complex openings, FEA should be used to explicitly assess the localized stresses.

2.2.2.11.1.2 ALLOWABLE STRESS CRITERIA

Peak stresses reflect the single, extreme lifetime seaways loading developed from a probabilistic assessment based on ship characteristics, operational environment and expected operating life. These peak stresses are not to exceed the yield stress of the material, F_y, in way of the opening for the seaway primary stresses.

For openings subject to combined primary and secondary stresses or secondary stresses only, the peak stresses shall not exceed the allowable stress, F_b, of the material. However, for these assessments, only 67 percent of the seaway primary stresses shall be used when combined with secondary stresses.

2.2.2.11.1.3 DESIGN OF SIMPLE OPENINGS

Simple openings have stress gradients isolated from the superimposed effects of other openings or discontinuities and have a basic geometric shape characterized by the variables shown in Figure 15. Specifically, an opening can be considered simple if it meets the following criteria:

- It is isolated from other discontinuities, such as another opening. To be considered isolated, the opening must be separated from another discontinuity by a distance of at least 4 times the width, b, of the smaller opening.

- It uses a standard radiused configuration at the corners.

- It falls within the following ranges of geometric parameters:

$$0.10 \leq r/b \leq 0.50 \tag{2.66}$$

$$0.25 \leq a/b \leq 4.00$$

where r =   radius for the corner of the opening,

a = Opening dimension parallel to the applied stress, and

b = opening dimension perpendicular to the applied stress.

- · It is reinforced with a ring (coaming) that meets the requirements for sizing the ring.

- It is reinforced with an insert plate that meets the requirements for sizing the insert.

- It is subject to uniaxial primary stresses, in combination with conventional normal loads.
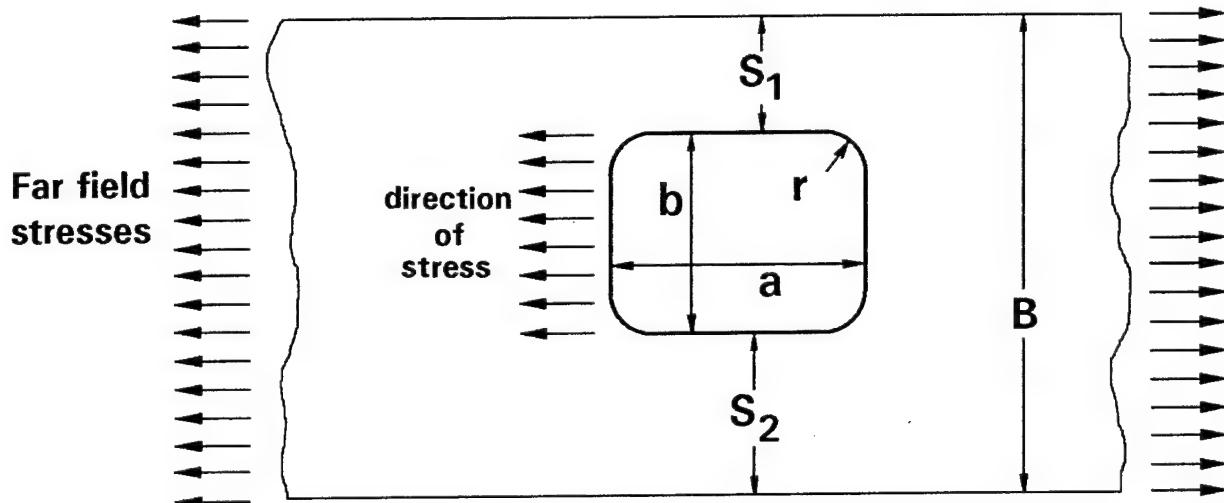
Figure 15. Characteristics of Simple Opening

Given the dimensions shown in Figure 15, the basic stress concentration factor, K_{b0}, for an unreinforced rectangular opening stressed uniaxially, in an infinite plate is determined from Figure 16.

$$SCF = K_{b0} \tag{2.67}$$

The amount that the basic stress concentration factor is reduced is based on reinforcements and possible eccentricity is provided as follows:

$$SCF = K_{b1} \; \phi \; \xi \tag{2.68}$$

where K_{b1} =   stress concentration factor for single unreinforced opening in a finite width panel. This is an adjustment of the basic stress concentration factor based on the location of the opening with respect to the distance from the structural boundary which produces the largest stress concentration.

ϕ = reduction factor if reinforcing ring (coaming) used.

ξ = reduction factor if insert plate reinforcement used.

Effects of opening configuration

The effects of the cutout and opening eccentricity shall be considered. Given the dimensions in Figure 15, the equations provided below adjust the stress concentration factors for these effects:

$$K_{b1} = \alpha_1 (1 + b/S_1)^{1/2} (S_2 + 0.5\ b)/(S_2 - S_1 + (S_1^2 + S_1\ b)^{1/2}) \qquad (2.69)$$

$$K_{b2} = \alpha_2 (1 + b/S_2)^{1/2} (S_1 + 0.5\ b)/(S_1 - S_2 + (S_2^2 + S_2\ b)^{1/2}) \qquad (2.70)$$

where, $\quad K_{b1} \quad = \quad$ the value for either forward or aft corner of opening on side S_1,

$\quad K_{b2} \quad = \quad$ the value for either forward or aft corner of opening on side S_2,

$\quad \alpha_1 \quad = \quad K_{bo} (2\ S_1/(2S_1 + b)) + (b/(2S_1 + b))$,

$\quad \alpha_2 \quad = \quad K_{bo} (2\ S_2/(2S_2 + b)) + (b/(2S_2 + b))$,

$\quad S_1 \quad = \quad$ smallest transverse distance from a structural boundary (shell or inner bottom) to the edge of the opening,

$\quad S_2 \quad = \quad$ largest transverse distance from a structural boundary (shell or innerbottom) to the edge of the opening.
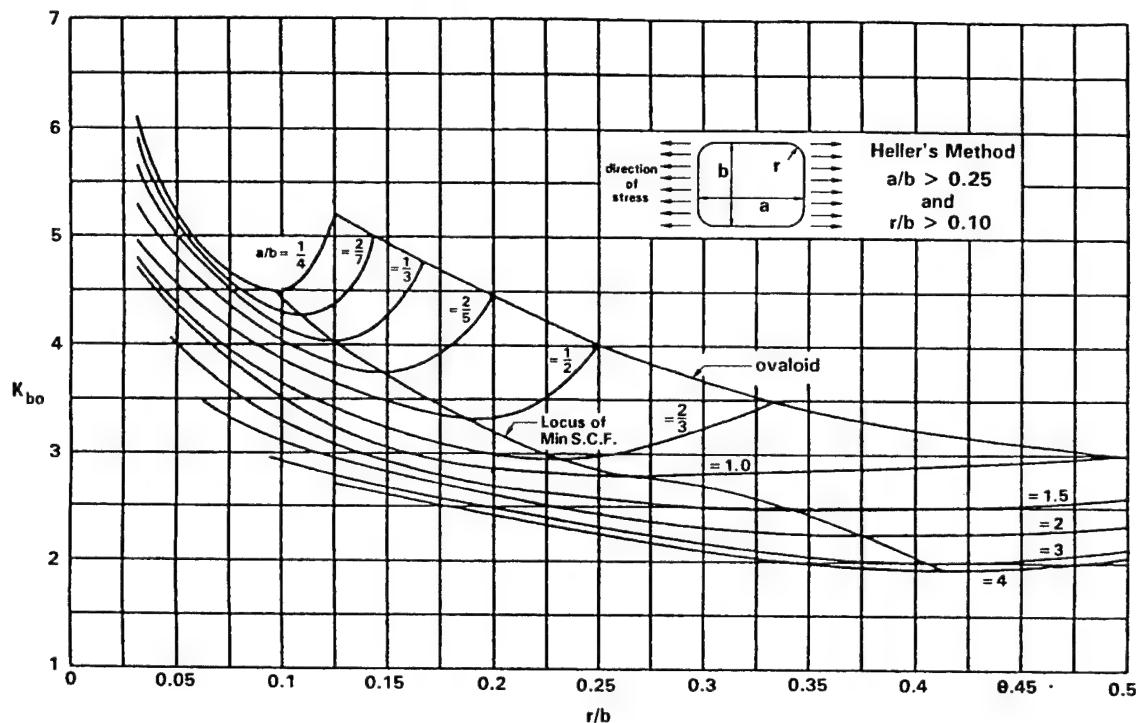
Figure 16. Basic Stress Concentration Factor, K_{bo}, for a Simple, Unstiffened Opening in Uniaxially-Loaded Plating

Effects of reinforcing rings (coamings)

Use of reinforcing rings reduces stress concentration. Reduction in the stress concentration factor due to the reinforcing ring is provided by the reduction factor, ϕ, as follows:

$$\phi = F_s F_n \phi' \qquad (2.71)$$

$$\phi' = F_l \left[2.0369 \left(\frac{r}{b} \right)^3 - 1.7668 \left(\frac{r}{b} \right)^2 - 0.044 \left(\frac{r}{b} \right) + 0.7584 \right]$$
where $\qquad (2.72)$

36

r = opening corner radius, inside of reinforcing ring,

b = opening dimension, inside of reinforcing ring, perpendicular to the applied stress,

F_t = stress reduction factor for thick coaming

= 1.0 if $t_c/t_w < 1.2$ (2.73)

= 0.96 if $t_c/t_w \geq 1.2$

t_c = thickness of reinforcing ring (coaming),

t_w = thickness of web or insert plate, if present,

$$F_n = 1 + \left(\frac{1-\phi}{\phi}\right)\left(\frac{8-\alpha_c}{7}\right)$$

(2.74)

α_c = lesser of h/t_c or 8.0,

h = width of reinforcing ring (coaming),

F_s = symmetry factor,

= 1.0 if reinforcing ring symmetrically aligned,   (2.75)

= 1.25 if reinforcing ring asymmetrically aligned.

    As general guidance, the thickness of the reinforcing ring (t_c) should be set between 1.0 and 1.2 times the thickness, t_w, of the web plate or insert plate. The width (h) of a reinforcing ring should generally not be less than 8.0 t_c. However, increasing the width of the coaming beyond 8.0 t_c does not lead to significant further reduction in stress concentration. Therefore, a reinforcing ring width of 10.0 t_c is recommended so that any in-service nicks and gouges along the edge of the reinforcing ring are out of the area of highest stress. To the greatest extent possible, the reinforcing ring should be symmetrically welded about the insert plate. Fatigue considerations require that coaming welds be 100 percent efficient full penetration welds. Reinforcing ring butt welds should be positioned in areas of minimum stress away from the stress concentrations.

    For evaluation of fatigue stresses, the coaming fillet welds are Category B details and any coaming butt welds are Category C details, as outlined in Section 3.

Effects of Insert Plates

    Further stress reduction in areas of high stress concentration can be achieved through the use of insert plates. The insert plate SCF reduction factor, ξ, is provided as follows:

$$\xi = 1 - \frac{\left(\frac{t_i}{t_p} - 1\right)}{3}$$

(2.76)

where t_i = thickness of the insert reinforcement plating,

       t_p = thickness of the parent plating.

As general guidance, insert plates may range from single, limited corner inserts to full-opening compensating inserts. Insert plates are not intended as an optional replacement for reinforcing rings, but are intended as a means of complimenting the reinforcement ring, primarily in situations where the stress reduction provided by the reinforcing ring is insufficient. Insert plates should be configured with butt welds in minimum stress areas well away from regions of stress concentration, and all welds must be 100 percent efficient, full-penetration welds. For fatigue stress evaluation, these butt welds are Category C details, as outlined in Section 3. In general, insert plates are to be continuously beveled along butt joints with the parent web plate to permit a smooth and continuous transition. This bevel should have a slope of 1:3 or less to minimize localized stress concentrations associated with the butt weld.

Stability Requirements

The presence of an opening in plating introduces a free edge, which weakens the plate. The plating adjacent to the opening shall be checked for adequate stability to preclude buckling. For adequate stability, the stress in the plating shall be less than the critical buckling stress. The edge of an opening parallel to the direction of primary stress shall also meet local stability requirements as an outstanding flange where the adjacent plating is considered as a free edge, or as a web with a reinforcing ring supported edge. A reinforcing ring, insert reinforcement or panel stiffening, or a combination of these alternatives may be used to increase buckling strength or maintain local stability.

2.2.2.11.1.4 STRESS RESULTS

The far-field stress from a finite element model is that stress where the change or slope of the stress gradient is negligible. With increasing distance from the opening, the rate of change in the stress gradient will decrease and eventually level off. This is the start of the far-field stress region. The SCF is calculated from the results of the finite element analysis by calculating the ratio of peak stress to far-field stress as follows:

$$SCF = \text{Maximum principal stress} / \text{Far-field stress} \qquad (2.77)$$

where the far-field stress is the uniform axial stress remote from the opening, or the stress, which would occur if the opening was not there.

2.2.2.11.1.5 DESIGN OF COMPLEX OPENINGS

Structural openings are classified as complex if they do not meet the requirements for simple openings as given in 2.2.2.11.1.3 Design of Simple Openings, above. Areas of the double hull that have complex stress fields, a complicated geometry, or a combination of the two effects would fall into this category. Finite element analysis is recommended for this sort of configuration, using a model that accounts for all possible geometric parameters and appropriate combined loads.

2.2.2.12 Transverse Panel Stiffeners

Plating design for the double hull panels, particularly those of the inner hull, is often governed by the high compressive secondary stresses. As can be seen in Figure 17, the highest secondary compressive stress for the inner hull occurs at the supports with the bulkhead, and is maximized in a fairly narrow band. As a result, this may force a severe thickness requirement on the inner hull plating which is overly conservative for most of the plating span. The governing effects are buckling and ultimate strength, both of which are strongly impacted by reductions in

plating span lengths. One alternative is to employ a local insert plate adjacent to the transverse bulkheads, leaving the most of the plating at acceptable thinner thicknesses.

By reducing the plating span, the buckling and ultimate strength can be significantly increased, thus reducing the plating thicknesses. One effective method of reducing the span length is to apply transverse plate stiffeners at sufficiently close intervals to partition the panel into sub-panels with the reduced span. Examples of such transverse stiffeners are shown in Figure 17. As can be seen, they are only applied in the end region where the compressive stresses are most severe. In this example, the stiffeners are sniped to preclude interaction at the panel boundaries. These stiffeners do not carry significant loads but effectively provide lines of support which greatly strengthen the plating in these regions. Because the span of these transverse stiffeners is so short, they can generally be specified as small bar stiffeners, which will have only a minor weight and producibility impact.
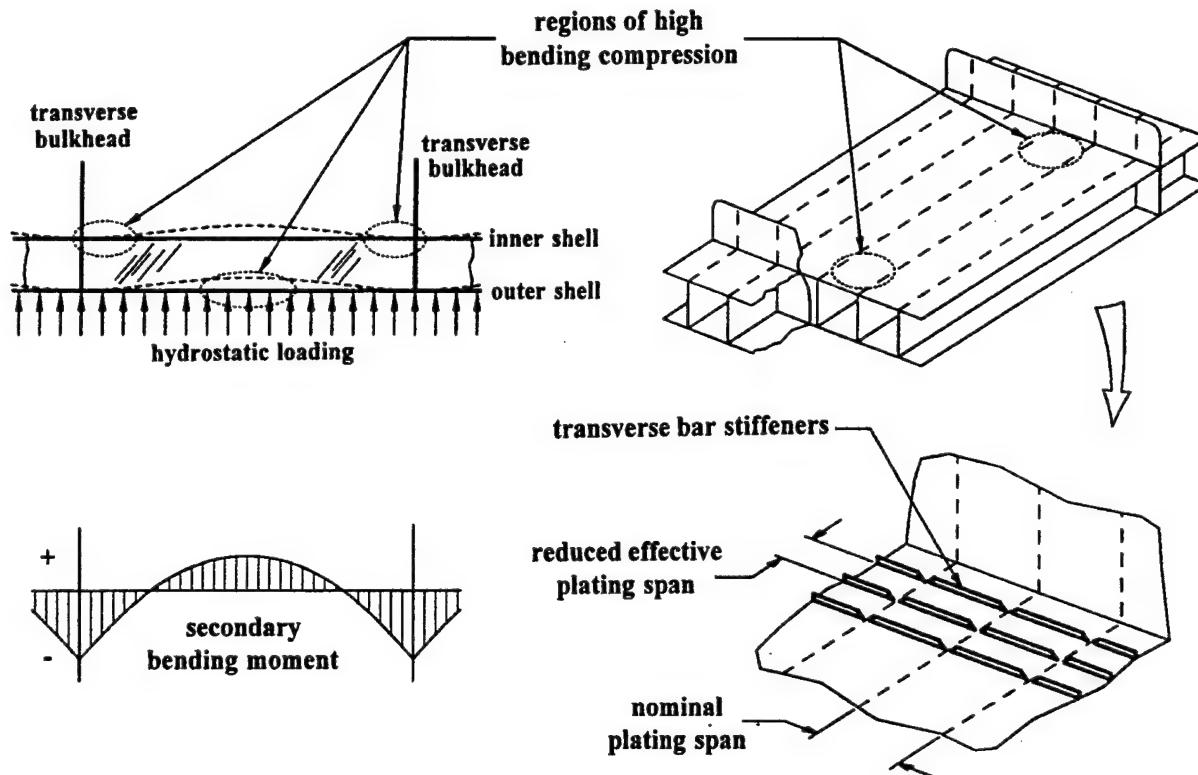
Figure 17. Transverse Panel Stiffener Concept for Inner Hull Plating

2.2.2.13 Deck Grillage Transitions and Advanced Deck Concepts

In many situations, it may be necessary to develop an advanced double hull ship with a conventionally stiffened main deck or interior decks. The deck configuration is often governed by spacing requirements that may preclude the use of a double deck. This will tend to have a greater depth requirement since it has fewer transverse frames, and results in much longer secondary spans. Thus, the designer may be forced to maintain the conventional deck, characterized as a grillage of transverse frames supporting longitudinally stiffened plating.

Conventional design philosophy requires transverse deck frames to be continuous with side shell frames and transverse bottom structures, and discourages discontinuous frame structures, which are viewed as sources of stress concentration and fatigue crack initiation. This design philosophy precludes the advanced double hull, as it has had its frames eliminated. Even a system of transitional partial frames, just around the deck intersections with the double hull would lead to structural complexity which would negate the advantages of the ADH concept.

Based on a series of scale-model tests and numerical studies conducted to evaluate the transitioning of conventional deck grillages into ADH structures, it was found that deck frames could be simply and abruptly fillet welded to the sides of the ADH cells, with essentially no backing structures or bracketing. Although it is recommended that the abrupt deck frame joint be applied in the preliminary design stages for joining conventional deck grillages to ADH side structures, it is strongly suggested that finite element analyses be conducted to ascertain the detail adequacy of using this deck frame joint concept.

As an alternative to double decks or conventional grillage decks, advanced deck concepts such as mechanically-fastened fiber reinforced plastics (FRP) decks or spaced-skin structural panels, such as Laser Corrugated Core (LASCOR) should be considered. These panels can either be welded or mechanically fastened to a margin plate along the boundary with the ADH inner hull.

3.0 Fatigue

The basis for practical fatigue strength assessment methodology easily dates back more than half a century. Although there are many fatigue damage accumulation models, some are very application oriented and difficult to adapt to situations with random loads. Still others require a number of empirical constants to be determined prior to use. Due to its simplicity and generally good predictive capability, the linear cumulative damage model (Miner 1945; Palmgren 1924) remains the method of choice and is often implemented in many engineering applications; this model is also the basis for most fatigue design codes.

Being an empirically based methodology, fatigue strength analysis or design must rely on test data to make predictions of fatigue behavior under service conditions. Much early fatigue data, considered only constant amplitude loadings; service loadings were often represented by a piecewise collection of constant amplitude block loadings. Fortunately, technology has improved over recent years to facilitate computer-controlled fatigue testing, enabling many types of variable amplitude loadings, including random amplitude loadings, to be investigated. Generation of such data is vital for comparison with predictions. Still, predicting the fatigue strength of welded ship structure can be difficult and often imprecise for several reasons.

Before proceeding, it is important to discuss the distinction between fatigue design and fatigue analysis. This document is concerned with fatigue design. Fatigue design employs

principles and applicable methodologies to perform a structural design against fatigue failure at an acceptable level of risk during the projected life of the structure. Input parameters may not accurately reflect actual values, but rather may be conservatively estimated. The projected operational profile is generally not known precisely, nor are the as-built cross-sectional properties and local imperfections. At this stage, one must make educated guesses at the fabrication quality, area of operations, and the behavior of the structure under load. The final product may in fact turn out to be better than expected, since some parameters may have been based on worse case scenarios. Fatigue analysis on the other hand usually involves defining input parameters as accurately as possible, so that the results reflect the actual behavior of the structure.

3.1 Background Guidance

Fatigue is the accumulated, irreversible damage in a structure that results from exposure to cyclic or oscillating stresses. The levels of stress necessary to cause fatigue damage can be very low, easily within the normal operating range of stress.

Although unavoidable, fatigue damage can be reduced by minimizing local stress concentrations such as notches, sharp corners, and openings. Fatigue can also be reduced by following good fabrication practice to minimize undercut at weld toes, avoid misalignment in plates, use of full penetration welds in critical areas of the ship where the weld runs perpendicular to the primary stress, and proper edge preparation and reinforcement.

Double hull structure is characterized by an assemblage of intersecting plates. As such, tests were planned and conducted on specimens representing various attributes of this basic joint detail (Kihl 1994a). Other joint configurations associated with curved hull plates were also tested (Dexter and Kaczinski 1994); these and other related results are not included here but can be found in supporting documentation provided in Appendix B of Sikora (2001). Fatigue behavior on additional joint configurations can be found in many fatigue design codes (AASHTO 1989; BSI 1980).

Testing on welded steel specimens has shown that fatigue strength does not increase with yield strength, except at very high levels of applied stress. Under most applications, use of welded higher strength steels will not increase resistance to failure by fatigue.

Tests conducted on specimens subjected to random loads indicate linear cumulative damage is generally accurate in predicting fatigue life. This conclusion is more thoroughly discussed in Sikora (2001). However , there is some scatter in the predictive capability; some results are conservative, while others are non-conservative. Using a ratio of actual to predicted fatigue life and mean S-N curves (S = applied stress and N = number of cycles to failure), shows a rough, bell-shaped frequency histogram centered on unity, indicating good predictive accuracy. The existence of non-conservative predictions leads one to consider the use of more conservative S-N curves. Such S-N curves are based on the standard deviation (σ) of the data about the mean S-N curve and are associated with a specific probability of failure assuming the fatigue life data follow a log-normal probability distribution. A mean minus two standard deviation S-N curve (2.3% probability of failure) generally shifts the frequency histogram of life ratios far enough to the conservative side to minimize failure. Linear cumulative damage, and the use of a "mean-2σ" S-N curve is used by most fatigue design codes worldwide.

Fatigue endurance at a given stress level also depends on many characteristics of the joint and weld material and geometry. The following conclusions are based on a fatigue life assessment of various test specimen configurations having non-load carrying full penetration fillet welds. The various configurations exhibit some degree of relative fatigue performance. Using Rayleigh Approximation to predict the fatigue life under a narrowband loading, root mean squared (RMS) fatigue strengths associated with one thousand cycles (low cycle) and one hundred million cycles (high cycle) were calculated for each joint detail. Considering a given detail as a reference baseline configuration, ratios of the RMS fatigue strength between the baseline and any of the other configurations were calculated and tabulated for low- and high-cycle applications at a mean probability of failure. A similar table of these ratios, or influence factors, was constructed for a 2.3% probability of failure (that is, mean minus two standard deviations). Appendix B of Sikora (2001) contains these tables of influence factors enabling one to determine the relative RMS fatigue strength between two different details and draw conclusions using any configuration as a baseline. Test data and results can also be found therein.

- A series of fatigue tests conducted on welded steel specimens with varying degrees of fabrication quality (straight full penetration non-load carrying fillet welds, and straight and misaligned full penetration load carrying fillet welds) has shown that full penetration load carrying fillet welds have 60% to 90% of the fatigue strength of full penetration non-load carrying fillet welds for straight members, and 40% to 60% of the fatigue strength of non-load carrying fillet welds if the load carrying member is misaligned by half the thickness. Considering full penetration load carrying fillet welds, misalignment of the load carrying member by half the thickness reduces the fatigue strength 33% to 50% of the fatigue strength of straight load carrying members.

- The fatigue strength of straight welded steel specimens having partial penetration load carrying fillet welds is about a third that of straight full penetration non-load carrying fillet welds. Misaligned steel specimens having partial penetration load carrying fillet welds also exhibit fatigue strengths which are about a third that of straight full penetration non-load carrying fillet welds.

- Fatigue tests on structural components (bulkhead penetration details) have shown them to have about half the fatigue strength of smaller straight specimens with non-load carrying fillet welds.

- Fatigue strength of thick welded plates (3/4" and 1") with non-load carrying fillet welds exhibit a third of the fatigue strength of similarly welded thinner (7/16" and 1/4") plates. The "fourth root rule" reasonably accounted for this effect.

- Fatigue tests on welded steel specimens at different mean stress levels indicate mean stress effects can reasonably be accounted for by using the Modified Goodman correction for tensile mean stresses; compressive mean stresses can conservatively be ignored, (Kihl 1994b).

- Fatigue tests conducted on full penetration cruciform specimens indicate fatigue strength under a bending load to be comparable at high stress levels and have two to three times the fatigue strength of axially loaded specimens at low stress levels.

Although these trends are observed using statistics associated with a mean probability of failure, they remain essentially the same using statistics associated with a 2.3% (mean minus two standard deviations) probability of failure.

3.2 Probability of Failure

Use of the fatigue data provided in this guide requires the designer to use appropriate factors of safety and global stress concentration factors to minimize risk of failure by fatigue. However, rather than using a factor of safety on the calculated mean fatigue life, the structure can be designed to fatigue lives associated with other, lower, probabilities of failure. To aid the designer, the mean constant amplitude S-N curve coefficients and standard deviation of the data about the best-fit straight line are provided for each of the configurations quantified. Probabilities of failure different from those considered can easily be determined by subtracting a multiple of the standard deviation from the life intercept (log(A)) parameter. Assuming a normal distribution, the standard deviation is a measure of the probability of failure. For example, two standard deviations produce a 2.3% probability of failure, three standard deviations produce a 0.1% probability of failure, and so on. Although any probability of failure can be used in design, fatigue design codes worldwide, generally use a mean minus two standard deviation S-N curve (2.3% probability of failure) for design.

Table 3 provides the S-N curve coefficients and standard deviation for various test specimen geometries and sets of data shown in Figure 18. Since this document focuses on double hull structure, the test data consist primarily of intersecting plate geometry. Data sets reflect different thicknesses, types of steel, alignment of load carrying member, and weld penetration.

$$N = 10^{\log(A)-2\sigma} S^B \qquad (3.1)$$

where B is the slope of the S-N curve.

Table 3. Fatigue S-N Curve Coefficients for Different Specimen Configurations

Steel Grade & Thickness (inch)	Component Type	Fabrication Location	Log(A)	B	Standard Deviation (σ)
HSLA80 7/16	Bending	Shipyard	13.617	-5.13	0.378
HSLA80 1/4	Continuous Cruciform	Shipyard	10.714	-4.087	0.350
HSLA80 7/16	Continuous Cruciform	NSWCCD	9.559	-3.21	0.185
HSLA80 7/16	Continuous Cruciform	Shipyard	10.432	-3.855	0.210
HSLA80 7/16	Continuous Cruciform	Shipyard & NSWCCD	9.947	-3.496	0.205
HSLA80 3/4	Continuous Cruciform	Shipyard	9.057	-3.134	0.172
HSLA80 1.0	Continuous Cruciform	Shipyard	8.389	-2.732	0.068
HSLA80 7/16	Discontinuous Cruciform	NSWCCD	9.601	-3.307	0.263
HSLA80 1/2	Misaligned Cruciform	NSWCCD	9.733	-3.949	0.227
HSLA80 1/2	Discontinuous Cruciform with Partial Penetration. Welds	NSWCCD	8.272	-2.686	0.139
HSLA80 1/2	Misaligned Cruciform with Partial Penetration Welds	NSWCCD	8.513	-3.349	0.208
High Strength 1/2	Continuous Cruciform	NSWCCD	11.289	-4.486	0.218
High Strength 1/2	Discontinuous Cruciform	NSWCCD	9.648	-3.417	0.252
High Strength 1/2	Misaligned Cruciform	NSWCCD	12.902	-6.416	0.142
Ordinary Steel 1/2	Continuous Cruciform	NSWCCD	10.566	-3.987	0.221
Ordinary Steel 1/2	Discontinuous Cruciform	NSWCCD	10.185	-3.752	0.304
Ordinary Steel 1/2	Misaligned Cruciform	NSWCCD	10.541	-4.924	0.149
HSLA80 & High Strength	Component	Shipyard & NSWCCD	9.192	-3.263	0.214

Effect of Applied Loading
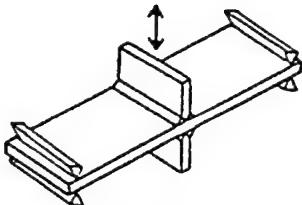
(A) Bending load (R = -1) applied to continuous cruciform.
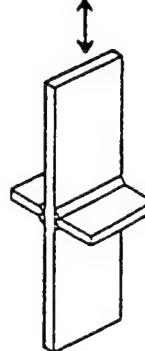
(B) Axial load (R = -1) applied to cruciforms having various attributes.
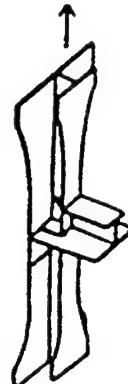
(C) Axial load (R = 0) applied to structural component, (shown in greatly reduced scale).

Effect of Fabrication Quality
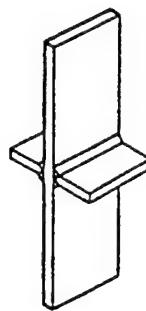
(D) Full penetration, no-load carrying fillet welds. Continuous member loaded
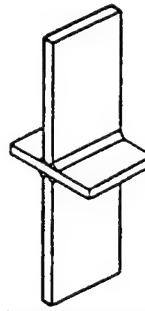
(E) Full penetration, load carrying filled welds. Discontinuous member loaded.
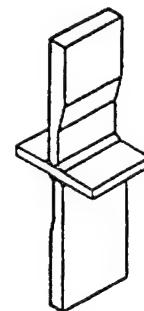
(F) Full penetration, load carrying filled welds. Misaligned member loaded.

Effect of Partial Weld Penetration
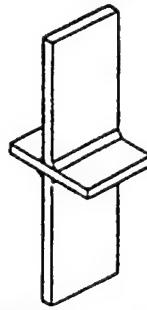
(G) Partial penetration, load carrying fillet welds. Discontinuous member loaded.
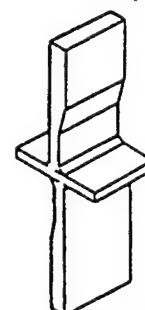
(H) Partial penetration, load carrying fillet welds. Misaligned member loaded.

Figure 18. Structural Details Pertaining to Double Hull Ship

3.3 Rules

To perform a fatigue design on ship structure, cyclic loadings that will act on the ship over its lifetime must either be estimated or assumed. The following method to determine global wave induced lifetime sea loads on ships is well documented and has been successfully used in many naval combatant designs and analyses (Sikora, Dinsenbacher, and Beach 1983). The method involves the use of longitudinal vertical bending moment response amplitude operators (RAOs) to quantify the ship's hull girder bending response per unit wave height for desired speeds and headings. Probabilities of occurrence of sea state, heading and speed must also be defined. This approach produces a lifetime fatigue load spectrum associated with a given time at sea. With an appropriate S-N curve and load to stress conversion, linear cumulative damage calculations are performed to determine the fatigue life at a given point on the ship. The method is outlined below.

1. Define the service life, percent operability (percent time at sea), and overall dimensions of the ship, that is, length between perpendiculars and beam amidships. The service life and percent operability are used to determine the time at sea. Ship dimensions may be used to generate RAOs from empirically based algorithms, if not available from other sources such as analytics or test data. RAOs are required for each of the speed and heading combinations chosen in the next step.

2. Define an anticipated operational profile consisting of the percentage of the ship lifetime that the ship is expected to operate at various speed, heading, and sea conditions. This information is used to calculate the time spent in each specific operating condition and is also used to determine the number of load cycles in each condition from the average encounter frequency. Typically, three speeds and four headings are considered for operations in low, medium and high sea conditions. An example of an operational profile is shown in Table 4.

    The time spent in each operating condition can be determined from the following equation.

    $$T_i = T_y \times P_1 \times P_2 \times P_3 \qquad (3.2)$$

    where T_y =   lifetime at sea,

    P_1 =   ship heading and speed probability,

    P_2 =   wave height probability, and

    P_3 =   wave spectral probability.

3. Select appropriate sea spectra to represent the wave conditions in the proposed region of operation and define wave height probabilities of occurrence. For example, sea spectra defined by the Ochi 6-parameter family of spectra can be used (Ochi 1978). Considering eleven bands of modal frequency (each with a given probability of occurrence) for the North Atlantic, and sixteen values of significant wave height produces 176 wave spectra. Together with perhaps twelve speed and heading combinations (RAOs), produces 2112 response spectra obtained by multiplying each wave spectrum times each RAO. Examples of wave height probabilities are shown in Table 5.

Table 4. Operational Speed and Heading Probabilities

a) Low Sea States (0-5 meters)

Relative Heading	Speed (knots)		
	5	15	25
Head (0°)	0.0125	0.0875	0.025
Bow (45°)	0.025	0.175	0.050
Beam (90°)	0.025	0.175	0.050
Stern Qtr. (135°)	0.025	0.175	0.050
Following (180°)	0.0125	0.0875	0.025

b) Medium Sea States (5-10 meters)

Relative Heading	Speed (knots)		
	5	15	25
Head (0°)	0.025	0.023	0.0025
Bow (45°)	0.375	0.338	0.038
Beam (90°)	0.023	0.020	0.005
Stern Qtr. (135°)	0.050	0.045	0.005
Following (180°)	0.025	0.023	0.0025

c) High Sea States (>10 meters)

Relative Heading	Speed (knots)		
	5	15	25
Head (0°)	0.020	0.0	0.0
Bow (45°)	0.808	0.142	0.0
Beam (90°)	0.0	0.0	0.0
Stern Qtr. (135°)	0.022	0.008	0.0
Following (180°)	0.0	0.0	0.0

4. Assuming the response processes are zero mean, narrowband, and Gaussian, the area under each response spectrum is the process variance, E (the mean squared value of the response). This parameter defines the distribution of load magnitudes that can be described by a Rayleigh probability function. The number of cycles contained in each response condition is determined by multiplying the time spent in the "ith" condition, T_i, by the average encounter frequency for that condition, $\overline{\omega}_{ei}$.

$$\overline{\omega}_{ei} = \sqrt{\frac{\sum\limits_{k} A_k \omega_{eik}^2}{\sum\limits_{k} A_k}}$$

(3.3)

where A_k =   area under an increment of the response function.

Table 5. Frequency of Occurrence of Various Sea States in the North Atlantic

Significant Wave Height (meters)	Frequency of Occurrence (NATO N. Atlantic)	Frequency of Occurrence (Atlantic, Station I)
<1	0.087	0.0503
1-2	0.192	0.2665
2-3	0.220	0.2603
3-4	0.157	0.1757
4-5	0.124	0.1014
5-6	0.080	0.0589
6-7	0.052	0.0346
7-8	0.039	0.0209
8-9	0.025	0.0120
9-10	0.013	0.0079
10-11	0.007	0.0054
11-12	0.004	0.0029
12-13	0.000	0.0016
13-14	0.000	0.00074
14-15	0.000	0.00045
>15	0.000	0.00041
	Total = 1.000	Total = 1.000

However, the encounter frequency must first be determined in terms of the wave frequency, ω, and the ship speed and heading.

$$\omega_e = \left| \omega + \frac{\omega^2}{g} V \cos\theta \right| \tag{3.4}$$

where, ω_e = encounter frequency

g = gravity constant (in consistent units with V)

V = ship speed

θ = ship heading = (0° head seas, 45° = bow seas, 90° = beam seas)

The number of cycles, n_i, exceeding a given magnitude, y, can be calculated for each response, (variance, E_i, and applied cycles, N_i), and summed over all the responses. By considering many different magnitudes and calculating the cumulative number of cycles exceeding that magnitude, a bending moment exceedance curve can be generated.

$$n_i = N_i e^{-y^2/2Ei} \tag{3.5}$$

5. Having calculated the primary (longitudinal vertical) bending moment exceedance curve, which results from exposure of the ship to the operational profile defined above, offset the

exceedance curve by the still water bending moment amidships, if known. The difference between cycles exceeded at adjacent points on the bending moment exceedance curve is the number of cycles contained in each increment. The corresponding bending moment amplitude is the average of the two bending moment magnitudes. This operation produces a histogram of bending moment amplitude and cycles applied over the life of the ship.

6. Select a candidate connection detail and generate a plot of midship section modulus (or design stress) versus fatigue life for the desired probability of failure, using linear cumulative damage calculations and fatigue data (in terms of an S-N curve) which best reflects the actual structure. Different probabilities of failure are associated with the S-N curve chosen and the number of standard deviations considered. Appropriate global stress concentration factors should be applied to properly compare service stress and stress applied to test specimens used to generate the fatigue data.

7. Select the minimum section modulus (or maximum design stress under a design bending moment) required to meet the desired level of reliability (probability of failure) and service life. Iteration between alternative details and corresponding fatigue data may be required as the calculations converge to an acceptable solution. The RMS fatigue strength ratios provided in Sikora (2001) may be of use in considering alternative details.

8. Check design stress levels against buckling and other strength criteria for consistency and repeat for other stations, as necessary (Sikora et al. 1995).

4.0 Foundations

4.1 Background

Historically, Navy foundations have been designed from shock considerations. The shock analysis method used the "Shock Design Factors" that consist of three curves of weight versus acceleration design numbers. This approach provided the analyst with a simple design methodology that was based on shock test results. The foundations resulting from this approach had heavy plate weldments with extensive manual fabrication operations and significant amounts of continuous, multi-pass welding. As a result, foundations designed by this approach were high in weight and high in cost. More recently, a foundation design approach using dynamic shock inputs for the mounted equipment and structural flexibility in the foundations has been developed. The Dynamic Design Analysis Method (DDAM) methodology takes into account the flexibility of the foundation structure to attenuate and reduce the shock loads. The DDAM approach has resulted in lighter foundation weights and reduced construction costs. Even with these advances, foundations are very labor intensive and cost ten times as much per ton to make as ordinary hull structure. Since over 200,000 labor hours are required to fabricate and install the foundations on a typical destroyer, further improvements can have significant cost savings.

Since the ADH structure is significantly different from conventional ships, it was not obvious whether foundations would be more or less difficult to design, fabricate, and install. Therefore, a three-pronged program was undertaken to develop design criteria for the foundations on ADH ships:

- First, the performance requirements were identified. A critique of current design methodologies was performed and an evaluation of the specifications, standards, and experimental backup data was conducted. The performance requirements, design criteria and allowables, construction tolerances and alignment constraints were all identified for a typical destroyer/cruiser.

- Next, candidate foundations were selected to include representatives supporting heavy weight, medium weight, and lightweight equipment. Ship motion analyses were performed on a typical destroyer/cruiser to generate the input loads for the foundations. Analyses were conducted on over 100 foundations to generate the loads on hull-to-foundation attachment details to ensure appropriate deflection and stress levels. They also identified stiffness characteristics of the combined foundation and hull structure to evaluate vibration performance.

- Finally, extensive tests were conducted to validate the fatigue performance of the structural details under cyclical axial, bi-axial, and bending loads. Based on the results of the fatigue testing, S-N diagrams were developed to assess fatigue resistance. Finite element analyses were conducted to determine stress concentrations for the candidate foundation details. These stress concentrations were included with extreme seaway loadings to complete the fatigue assessments and validation of the proposed foundation design methodology.

As a result of these studies, the proposed design guidelines presented in the following section were developed. These guidelines can result in a number of benefits. It was found that ADH foundations can be located at the optimum locations for the equipment rather than being dependent on the existing structure as on conventional ships. This greatly simplifies the design, drawing, and engineering costs of both the foundations as well as the electrical and piping arrangements and connections for the equipment. Furthermore, far fewer brackets and backup structure were needed for the ADH foundations. There is a reduction in re-work because of the fewer pieces and the use of fewer, common designs. The fewer pieces result in reduced logistics, handling, and storage of components. For a number of candidate foundations, it was found that an average of 33 percent could be saved on foundation weights and 61 percent saved on welding costs. The labor savings of the more producible ADH foundations contribute to a reduced time of delivery for the ship. Therefore, foundations can be more easily designed, fabricated, and installed on ADH ships than on conventional ships.

4.2 Rules

4.2.1 Rules for Equipment Foundations

1. Choose a foundation configuration and estimate the worst-case eccentricity.

There are three types of foundations (excluding the main machinery foundations) commonly used on ships: frames, trusses, and grillages (Figure 19). A frame is the simplest and lowest cost option but has significantly greater moments at the attachments than the others. Diagonals can be added to make a truss if required to satisfy design criteria. Eccentricity can be limited with a specified tolerance and backup structure can be used to bridge longitudinal girders.

Frame   **Truss**   **Grillage**
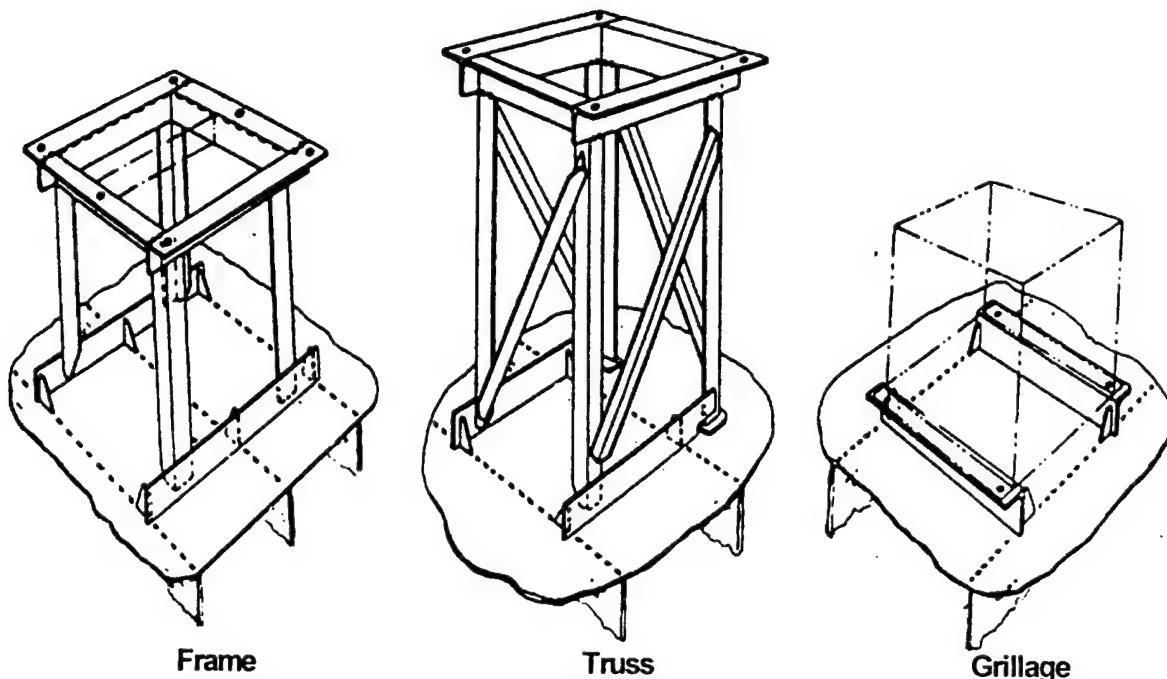
Figure 19. Types of Equipment Foundations

Select a foundation configuration and develop a "first cut" sketch of the foundation. Develop an initial design drawing, as in Figure 20, showing the attached equipment and any system interferences that must be accommodated. Incorporate producibility considerations: (1) square cuts of angles and bars are the most producible, (2) fillet weld the angle sections directly to the inner hull plating without necessarily landing them over the web girders, (3) eliminate backup structure where possible.

The shock requirements for grillages supporting alignment-critical items limits the maximum equipment weight to about 400 pounds. For equipment that is not alignment-critical, the shock requirements allow equipment weight up to 2200 pounds. The allowable equipment weight for grillages is not typically limited by vibration or fatigue. Therefore, grillage-type foundations can be landed almost anywhere on the double hull and would meet all applicable criteria without the use of backup structure.

The maximum equipment (alignment critical) weight determined by shock requirements for narrow frames (less than 13 inches) without backup structure is: (1) 300 pounds when the eccentricity is 1.4 inches, (2) 200 pounds when the eccentricity is 2.4 inches, and (3) 350 pounds at 18-inch, or mid-panel, eccentricity. The maximum equipment weight for wider frames (greater than 34 inches) without backup structure is (1) 1100 pounds when the eccentricity is 1.4

inches, (2) 380 pounds when the eccentricity is 2.4 inches, and (3) 700 pounds at mid-panel eccentricity.
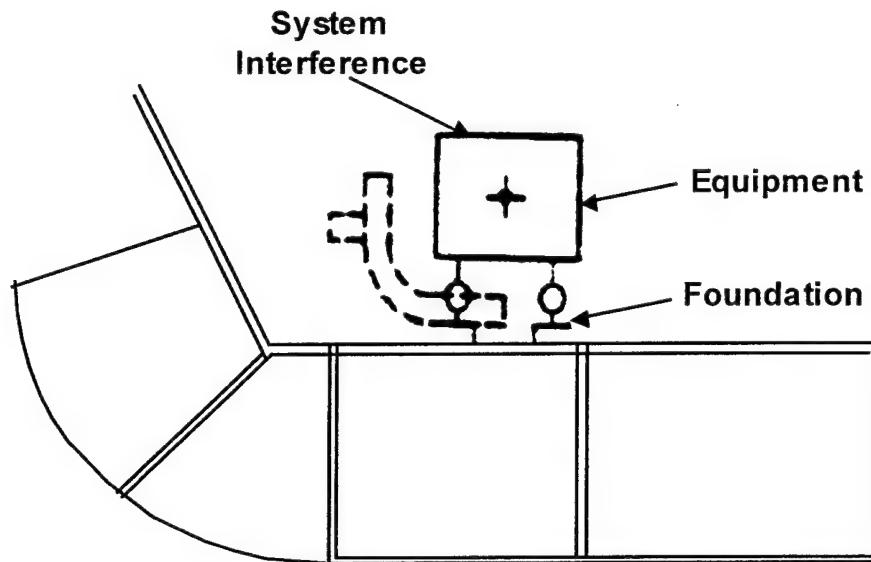
Figure 20. Integration of Foundation Design with Equipment and Ship

2.   Calculate the effective root mean cube (RMC) acceleration in both the vertical and lateral directions.

Table 6 and Table 7 summarize the RMC accelerations for a typical destroyer/ cruiser at ten locations on the ship. A seakeeping analysis should be performed for other ship types. Also included in the tables are the numbers of lifetime acceleration cycles to be used in the fatigue calculations for the foundations. To calculate the effects of slamming as a parameter of slamming severity, the number of cycles are multiplied by a cycle-per-slam ratio of 1 to 5 while the corresponding accelerations are multiplied by a factor of 1 to 2.

Table 6. Foundation Vertical Accelerations

Location Point	Root-Mean-Cube Vertical Acceleration Amplitude					
	Cyc/Slam = 1	Cyc/Slam = 3	Cyc/Slam = 3	Cyc/Slam = 3	Cyc/Slam = 3	Cyc/Slam = 5
	Fac=1.0	Fac=1.0	Fac=1.25	Fac=1.5	Fac=2.0	Fac=2.0
Fwd. Perpendicular	0.239	0.244	0.250	0.256	0.270	0.292
Fr 174, CL, InBtm	0.135	0.138	0.141	0.145	0.153	0.165
Fr 174, SdSh, InBtm	0.139	0.141	0.145	0.149	0.157	0.170
Fr 174, MnDk@Side	0.141	0.144	0.147	0.151	0.160	0.174
Center of Gravity	0.088	0.089	0.091	0.093	0.098	0.106
LCG, SdSh, InBtm	0.090	0.092	0.094	0.097	0.102	0.110
LCG, MainDk@Side	0.092	0.094	0.096	0.098	0.104	0.112
Fr 346, CL, InBtm	0.076	0.077	0.079	0.081	0.085	0.091
Fr 346, SdSh, InBtm	0.075	0.077	0.078	0.080	0.084	0.091
Fr 346, MnDk@Side	0.075	0.077	0.078	0.080	0.085	0.091

Location Point	Number of Lifetime Vertical Acceleration Cycles (Millions)					
	Cyc/Slam = 1	Cyc/Slam = 3	Cyc/Slam = 3	Cyc/Slam = 3	Cyc/Slam = 3	Cyc/Slam = 5
	Fac=1.0	Fac=1.0	Fac=1.25	Fac=1.5	Fac=2.0	Fac=2.0
Fwd. Perpendicular	63.93	64.33	64.33	64.33	64.33	64.72
Fr 174, CL, InBtm	63.32	63.72	63.72	63.71	63.72	64.11
Fr 174, SdSh, InBtm	63.07	63.46	63.47	63.47	63.46	63.87
Fr 174, MnDk@Side	61.96	62.36	62.35	62.36	62.36	62.76
Center of Gravity	60.39	60.78	60.78	60.78	60.78	61.18
LCG, SdSh, InBtm	61.30	61.70	61.69	61.70	61.69	62.09
LCG, MainDk@Side	61.20	61.60	61.60	61.60	61.60	62.00
Fr 346, CL, InBtm	57.15	57.54	57.54	57.54	57.55	57.94
Fr 346, SdSh, InBtm	57.72	58.12	58.11	58.11	58.11	58.51
Fr 346, MnDk@Side	57.73	58.12	58.12	58.13	58.12	58.53

3. Calculate the stiffness coefficients of the attachments and the stress concentration factors (SCF) from thin shell finite element models.

Develop thin shell finite element models of the bottom 24 inch or more of the foundation angle support, at least one cell width of the inner bottom or side shell, and at least the same length in the longitudinal direction to simulate contiguous structure. Use an element size of 1 inch or less in the critical attachment regions. Apply unit forces and moments at the base of the angle and calculate the stiffness coefficients of the attachment and the SCF. These analyses can be performed in advance of the standard angle section at a variety of eccentricities and the results presented in graphical format or as curve fit algorithms.

52

Table 7. Equivalent Constant Acceleration Amplitudes

Root-Mean-Cube Acceleration Amplitude (G's)			
Location Point	Horizontal (without roll)	Horizontal (with roll)	Longitudinal
Fwd. Perpendicular	0.052	0.132	0.020
Fr 174, CL, InBtm	0.038	0.122	0.027
Fr 174, SdSh, InBtm	0.038	0.122	0.027
Fr 174, MnDk@Side	0.043	0.122	0.019
Center of Gravity	0.039	0.119	0.020
LCG, SdSh, InBtm	0.034	0.116	0.027
LCG, MainDk@Side	0.042	0.123	0.019
Fr 346, CL, InBtm	0.033	0.116	0.027
Fr 346, SdSh, InBtm	0.033	0.116	0.027
Fr 346, MnDk@Side	0.042	0.125	0.019
Number of Lifetime Acceleration Cycles (Millions)			
Location Point	Horizontal (without roll)	Horizontal (with roll)	Longitudinal
Fwd. Perpendicular	40.76	38.42	47.86
Fr 174, CL, InBtm	39.96	36.70	51.28
Fr 174, SdSh, InBtm	39.96	36.70	51.11
Fr 174, MnDk@Side	37.15	35.30	53.92
Center of Gravity	37.22	34.74	47.86
LCG, SdSh, InBtm	38.44	36.35	50.52
LCG, MainDk@Side	37.12	35.13	54.07
Fr 346, CL, InBtm	37.73	35.95	51.28
Fr 346, SdSh, InBtm	37.73	35.95	50.54
Fr 346, MnDk@Side	38.78	36.30	54.07

4. Analyze the foundation as a beam model with a concentrated mass at the center of the equipment.

Determine the mass of the foundation and the equipment. Calculate the stiffness of the attachments from the finite element shell model (Rule 3). Where distortion of the ship structure under hydrostatic load is probable, estimate possible differential displacements between longitudinal girders. Use a simple beam model to assess the member forces from differential displacements.

5. Use the beam model to calculate the resonant frequency.

The following equation may be used to calculate the resonant frequency. To avoid excitations, the resonant frequency must be greater than 1.25 times the maximum blade (propeller) rate frequency; for example, greater than 15 Hz for the destroyer/cruiser. For foundation attachments with limited eccentricity relative to the longitudinal girders, the vibration

criteria need not be applied in the forward two-thirds of the ship. However, all foundations on unsupported plating should be checked against these criteria.

The system natural frequency in radians/second is given by:

$$\omega = (Kg/W)^{1/2}$$

where K is the spring constant and g/W is the reciprocal of the mass. A plot of displacement for a simple spring-mass system times a scaling factor as a function of the system natural frequency is termed a "shock spectrum" and is usually specified for Navy shipboard equipment in terms of $X\omega$.

The width of the foundation and position of the legs relative to the longitudinal web members significantly affect the frame's natural frequency. Foundations that have one set of legs landing in the center of the panel and the other set of legs near the center of another panel will have the lowest natural frequencies. For items mounted in the center of the panel, the vibration natural frequency will be governed by panel stiffness. Foundation members can bridge across the panel to increase the foundation natural frequency where required.

6. Multiply the accelerations by the equipment mass plus one half of the foundation mass to estimate shock forces and associated nominal stresses in the member.

Obtain shock accelerations from DDS-072, following NAVSEA 0908-LP-000-3010 (Naval Sea Systems Command 1977). Use the beam model to calculate member forces. Check the shock forces in compression with respect to allowable reaction forces from the web crippling design equations. Multiply nominal stress by SCF to estimate the peak stress due to shock. (The shock criteria are very uncertain in this application.) If the structure is alignment critical, this maximum stress is limited to the yield strength. For non-alignment-critical structure, the limiting shock stress is two times the yield strength.

The web failure modes arise from patch loads centered on a web member and consist of web crippling, web yielding, and shear buckling of the web. The American Institute of Steel Construction (AISC 1991)) design curves (Figure 21) are to be used to calculate web strength for foundations (a single patch load centered over a longitudinal web member) and dry-docking loads (a patch load centered over two or more longitudinal web members).

7. Compare the root mean cube (RMC) peak stress range to the fatigue strength at the lifetime number of cycles.
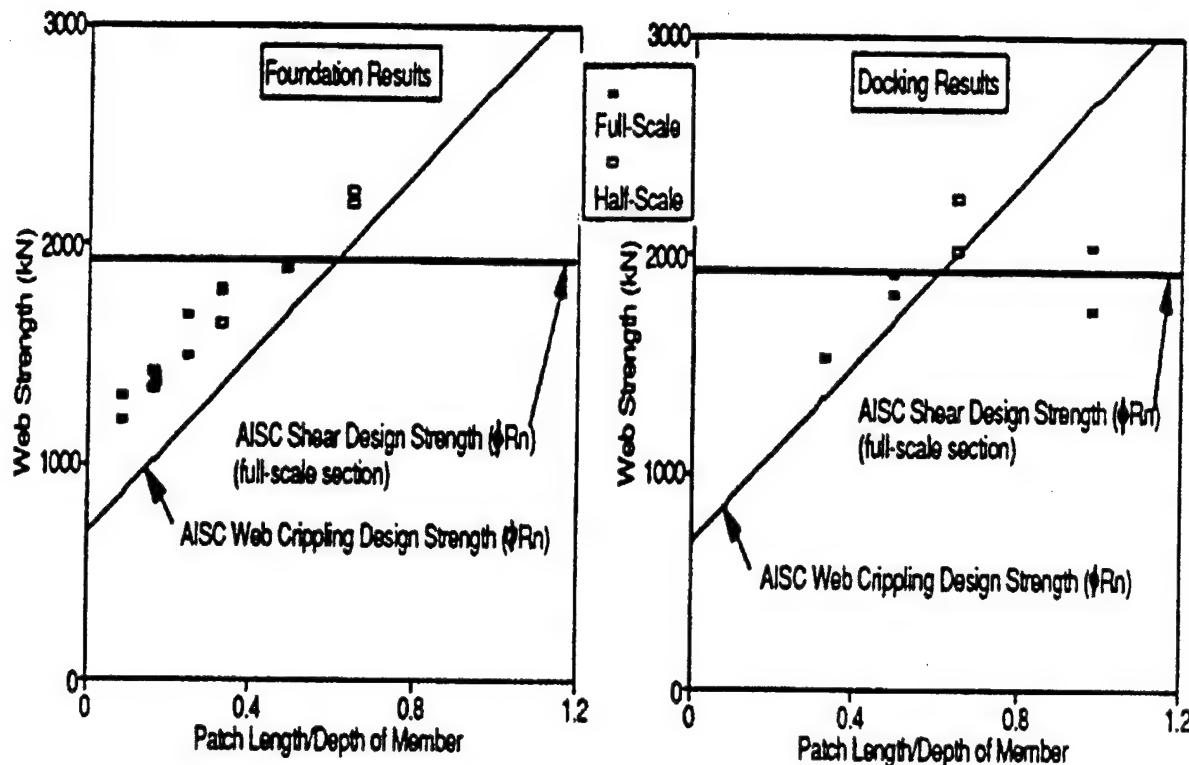
Figure 21. Web Crippling Strength Curves (AISC 1991)

For both the vertical and lateral accelerations, multiply the RMC accelerations amplitudes by the mass (equipment plus one half of the foundation mass) and estimate the RMC force amplitudes. Obtain the RMC member forces from the beam model, calculate the RMC nominal stress range (double the amplitudes), and multiply by the SCF to obtain the RMC peak stress range. Use the larger of the RMC peak stress range resulting from either the vertical or lateral accelerations; that is, do not combine the accelerations or the resulting stress ranges. Compare the RMC peak stress range to the fatigue strength at the number of cycles appropriate to the lifetime at sea. If the lateral accelerations govern (as is typical), the fatigue strength at 60 million cycles (for a thirty year life) of 4.7 ksi (32 MPa) is used as the limiting RMC stress range. (It was found from several sensitivity studies that variations in the number of cycles do not significantly change the fatigue strength.) If vertical accelerations govern, the fatigue strength at 100 million cycles (for the same thirty year life) of 4 ksi (28 MPa) is to be used.

The AASHTO (1989) Category C S-N curve, shown in Figure 22 is to be used in the fatigue analysis. This curve (which is the same as the AISC or the American Welding Society (AWS) Category C) represents the fatigue strength of a transverse weld when failure results from a crack at the weld toe. The loading and stress analysis can be considered independently because the stresses in the orthogonal direction were not found to influence the fatigue life.
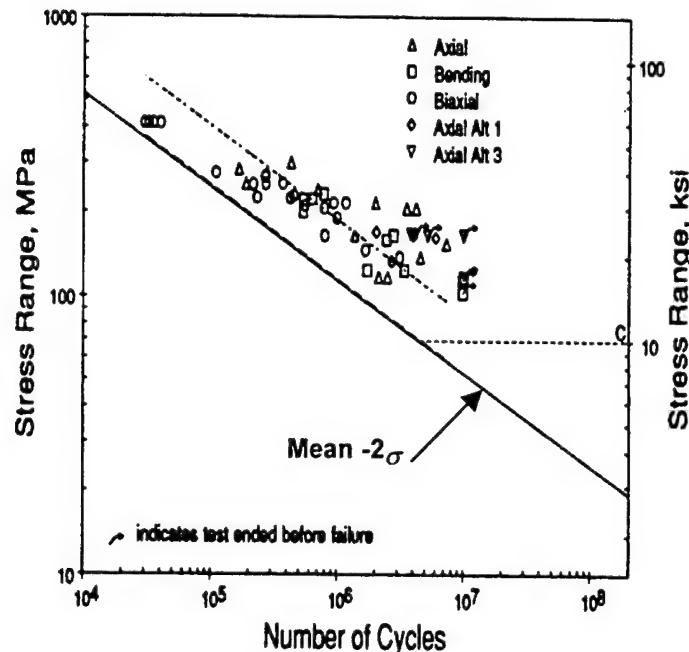
Figure 22. AASHTO S-N Curves (AASHTO 1989)

4.2.2 Rules for Propulsion Plant and Main Machinery Foundations

The very large foundations supporting the propulsion plant and main machinery are tied into the primary hull structure to such an extent that an analysis of the entire compartment is needed. The hydrostatic and hydrodynamic pressure loads cause local structural deformations in addition to the overall hull girder deflections. In order to consider the interaction of these effects on the foundations, a comprehensive finite element model of the entire compartment and the machinery foundations must be performed.

1. Generate the finite element models of the hull structure of each machinery room compartment without the equipment foundations.

The mesh size should be sufficiently fine such that there are at least two elements in the depth of the longitudinal web members and at least one element on the inner and outer shell plating between longitudinal members. Longitudinally, the length of the elements should be approximately equal to the web spacing. Next, assess the basic structural behavior of the compartments under hydrostatic loading.

The structural behavior of the ADH ship can be quite different from that of a conventional ship because of the absence of transverse web frames. The vertical deflection of adjacent longitudinal web girders can be independent of each other because there is no shear connection.

2. Add the large machinery foundations to the finite element models of each compartment.

The element mesh size for the foundations should be of comparable size to those in the hull structure. All beds, pedestals, and brackets should be included in the foundation model; see Figure 23. Model the piping attached to the machinery mounted on the foundations to include

the piping loads from hull girder bending induced on the foundations. Assess the potential for shaft alignment problems due to hull deflection under hydrostatic loading, deadweight loads, and thrust and torque loads on the shaft.

The differential flexure between longitudinal web girders in the ADH may pose problems for some of the foundations and attached piping. Additional stiffening to relieve these problems can be achieved by employing large foundation rafts or by adding ring frames to the inside of the inner shell. In the destroyer/cruiser examples evaluated, a modest tee-beam was sufficient as a ring frame (an 8" x 3/8" web with an 8" x 5/8" flange).
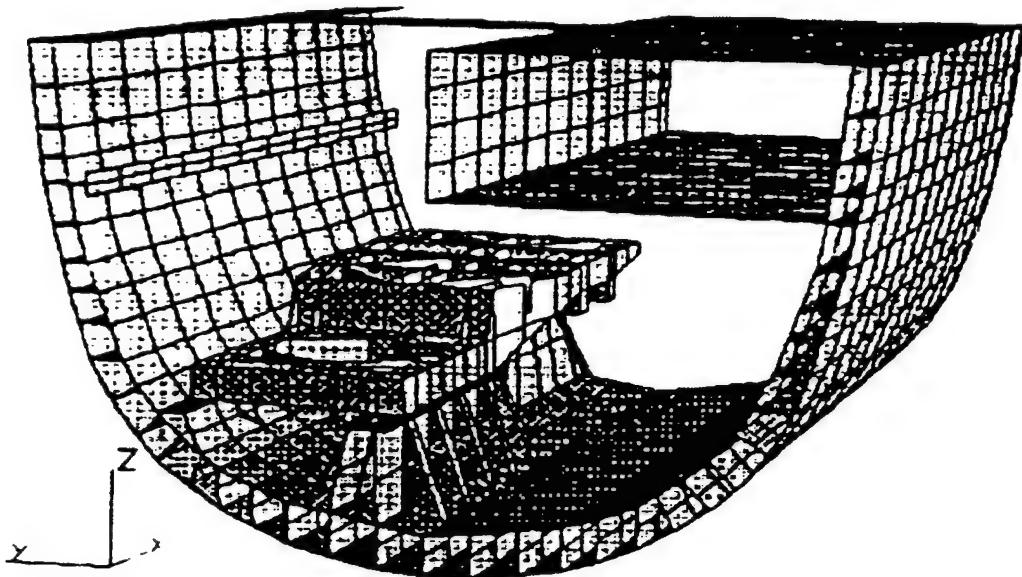
Figure 23. Sample Finite Element Model of Main Machinery Room on ADH

5.0 Grounding

5.1 Background

Oil spill pollution resulting from tanker hull rupture during grounding and stranding accidents has become a growing concern. In response to this concern, the Oil Pollution Act of 1990 (OPA'90) mandates that all tank vessel construction contracts awarded after 30 June 1990 must be of double hull configuration if they are intended to transport oil in navigable waters of the United States. Existing tank vessels built without double hulls will not be permitted to operate in U.S. waters after reaching the specific age and date specified in the Act.

In response to this Act, a study was undertaken to investigate the grounding behavior of double hull and double bottom tankers. Grounding occurs when a moving ship strikes a fixed object. In addition to the vertical forces pushing upward on the bottom of the ship, there are also longitudinal forces from the forward velocity which must be dissipated. The study of this complex phenomena consisted of numerical, analytical, and most importantly, experimental efforts of conventional double hull and ADH configurations.

First, the rock penetrates the outer hull, and, if it is sufficiently large, it will cause the inner shell to deform (Figure 24). As soon as the inner shell is deformed upwardly, it becomes stressed as a membrane. As the rock penetrates through the next heavy transverse member, rupture of the inner shell is always initiated by a crack propagation from the transverse plating penetration into the inner shell plating, which is highly stressed, resulting in a catastrophic rupture of the next oil tank. Figure 25 and Figure 26 show the initiation of tank rupture at the transverse bulkhead in the ADH grounding tests. Three distinct inner shell rupture sequences were identified in the NSWCCD grounding experiments and are discussed in detail by Sikora (2001). The "Achilles heel" of an oil tanker is the welded intersection between any heavy transverse plating (usually the bulkhead) and the inner shell. Since the advanced double hull tanker has no transverse frames, inner shell rupture initiation will almost certainly occur at the transverse bulkhead. Efforts to prevent inner shell rupture initiation are to be focused on transverse bulkhead design.

3 meters
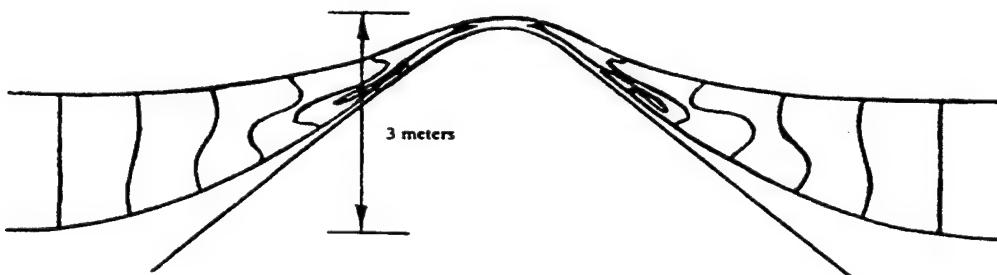
Figure 24. Double Hull Deformation Profile during Grounding

Figure 25. ADH Grounding Damage - Looking Aft

Figure 26. Transverse Bulkhead Damage

The number of tanks that are ruptured is a function of the energy dissipation of the double bottom structure. The energy dissipation in a grounding event is primarily governed by the amount of longitudinal structure that must be crushed, torn, or deformed by the rock. Since the ADH configuration has more longitudinal structure relative to a conventional double hull, it has better energy dissipation characteristics.

Any double hull design is resistant to oil spill damage: however, the advanced double hull design showed the best performance in the grounding experiments due to its high energy dissipation and the no-frame configuration (no transverse frames to initiate tank rupture).

5.2 Guidelines for Grounding Protection

Current double hull anti-pollution guidelines for tankers (OPA'90) call for a double bottom spacing of B/15 (B = maximum beam of ship) or 2 meters (approximately 6'7"), whichever is less, with a minimum of 1 meter. This is a formal requirement for all new tankers - other guidelines listed below offer a much-improved resistance to grounding damage, but are suggestions only.

Two important aspects of grounding protection are greatly influenced by the structural design of a double hull tanker:

- **Inner shell rupture initiation** at a heavy transverse member (usually the bulkhead)

- **Energy dissipation** characteristics of the structure which bring the ship to a stop, thereby limiting the number of tanks breached.

5.2.1 Inner Shell Rupture Initiation

If possible, a valuable additional safety measure can easily be incorporated into the forwardmost tank by using an inclined inner shell which extends from the forward tank bulkhead (at a height of 2.5 to 3 meters), sloping to 2 meters at the tank's aft bulkhead. Arrangements, fabrication, and/or operational economics may preclude this design feature.

Outer shell, inner shell, and longitudinal girder thicknesses should be determined by traditional strength and fatigue considerations. For example, a slightly thicker inner shell would

increase its resistance to rupture, but may result in a slightly heavier design for the same sectional strength.

A vertically-collapsing section at each transverse bulkhead can provide greater upward deformation of the inner shell, which permits the intruding rock to pass underneath the critical intersection with reduced vertical forces. This action can be provided by the use of a stooled, or haunched area at the intersection of a double-plate transverse bulkhead and the inner shell. This haunch is normally used to reduce tank liquid sloshing loads on the bulkhead plating and is present on both forward and after sides of the bulkhead. As shown in Figure 27, the haunch should be 45°, as large as possible, with the inclined plating stiffened by bulb stiffeners, rather than by using a full plating extension of the longitudinal girders into the haunch area. This haunch stiffener construction leaves an opening in the center beneath the bulkhead that provides a 'soft' area to allow the haunch collapse to initiate under threshold grounding loads, yet the stiffeners and plating can be designed to withstand lifetime service loads. The inner shell plating should be longitudinally continuous under the haunch from one tank to the next. Since several haunch panels buckle and collapse on each side of the rock location, the overall effect of haunch collapse during a grounding is that a more global deformation of the inner shell results, which, in turn, causes reduced membrane stresses and less likelihood of tank rupture. Bulkheads aft of midships do not need this treatment.
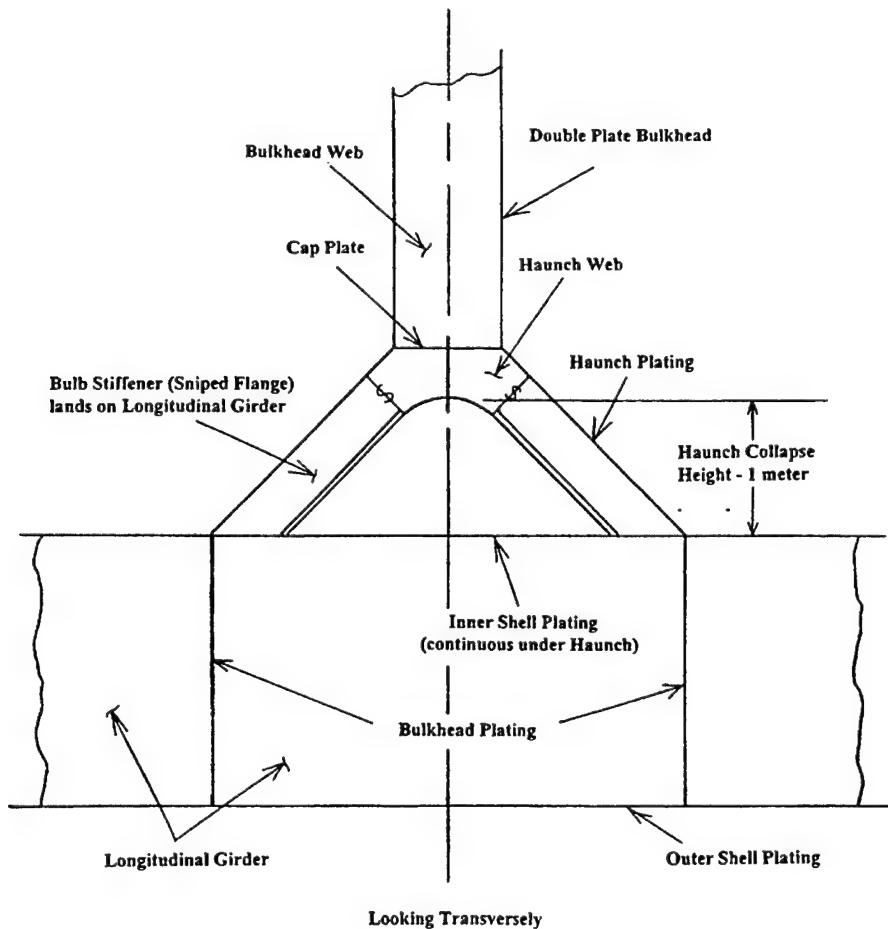
Figure 27. Collapsing Bulkhead Haunch Configuration

Longitudinal girders should be stiffened by longitudinally oriented stiffeners rather than vertical stiffeners. Experiments indicated that the use of tightly spaced vertical stiffeners here did not improve the grounding performance, and actually caused numerous punch-through ruptures of the inner shell.

5.2.2 Energy Dissipation

The spacing and thickness of ADH longitudinal girders in the double bottom have a great influence on the energy dissipation. A dangerous rock pinnacle shape that is high enough to cause inner shell rupture can only travel through this structure by deforming a large array of longitudinal girders that are in the path of the rock. Figure 28 shows the superposition of the ADH bottom structure and a rock pinnacle to illustrate the material that must be displaced during the grounding. The longitudinal girders and the inner and outer shell plating must be displaced around opposite sides of the rock, resulting in a great dissipation of energy by distortion, tearing, and friction. The higher the energy dissipation, the shorter the stopping distance, resulting in fewer tanks breached.

A tight spacing of ADH longitudinal girders is desired for improved energy dissipation during a grounding incident. Experiments show that increasing the number of girders in the double bottom by 50% results in a doubling of the energy dissipation, which roughly halves the stopping distance. For example, the grounding tests indicate that for a 40,000 ton tanker running aground at 14 knots on a rock pinnacle with a 4-meter height above the keel, the ADH double bottom structure with a web spacing of 46" provides the energy dissipation to bring the ship to a stop in approximately 190 feet, rupturing three oil tanks. However, an ADH tanker structure with a tighter web spacing of 33" can bring a similar ship to a stop in only 100 feet. This would allow the rock to penetrate only the bow and into the first oil tank, causing a small spill at the very worst. Note that the additional use of an inclined inner shell in the first tank as noted above may result in no tank rupture at all.
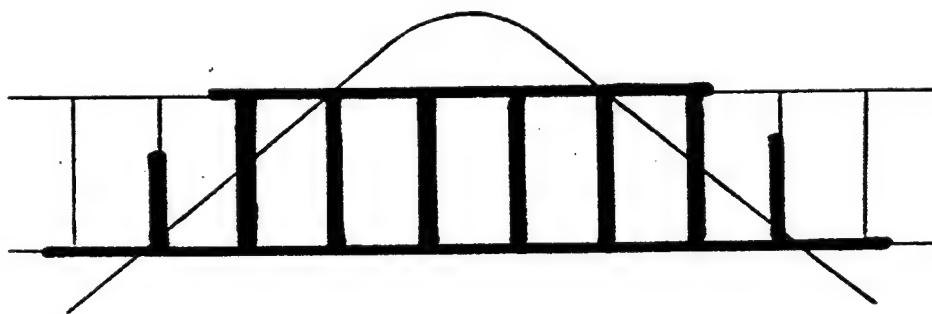
Figure 28. ADH Undeformed Bottom Structure in Path of Rock

5.2.3 Post-Accident Considerations

After a grounding incident occurs and the ship is stranded, subsequent ship motions in heavy weather or tidal changes may easily cause a widening of the rock damage site, resulting in deeper vertical penetration into the ship structure. Although initial rupture of the oil tanks may

not have occurred at the time of the grounding, an oil spill becomes more likely with time if the ship is not removed from the rock pinnacle quickly.

The short stopping distance during a grounding for an ADH design with a tight spacing of longitudinal girders suggests that with transfer of cargo the bow might be lifted clear and the ship pulled from the rock before heavy weather causes increased damage and spill pollution.

These observations and conclusions suggest that the ADH design for oil tankers can offer excellent protection against oil spill pollution in the event of a grounding accident.

6.0 Joining and Welding Guidance

6.1 Background

The use of the ADH configuration greatly simplifies the geometry of the structure through the elimination of the transverse frames. Not only are the weld runs uninterupted in the longitudinal direction, but nearly all of the chocks, collars, and brackets are eliminated. Thus, more efficient automated welding processes can be used to the fullest extent. Several studies have been conducted on the various automated welding processes and joint designs with potential applications to the ADH configuration. Included in this research are flux cored arc welding (FCAW), gas metal arc welding (GMAW), submerged arc welding (SAW), electrogas welding (EGW), electron beam welding (EBW), and laser welding. Much of this research focused on a variety of one-sided weld joint designs.

In the current economic environment, efforts to reduce construction costs have become increasingly important. A cost comparison (Sikora and Devine 1997) of an ADH variant was conducted with the conventional DDG-51 class to quantify potential cost reductions. An 8.3 percent savings in the cost of fabricating the primary hull structure was attributed to reduced welding costs from a reduced number of linear feet of weld required. Other factors contributing to reduced welding costs, such as increased use of modern, automated welding, were not included in the analysis. Although this study was conservative, the findings reveal the potential of the ADH configuration to reduce welding costs.

Most structural welds on naval ships with conventional stiffened plate configurations are accomplished using conventional two-sided welding practices. Although most of the welds on an ADH vessel can also be performed with these same practices, there are situations were single-sided welding would be invaluable because of spatial constraints imposed by relatively small cells. The Center for Advanced Technology for Large Structural Systems (ATLSS) at Lehigh University conducted a study to demonstrate automated one-sided welding processes for use in ADH structures with current shipyard technology and materials. Weldability tests were conducted on candidate one-sided T-joint weld details fabricated from 9.5 mm and 12.5 mm thick HSLA-80 steel. These tests revealed the effect of welding parameters on the quality and

producibility of the candidate joints. Metallurgical and mechanical property tests were performed to characterize weld discontinuities and assess their effect on joint strength. Large scale I-section fatigue tests and tests to characterize the effect of weld heat input and notch toughness were performed. Finally, this study identified weld joint designs and welding processes that result in acceptable quality and producibility for typical HSLA-80 T-welds.

Metro Machine Corporation has demonstrated the feasibility and design acceptability of joining three plates with one, vertical up electrogas weld (Juers and McConnell 1994). The method uses large alignment towers to locate and clamp shell and longitudinal plates for welding. Multiple towers are arranged to allow fabrication of entire hull cross-section modules (30 feet long) with all welds being made simultaneously in under two hours. A series of fatigue and Charpy V-notch toughness tests were performed on these electrogas welds by ATLSS and approved by the American Bureau of Shipping (ABS). This has demonstrated that welding time and costs can be significantly reduced through the effective use of automated welding processes.

The use of high energy density weld processes, such as electron beam and laser welding, are well suited for the exterior (blind-sided, through plate welding) closure of the double hull cells. Non-vacuum electron beam and CO_2 laser welds were fabricated and tested under a Navy Joining Center contract. The results were promising and indicated that more cost effective and better quality welds were possible than with traditional processes. A limited number of fatigue tests were performed on these welds and were found to be acceptable. The state of the art for high energy density welding processes is rapidly advancing, making them worth serious consideration.

6.2 Rules

The recommendations made in this section dealing with conventional shipyard welding processes consisting of single pass fillet and single-sided welds are based on results from tests conducted with specific material systems and scantling geometries. Informed decision should be made about their applicability when other materials or geometries are being used. For further details on the baseline material systems and scantling geometries refer to Sikora (2001).

6.2.1 Fillet-/T-Welds

Automated/mechanized flux-cored arc welding (FCAW) and gas-metal arc welding (GMAW) are the preferred processes for standard fillet/T welds. Overhead welding should be avoided.

6.2.1.1 Single-pass Fillet Welds

Automatic/mechanized FCAW is the preferred process for single-pass fillet welds. These welds can be made in any position; however, whenever possible, overhead welding should be avoided. Recommended welding parameters can be found in Appendix E of Sikora (2001). See Figure 29.
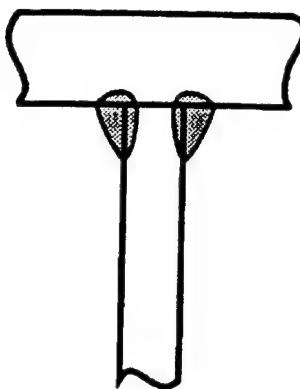
Figure 29. Single Pass Fillet Welds

6.2.1.2 One-sided T-Welds

For one-sided welds the single bevel-T joint or a non-standard joint referred to as a "butt-T" joint is preferred. See Figure 30.

Butt-tee Joint

Single Bevel-tee Joint
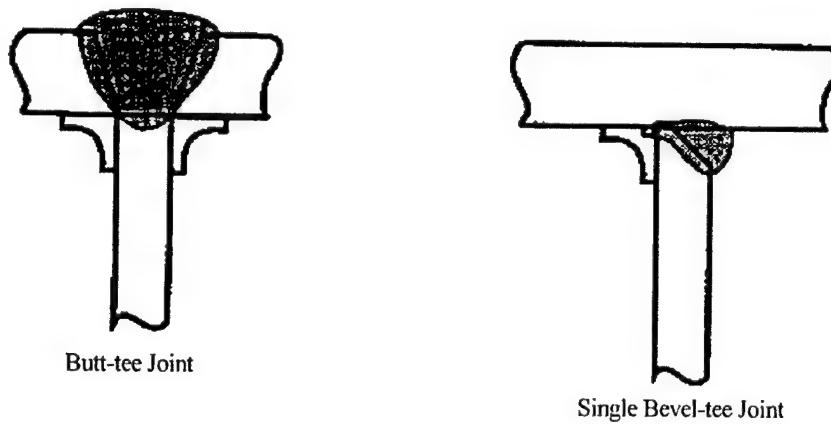
Figure 30. Butt-T and Single-Bevel-T Joints

When making one-sided, full-penetration welds, the use of ceramic backing and a high degree of joint fit-up control are needed. Without ceramic backing the allowable range of weld parameters and joint fit-up are likely to be too restrictive for a production environment, resulting in difficulty in controlling melt-through. The development of an automated method for application and removal of the ceramic backing should be considered to enhance productivity.

One-sided, full-penetration T welds should not be made in the overhead position, even with ceramic backing since backing is ineffective in this position.

In the case of one-sided single-bevel joints, when critical loading is tensile and reduced joint ductility is not a concern, nearly-full penetration joints should be considered in lieu of full penetration joints. This is because, when using the automatic/mechanized FCAW process and reducing the root opening to zero, welds can be made in all positions without ceramic backing.

One-sided, full-penetration single bevel-T and butt-T joints with matching strength filler material are fully or near fully efficient connections in tension.

One-sided, partial-penetration joints (single bevel-T and butt-T) should be near fully efficient in tension provided the unfused root is less than 15 percent of the discontinuous/thinner member (that is, 1.6mm unfused root with a 9.5mm member). However, they are not preferred because of corrosion issues.

The longitudinal shear capacity of one-sided butt-T joints can be evaluated from the net fused area at the weld root and the weld material shear strength.

The AASHTO Category B' curve can be used for design against longitudinal fatigue of full penetration T-joints. A limited number of tests suggested the Category B' curve could also be used for fully efficient partial penetration T-joints since no significant differences from full penetration joints were observed.

A fitness-for-purpose assessment of the effect of weld discontinuities, particularly incomplete weld root penetration, associated with single sided joints will be required before they can be used.

Whenever possible, one-sided, full-penetration butt-T welds using the automatic/mechanized FCAW process should be made in the flat or horizontal position as this aids in improved backside weld contour.

Partial-penetration butt-T welds can be made without ceramic backing using the FCAW, SAW, and GMAW processes. When using the GMAW process in spray mode, a desirable weld root condition could be more easily obtained and may be preferable to FCAW or SAW, especially for the root pass. Shallow penetration and intermittent lack of fusion at the weld root can be more of a problem with the FCAW and SAW processes.

6.2.2 Butt Welds

For heavy sections, greater than or equal to 1 inch thick, the Electrogas/Electroslag vertical up process is preferred. All other positions should be avoided for this process.

For thin sections less than 1 inch, automated/mechanized SAW, FCAW, or GMAW in the flat position is preferred. Avoid the use of SAW for out-of-position welding.

6.2.2.1 One-Sided Butt Welds (with FCAW)

For out-of-position welding, the FCAW process is preferred.

With the FCAW process, a 60-degree bevel angle and zero root opening produces the deepest joint penetration with the least risk of burn-through. Less bevel angle reduces penetration and more bevel angle increases chance of burn-through.

Full penetration joints can be produced in the horizontal and vertical positions but reproducibility is marginal. Achieving full penetration is most difficult in the vertical position due to the propensity for burn-through.

Ceramic backing improves penetration and backside contour, and limits burn-through in the flat position but may not reduce the likelihood of burn-through in the horizontal or vertical position due to removal of backing from arc forces.

6.2.2.2 Electrogas T-/Butt-Welds

The electrogas welding process (EGW) should be performed in the vertical up position. The vertical up EGW process should be used to join three structural members in one welding operation, the internal longitudinal girder and two adjacent inner or outer shell plates. The internal longitudinal girder should act as a spacer for the adjacent shell plates prior to its being incorporated into the structure.

High deposition rates (50 lbs/hr) and rapid joint completion rate (15-20 ft/hr) when using the electrogas welding process can be expected.

When using either ABS Grade CS or Grade A steel (mild steels with a minimum yield strength of 34 ksi and a tensile strength range of 58 through 71 ksi), the EGW filler metal that should be used is a Lincoln Electric Innershield type of electrode, designated Lincoln NR-432, which generates its own protective shielding gas (self shielded) and fluxing agents. Occasional gross porosity and arc instability problems have been identified when using Lincoln NR-431, an earlier version of this type wire. Therefore, the use of NR-431 should be avoided. Weld metal property requirements are those specified in the American Welding Society (AWS) filler metal specification AWS A5.26-91 for Class EG-82T-G welding wire.

When designing with the plate and filler metal mentioned above, to assure adequate fatigue performance, a conservative lower boundary estimate for fatigue strength of electrogas welds is the AASHTO category B' S-N curve.

Sufficiently rigid towers must be designed and built to accommodate the necessary fixturing and the vertically mobile EGW welding machine platform.

The mobile EGW welding machine platform should be designed to carry the spool of wire, wire feeder, arc controller (volts, amps), cab speed controller, oscillator controller, compressed air and cooling water manifolds, manual torch positioning slides and the welding operator.

Adequate clamping forces must be applied to the weld joint to prevent material movement during the welding operation and to assure structural dimensions are being held to the required tolerances.

All the clamps should be directed toward applying forces toward the weld joint and therefore maintain joint dimensions and location. An adequate combination of hard and soft plate stops must be included to maintain sufficient control of dimensional tolerances.

There should be special water-cooled shoes on all sides of the weld joint, which, in addition to aiding in maintaining proper alignment, serve to contain the molten weld metal and form the weld contours.

The water-cooled shoes must have an appropriate geometry and be held with enough pressure to maintain an adequate seal that will prevent loss of the weld pool.

It is important that the operators maintain the straightness and continuity of the segmented backing bar.

6.2.3 *Concentrated Energy Processes*

These processes are not as fully developed as the "conventional" processes, but notable advances have been made and the frequency of use in production environments is increasing. However, these processes require some shipyard commitment to install.

The concentrated energy processes, when available, are preferred for butt and butt-T welds and should be avoided for use in fillet welding.

6.2.3.1 Electron Beam Welding

For electron beam vacuum or non-vacuum welding, the work piece and electron beam generator must be inside an enclosure designed to attenuate the X-rays generated as the electrons strike the weld metal surface.

For vacuum electron beam welding, an enclosure designed for an external pressure of 15 psia (atmospheric pressure) is required. For large ship structures, a large vacuum chamber is not cost effective.

Good weld piece fit-up is required for electron beam welding. Weld surfaces should be cleaned of paint, dirt, mill scale, and other impurities to prevent weld contamination. Because of the very small weld beam diameter, the work piece and beam generator must be isolated from excessive vibration inputs.

For electron beam welding, a shield gas is required (except welding in a vacuum) to prevent weld contamination from the oxygen and nitrogen in the atmosphere. Service systems, that is, cooling of beam generators, vacuum required for the electron beam generator, and electrical power requirements must be considered.

Where work fit-up gaps are large, a gap filler material and weld feed wire are necessary for a geometric weld configuration.

7.0 Outfitting of Distributed Systems

7.1 Background

Distributive systems consist of the piping, electrical cabling, heating, ventilation and air conditioning (HVAC) ducts. For conventional ships, these systems must be routed around or through the transverse frames, thus increasing their cost and complexity. For advanced double hull ships, the smooth, uninterrupted surfaces of the inner shell greatly simplifies the routing of distributive systems, eliminates many bends, shortens system lines, and significantly reduces installation costs. A cost comparison (Sikora and Devine 1997) was conducted for electrical, HVAC, and piping systems in a DDG-51 class ship. Using conservative assumptions, this

analysis estimated that the use of an ADH configuration would result in a 17.5% labor hour savings in the electrical craft, a 17.9% labor hour savings in the sheet metal craft (ventilation ducts), and a 23.6% labor hour savings in the piping craft. Since almost half of the four million trade craft hours are used to install distributive systems, this results in a third of a million labor hours saved. Reducing the length of the system runs results in 118 ltons of weight savings and $4M reduction in material costs.

When using the ADH configuration, there is the option to either place the distributive systems on the inner surface of the inner hull or, if the cell size is adequate, inside the cells (the space between the inner and outer hulls). Although the functional requirements of certain distributive systems can dictate their location, improved space use and accessibility can be achieved through careful planning. This is especially a concern for volume-limited, small combatants.

It is generally easier to install and maintain distributive systems when located on the inner surface of the inner hull than when placed within the cells. However, intrashell installations are possible. Ingalls Shipbuilding and the Center for Advanced Technology for Large Structural Systems (ATLSS) at Lehigh University performed a physical study (Sizemore et al. 1994) that characterized the constraints on access to, and work associated with, distributive systems being conducted inside intrashell spaces. Full-scale mockups were used to evaluate installation, repair, and maintenance of typical combatant distributive systems inside cells. Requirements and strategies for movement of personnel, handling and conveyance of materials and equipment, and the conduct of work were identified. As part of this study, a multi-purpose conveyance device was designed, prototyped, and tested. The device provided personnel with improved body support when performing work in awkward positions. Specialty tooling for lifting and positioning material were also designed, prototyped, and tested. This work provided valuable insights into safe and efficient work procedures associated with the location of distributive systems inside intrashell spaces.

On conventionally framed ships, distributive system attachment points are generally located at hard spots associated with frames. Current military standards place many constraints on attachment point designs – driving up costs. Ingalls Shipbuilding developed various alternative pipe hanger attachments that can be welded anywhere on the shell surface. Since they represent a significant departure from military practice, Ingalls Shipbuilding and ATLSS developed new guidelines to evaluate the fatigue strength of these design alternatives. As was previously done for ADH foundations, the design procedure used a "hot spot stress range" procedure from the American Welding Society. The method makes use of the stress range close to the weld toes where fatigue cracking is expected to occur. Full-scale fatigue testing characterized and validated the fatigue strength of alternative attachments. This work provides an alternative attachment method which allows designers to take advantage of the reduced constraints associated with the ADH configuration.

7.2 Rules

7.2.1 Placement of Distributive Systems

- Functional requirements of certain distributive system may dictate their location. The location of these systems should be established first.

- When installing systems, particularly those in small intrashell spaces, the blockage envelope formed by the location and density of the distributive systems should be carefully evaluated to avoid excessive or unnecessary blockage.

7.2.2 *Monitoring Distributive Systems Condition*

- Due to the large number of intrashell spaces, each space should be permanently labeled with tags having machine-readable and man-readable data providing pertinent information about the contents and history of the space.

For intrashell spaces, minimally invasive procedures should be used to identify the locations that require entry. Pressurization, gas content, and estimates of coating degradation or mechanical damage to distributive systems can be accomplished through small ports. Bore entry video instruments should also be considered to minimize the need for personnel entry into intrashell spaces.

7.2.3 *Intrashell Work*

- Strict use and application of carefully chosen safety appliances and procedures is of heightened importance during work in intrashell spaces due to their highly confined nature.

- Adequate ventilation of the intrashell space must be provided to reduce to a minimum the work generated smoke, fumes, and airborne particulate.

- Evacuation plans and procedures should be established for removal of injured personnel.

- In small cells where movement is difficult, conveyance devices should be used for movement of personnel and materials. Personnel conveyance devices should also provide proper support for personnel during installation, repair, and maintenance operations.

- In small cells, specialty tools should be used for lifting and positions that take advantage of the cell geometry to avoid the need for installation/removal of temporary padeyes.

7.2.4 *Attachment Fatigue Design*

- Determine the lifetime history of inertial loads at all critical weld details.

- Determine the hot-spot stress (perpendicular shell bending stress 6 mm from the weld toe of interest) due to surge, sway, and heave individually.

- Assume that Miner's rule (Miner 1945) for cumulative damage is valid to allow simple conversion of stress range to the constant amplitude equivalent.

- Calculate the root mean cube (RMC) hot-spot stress range in each of the three principal directions.

- Compare the largest of these RMC stress ranges to the fatigue strength obtained using the AASHTO, Category C, S-N design curve at anticipated lifetime number of cycles (AASHTO 1989).

- Modify the design if necessary or appropriate and repeat the above procedure.

8.0 Corrosion

8.1 Background

The cost of corrosion maintenance and repair of surface and sub-surface Naval ships has been roughly estimated to be at least 1.2 billion dollars annually for approximately 360 ships (Thurston 1997). These costs can be minimized for new ships with close attention to design, manufacturing techniques, quality control, materials selection and other corrosion control techniques.

Corrosion control of structures exposed to seawater is traditionally accomplished through the combined use of coatings and cathodic protection and through the selection of corrosion-resistant materials. Several aspects of the advanced double-hull (ADH) construction concept present significant challenges to the traditional technologies of cathodic protection and coatings and are discussed below. There are also two unique features of all double-hulled ships, which increase corrosion susceptibility versus single-hulled ships. One is moisture condensation inside double hull cells caused by a variation in temperature between the inner and outer cell walls. The other is the increased amount of horizontal surface on which water may accumulate.

The ADH concept consists of inner and outer hulls separated by only about 1 meter, with solid longitudinal connections every 1 meter. As with the commercial tanker ADH design, traditional corrosion control techniques are well established for the seawater side (cathodic protection and coatings) and the interior-crew and machinery spaces (coatings). This ADH design results in long cells (with a 1-m^2 cross-section) which need corrosion protection on the inside as well as the outside. The corrosion control challenge presented is due to the limited access and visibility for preservation, inspection and maintenance of the inner portions of the cells. This includes problems of surface preparation and application of corrosion-control measures such as coatings. Additionally, restricted inspection and maintenance periodicity requires any corrosion-control methods used to be of extremely high reliability. Finally, the all-welded construction of ADHs leads to a situation where traditional coatings applied inside cell spaces can be burned off at welds during final assembly.

Because the size of the tanker ADH cells will allow relatively easy access, the corrosion control emphasis for commercial ships will be to minimize the acquisition and life-cycle costs using traditional technologies such as coating and cathodic protection. The ADH cells on naval

combatants do not allow easy access. Consequently, traditional coating methods for corrosion control are not suited and alternative technologies are addressed to minimize acquisition and life-cycle costs.

8.2 Corrosion Guidelines for Interior Cells of ADH Sealift Ships

These guidelines were summarized from previously issued Carderock Division Naval Surface Warfare Center technical reports. A summary of the supporting data is presented in Appendix G of Sikora (2001).

8.2.1 Design

8.2.1.1 Scantlings

Scantlings must be designed with a corrosion allowance between 1.5 mm (0.06 in.) and 3.0 mm (0. 1 2 in.), taking into account the allowable steel mill plate thickness tolerances. Either tighten the rolling tolerances or increase the corrosion allowances accordingly. For combatants, access must be provided at the forward and aft ends of each cell. Minimum opening sizes for horizontal plates should be 450 mm by 600 mm (18 in. by 24 in.) or 570 mm (22.4 in.) in diameter. Minimum opening size for vertical surfaces should be 600 mm by 800 mm (23.5 in. by 31.5 in.). Wing tanks must have access hatches and vertical ladders at both their forward and aft ends for safety/emergency egress purposes.

8.2.1.2 Piping

Piping should be installed to allow forced air ventilation of the cells, particularly those in the bottom of the vessel. This can also help prevent coating blisters or damage due to solvent entrapment during maintenance coating. A purge pipe to the weather is suggested. Positive drainage must be provided from all horizontal plates or stiffeners. Provide air escape paths for all seawater ballast tanks to prevent the formation of air pockets and to improve the effectiveness of sacrificial anodes, particularly in bottom tanks.

8.2.1.3 Sacrificial Anodes

Sacrificial zinc or aluminum anodes should be used in seawater ballast tanks and designed for a minimum life of 8 years. Aluminum anodes should never be used in oil tanker ballast tanks or seawater ballast tanks where there is a potential of explosive atmosphere because of their tendency to cause sparking if they become loose and fall. Aluminum anodes should have height restrictions in cargo tanks such that their weight-at-height factor does not exceed a potential energy of 275 Joules.

8.2.1.4 Outfitting

Glass-reinforced epoxy, or other nonconductive composite materials should be used for all ladders, walkways, gratings, handrails, and so forth, to the maximum extent possible. Carbon fiber-reinforced composites should not be used. Any fastener used with glass reinforced epoxy or composite material for ladders, handrails, or other outfitting inside the ballast tanks should be of a high nickel alloy, such as Monel 400.

8.2.1.5 Welds

Full-penetration welds must be used in lieu of partial penetration fillet welds for all stiffeners to prevent entry of corrodent into the joint crevice in the event of a cracked weld.

8.2.1.6 Stringers

Longitudinal stringers should be used with a maximum spacing of 4 m (13 ft) in the double-side tanks. This would serve to stiffen the structure, resulting in less cracking of coatings and additionally, aid inspections by serving as inspection walkways.

8.2.1.7 Stiffeners, Cutouts, Brackets, Structural Support Members

The number of stiffeners, cutouts, and small pieces or brackets having sharp corners where coatings tend to fail prematurely should be minimized. For combatants, the only structural sharp edges that should be present are those at access openings from cell to cell. For tankers, plates should be used instead of stiffeners, where possible, to provide a stiffer structure and to minimize sloshing of the ballast, which erode coatings. Standard foundation designs should be used. Structural features that can cause shadowing of areas during paint spraying should be minimized. Structural support members should be of simple shapes, such as smooth round bars or pipe for ease in applying coatings. Bulb angle stiffeners or rounded profiles should be used whenever possible. If the concept of diagonal stiffening is reinstituted, these cells should be designated as dry voids because the stiffeners will render the cells difficult to inspect. All surfaces of the tank interior should be readily accessible for surface preparation and coating application.

8.2.1.8 Distributed Systems

Distributed systems such as piping, conduit, cabling, and so forth, should not be installed in any cells that will be used for fluid service, such as seawater, potable water, collecting and holding (sewage), fuel oil, and so forth If a conventional method of painting is used, major painting should be done before the distributed systems are installed. This will ensure the optimum line of sight and accessibility for good paint coverage. When the distributive system is installed, paint touch up must be done at the weldments and on the other side of the weld.

8.2.1.9 Alternative Designs

Two alternative configurations for commercial tanker ballast tank placement (Hah and Akiba 1994) should be considered for use. To facilitate inspections of ADH cells and to reduce the possibility of piping leakage, discharge piping (ballast tank, bilge, and so forth) and blowdown piping should be incorporated into a separate compartment complete with removable cover plate or access cover. Design consideration should also be given to Hah and Akiba's proposed valve compartment concept shown in Figure 31.
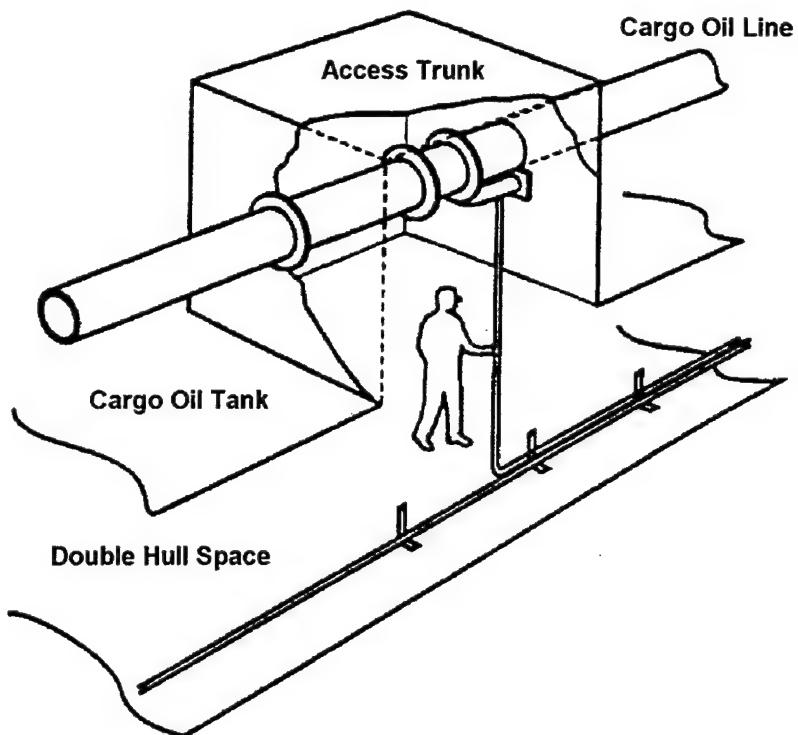
Figure 31. Piping Inspection Layout in Tanker Bottom

8.2.2 Construction

8.2.2.1 Welds

Prohibit intermittent welding, also called staggered, stitch, or skip welding. Full-penetration welds must be used in lieu of partial penetration fillet welds for all stiffeners, transverse girders, deck hangers for composite decks, and the resilient mounts to the inner hull shell, to prevent entry of corrodent into the joint crevice in the event of a cracked weld. Badly undercut welds must be removed and re-welded. Butt-welded joints should be used whenever possible. Weld spatter, arc strikes, and so forth, must be ground smooth before painting. Areas where welding was performed after the paint step should be touched up, with extra attention paid to weld seams.

8.2.2.2 Connections, Joints

Bolted, riveted, or lap joints must be prohibited. Threaded connections should not be used or, when necessary, should be made using corrosion-resistant materials. Butt-welded joints should be used whenever possible. Prohibit intermittent welding, also called staggered, stitch, or skip welding. Weld spatter, arc strikes, and so forth, must be ground smooth before painting.

8.2.2.3 Cutouts, Structural Support Members

A minimum radius of 3.2 mm (1/8 in.) should be required on all edges prior to coating. A radius of 6.4 mm (1/4 in) is preferred.

8.2.2.4 Attachments

For either conventional or electro-deposited epoxy (E-coat) paint systems, attachments should be installed prior to coating. Brackets for bolting any ladders, walkways, handrails, and so forth, should be installed prior to coating. Deck, foundation, and distributive system attachments should be welded into place before coating. All temporary construction fixtures and brackets, and all weld spatter, arc strikes, and so forth, must be ground smooth before painting or dipcoating. Badly undercut welds must be removed and rewelded. If the electrodeposited E-coat system is used, access openings must be in place before coating. Full-penetration welds should be used to attach transverse girder, deck hangers for composite decks, and the resilient mounts to the inner hull shell.

8.2.2.5 Distributive Systems

Upon completion of the coating step, any distributive system that will be used should then be installed.

8.3 Coatings

A trained coatings inspector must be used throughout the entire coatings process. Specific inspection checkpoints should be established and passed in order to continue to the next step. Coatings inspectors should be used for any significant coating-repair operations.

8.3.1 Pre-construction

Surface preparation is a crucial step in optimizing a high-performance coating system. Before construction, structural steel must be abrasive blasted to a near-white metal finish (NACE 1991). A pre-construction primer should be used. A weld-through pre-construction primer of inorganic zinc (IOZ) of 25 to 50 µm (1 to 2 mils) dry film thickness (DFT) is recommended for all structural members. Questions remain as to whether this pre-construction primer should be removed by abrasive blasting or left on as a final primer with minimal power tool cleaning (equivalent to SSPC-SP-3) as Japanese shipbuilders sometimes do (NSRP 1987). For Navy ships, however, zinc-based coatings are not used in final coating systems for underwater hulls or ballast tanks due to poor past performance. Possible future environmental regulations concerning zinc as a pollutant must also be considered in deciding whether or not to remove or leave the IOZ pre-construction primer in the final coating system.

8.3.2 Construction

For either conventional or E-coat paint systems, attachments such as: brackets for bolting ladders, walkways, handrails, and so forth, and deck, foundation, and distributive system attachments, should be installed prior to the final coating system application. All temporary construction fixtures and brackets, and all weld spatter, arc strikes, and so forth, must be ground smooth before painting or dip-coating. Badly undercut welds must be removed and re-welded. If the E-coat system is used, access openings must be in place before coating. A minimum radius of 3.2 mm (1/8 in.) should be required on all edges prior to the final coating: a radius of 6.4 mm (1/4 in) is preferred.

8.3.3 Surface Preparation

Upon completion of all fabrication, welding, and edge preparation, either power tool cleaning, solvent cleaning, or abrasive sweep blasting should be used to spot clean all rusted areas. In the U.S., IOZ pre-construction coatings are usually removed by abrasive blast cleaning after fabrication due to blistering of topcoats over this primer. However, some Japanese shipbuilders incorporate a well-cured IOZ primer into the final protective coating (NSRP 1987).

Soluble salts must be removed before coating. Requirements for soluble salt limits should be incorporated into new construction and repair specifications. Abrasive blasting is not sufficient to remove soluble salts. High pressure, preferably high purity, water blasting, or phosphoric acid (5%) washing is required for salt removal. Inspection and testing must be conducted to ensure that soluble salts are removed from the surface to the specified level of cleanliness, using the appropriate test procedure. The Navy currently requires a salt level of 3 $\mu g/cm^2$ for immersed surfaces and 5 $\mu g/cm^2$ for non-immersed surfaces.[1] The Navy's guidelines may be augmented by a joint standard on surface preparation by high and ultra-high pressure water jetting, issued by NACE International (NACE 1991) and the Steel Structures Painting Council (SSPC). Caution must be taken to prevent re-contamination prior to coating. Control of flash rusting and acceptance levels should also be addressed by the surface preparation standard selected.

8.3.4 Coating Selection & Application

A light-colored, volatile organic compound (VOC) regulation-compliant, surface-tolerant, flexible, high-build, two-coat, 100-percent solids epoxy paint system should be applied using airless spray equipment, with a minimum dry film thickness (DFT) of 250 μm (10 mils). The use of coal tar epoxies, which tend to be dark, must be avoided. Do not use soft coatings, even temporarily. Coatings specified must be resistant to mechanical abrasion damage, which tends to occur during final outfitting of a vessel. A commercially available fluoropolyurethane paint[2] developed by the Naval Research Laboratory indicates excellent resistance to microbiologically induced corrosion, and excellent corrosion resistance in seawater environments. While there is at least one drawback to using this coating (initial cost and, possibly industrial hygiene issues), this material should be considered for use. Several coatings were evaluated for ADH applications (Holder 1995). As a group, high-build epoxies performed the best in both long and short-term exposure tests. Many of the high-build epoxies outperformed the standard Navy epoxy F150/151 system.

Two stripe coats must be used on all edges and welds, quality control must be enforced in these areas. After welding, all weld spatter, arc strikes, and so forth, must be ground smooth before painting or dip-coating. Opposing sides of the weldments must be touched up. The entire tank or cell space should be coated. Coating the overheads of tanks must be specified because sacrificial anodes will not provide protection in this area. For tankers, a special erosion resistant topcoat should be considered for use around openings where the seawater velocity may be

---

1 At present, Navy guidelines for surface preparation by hydro-blasting (to remove coatings and/or salts) are in the form of a Naval message. These will eventually be issued as a Uniform Industrial Procedure Instruction (UIPI) and referenced in the Naval Ship's Technical Manual (NSTM) Chapter 631 as an Advanced Change Notice (ACN).

2 Manufactured by 21st Century Coatings Inc., 310 North Fairfax St., Suite 100A, Alexandria VA 22314.

higher. Additional attention must also be paid to all horizontal surfaces where water can accumulate. Upon completion of construction (for example, installation of distributive systems), damaged coatings should be repaired.

8.3.5 *Coating Maintenance and Repair*

For in-service maintenance/repair coating operations, surface-tolerant epoxies should be used in conjunction with small, vacuum-assisted power cleaning tools or vacuum blasting. Any areas of damaged coating must be re-coated before returning a tank to service. Vacuum blasting should be used for surface preparation for spot coating repairs. Two stripe coats must be used on edges and welds during touchup coating.

A coating life of 15 to 20 years is not an unrealistic goal, assuming coating maintenance is periodically applied. Regular inspections for coating repair and anode replacement will be necessary to maintain the long life of these systems.

8.4 Alternative Corrosion Control Methods for Dry Cells

For dry cells of combatants, only one of the corrosion protection systems tested was judged to be feasible for the double-hull application: the desiccant wheel (DEW) dehumidification system (Bowles 1997). The airflow configuration as well as the performance, reliability and capacity of the dehumidification unit under realistic conditions need to be addressed. However, dehumidification should only be considered if a forced-air flow system will be installed. Additionally, ship survivability should be addressed since this corrosion control method requires the interconnection of cells.

Another alternative is to hermetically seal uncoated or coated cells (with a one-time coating) (Bowles 1997). This control method could work in conjunction with rigorous, remote environmental sensing (for example, humidity or wetness) to ensure that low humidity conditions are maintained and that air or seawater breachment is detected. However, scheduled inspections are still recommended and sensors may need periodic replacement that raises the problem of access to hermetically sealed cells.

Inert gasses such as argon or nitrogen should not be used for corrosion protection in accessible cells used dry or as storage because of the potential problems that may be encountered in obtaining a breathable atmosphere in these cells for inspections.

8.5 Maintenance

The knuckle joint area at the forward and aft ends of a ship where the horizontal and vertical members of the sides and bottom converge will probably need increased corrosion protection and inspections. Robotic inspection appears ideal for combatant cells where access by human inspectors may be very difficult (Gallagher, Barbera, and Bankard 1994). Its use should be considered.

Inspections should concentrate on any horizontal surfaces which will trap mud and debris because this is where most coatings failures initiate. For combatants, inspection criteria and nondestructive inspection methods for the installed damping material and the underlying metal must be established. Possible methods of inspection are laser shearography and infrared thermal imaging. Life-cycle enhancement for commercial and combatant ADH ships can be improved

by using cell maintenance and corrosion tracking databases. The use of the NAVSEA/PERA-CV (1991) database is recommended

If regular visual inspections are not possible, corrosion or corrosivity sensors are recommended for all unprotected spaces or spaces protected by hermetic sealing or dehumidification. Automated inspection devices, if used, should be designed to impart a minimum of potential damage to any coating system or acoustic damping material.

Periodic inspections for coatings repair and anode replacement are required in combatant cells and must be implemented via the U.S. Navy's periodic maintenance schedule (PMS). A maintenance requirement card (MRC) should be developed combining the best features of the standard inspection forms contained in ASTM F1130 (ASTM 1999) and the International Association of Classification Societies and Tanker Structure Cooperative Forum Guidance Manuals for the Inspection of Double and Single Hull Tankers (TSCF 1995). Such a form will decrease the amount of time needed to conduct an inspection and can provide a standard that can be easily used by the ship repair community to prepare clearly understood work specifications. The U.S. Navy must also anticipate the need to gas-free every cell of a combatant vessel before an inspection to eliminate any pockets of unbreathable air.

A coating life of 15 to 20 years is not an unrealistic goal, assuming coating maintenance is periodically applied. Regular inspections for coating repair and anode replacement will be necessary to maintain the long life of these systems.

Inert gasses such as argon or nitrogen should not be used for corrosion protection in accessible cells used dry or as storage because of the potential problems that may be encountered in obtaining a breathable atmosphere in these cells for inspections.

8.6 Operation

When bottom tanks are ballasted, they should be 100 percent full in order to minimize ballast sloshing and to maximize the effectiveness of sacrificial anodes. A dispersant such as "Mud Out" should be used in ballast tanks.

8.7 Recommendations

Where cells will remain dry, additional work is necessary for the use of dehumidification or hermetic-sealing of cells as a corrosion control method. A thorough analysis of available sensor technology should be conducted for monitoring the environmental condition of hard-to-access combatant cells. Additionally, use of sensors could have the additional benefit of enhancing survivability by pinpointing areas of seawater leakage. For combatants, the optimum desiccant wheel (DEW) system configuration and performance should be determined, including the number of cells to be connected to each unit, the design of an appropriate valve system to enhance survivability, the use of dampers to allow the system to respond to humidity variations in different areas of the hull, and the location of DEW systems onboard ship and storage of spare parts. However, indications are that these technologies could reduce corrosion to the point where coating and frequent visual inspection would not be required.

A longer-term test should be conducted to fully evaluate the performance of the Rubatex R-416-H material. The material selected for the final acoustic damping should be evaluated for compatibility with the fluids to which it will be exposed. Further work should be conducted to

determine the optimum and most economical surface preparation method that will produce a high degree of confidence in the life of the resulting coating system.

Further research should be performed regarding the use of a 0.7-mil DFT IOZ primer, which is not removed before applying the final paint system, as is current practice in Japan. Testing of the E-coat system should include an evaluation of the effects of residual primer on the deposition and subsequent adherence of the E-coat.

9.0 Miscellaneous Topics

During the course of the ADH research projects, a number of technical issues were raised on other topics. Although no design guidelines are offered, it is important that they be addressed.

9.1 Inspection, Maintenance and Repair

The small size of the cells (approximately 3 feet by 3 feet) on combatants is frequently perceived as an inspection and maintenance problem. Although it was shown in Section 7 that personnel can readily work inside of these cells, unmanned methods would be preferred. Gallagher (1994) developed a remotely controlled vehicle which has been demonstrated to inspect, clean, paint, and keep a maintenance history of 3-foot by 3-foot cells. This self-propelled robot can be inserted in a 12-inch by 12-inch access opening.

9.2 Damage Control

Damage control measures must address both the hydrostatic stability of a partially flooded vessel and the emergency procedures needed to plug a hole. Kopp (1994; 1995; 1994) performed a series of model tests to investigate damage stability of ADH combatants. The current Navy criteria was found to apply to the ADH configuration. Since it is somewhat more difficult to design an ADH combatant with acceptable damage stability than a conventional ship, the designer must consider damage stability early in the design cycle.

Ex-*Shadwell* tests suggested an inflatable bladder inserted inside a cell would plug a hole better than current methods.

9.3 Equipment Shock

The Naval Surface Warfare Center's Underwater Explosions Research Department (UERD) (Dawson and Handleton 1996) conducted an extensive numerical analysis of an ADH cruiser subject to an underwater explosion. They showed that an ADH was better at attenuating shock on equipment than a conventional ship because it reduced accelerations and peak

velocities, and had similar or larger absolute displacements. Snyder (1997) showed that internal decks and platforms on ADH ships could be shock isolated.

9.4 Signature Control

Infrared energy from machinery, equipment, and so forth is emitted from that portion of the ship which is above the waterline. Cervenka (1994) has shown that air filled cells in the ADH has an inherent insulating value of one inch of insulation. Furthermore, the ADH cells tend to reduce the high thermal gradients on the ship. Additional potential control measures would be to spray a fluid inside of the cells.

The ADH configuration has no potential benefits nor any penalties associated with radar or magnetic signatures. Anything that can be done to reduce these signatures on conventional ships can also be applied to an ADH ship. However, the ADH configuration is compatible with replacing the ordinary shipboard steels with non-magnetic materials (such as stainless steel, aluminum, or titanium) to significantly reduce magnetic signatures.

10.0 References

AASHTO. 1989. *Standard Specification for Highway Bridges.* 14th ed. Washington, DC: American Association of State Highway and Transportation Officials.

AISC. 1991. *Manual for Steel construction, LRFD.* First or ASD 9th edition ed. Chicago, IL: The American Institute for Steel Construction.

ASTM. 1999. *Standard Practice for Inspecting the Coating System of a Ship,* Volume 01.07, Test Method F1130-99, West Conshohocken, Pennsylvania: Américan Society for Testing and Materials.

Bleich, F. 1952. *Buckling strength of Metal Structures*: McGraw-Hill Book Company.

Bowles, C., K. Lebègue, et al. 1997. *Testing of Alternative Corrosion Control Methods to Coatings for Advanced Double Hull Naval Combatants,* NSWCCD-TR-61-97/04, West Bethesda, MD: Naval Surface Warfare Center, Carderock Division.

Bruchman, D., and J. Atwell. 1991. *Design Criteria for Advanced Double Hull Ships in Support of the Fast Sealift Program,* SSPD-92-173-33, Bethesda, MD: David Taylor Research Center.

BSI. 1980. *Steel, Concrete, and Composite Bridges, Part 10, Code of Practice for Fatigue,* BS5400, London, UK: British Standards Institute.

Cervenka, P., D. Weiss, and R. Ratcliffe. 1994. *Infrared Implications in Double Hull Surface Ship Design,* TR-94/010, August 1994. West Bethesda, MD: Naval Surface Warfare Center, Carderock Division.

Dawson, R., and R. Handleton. 1996. *An Analytical Comparison of Equipment Shock Responses in Conventional and Advanced Double Hull Cruisers Due to a Noncontact Underwater Explosion,* SSM-66-96/6, May 1996. : Naval Surface Warfare Center, Carderock Division.

Dexter, R. J., and M. Kaczinski. 1994. Large Scale Fatigue Tests of Advanced Double Hull Weld Joints, Paper No. 8. Paper read at Proceedings of the Advanced Double Hull Technical Symposium, Oct. 25-26, 1994, at Gaithersburg, MD.

Ford, H., J.M. Grassman, and R. Michaelson. 1994. Stress Behavior of Advanced Double Hull Structures, Paper No. 10. Paper read at Advanced Double-Hull Technical Symposium, 25-26 Oct 1994, at Gaithersburg, MD.

Gallagher, M., T. Barbera, and M. Bankard. 1994. Inspection and Maintenance of Advanced Double Hull Cells, Paper No. 17. Paper read at Advanced Double-Hull Technical Symposium, 25-26 Oct. 1994, at Gaithersburg, MD.

Hah, J., and T. Akiba. 1994. Environmental Concern: A Revolutionary Concept in Double-Hull Tanker Design. Paper read at Singapore 1994 Conference, 22-25 March 1994, at Singapore.

Holder, A. G. 1995. *Coatings for Advanced Double-Hull Ships*, CARDIVNSWC-TR-64-95/06, June 1885. West Bethesda, MD: Naval Surface Warfare Center, Carderock Division.

Hughes, O.F. 1988. Ship Structural Design, A rationally-Based Computer-Aided Optimization Approach. *SNAME Publications*.

Juers, R., and F. McConnell. 1994. Electrogas Welding of Advanced Double Hull Subassemblies, Paper No. 13. Paper read at Advanced Double Hull Technical Symposium, Oct. 25-26 1994, at Gaithersburg, Md.

Kihl, D.P. 1994a. Axial Fatigue Behavior of Advanced Double Hull Combatant Weld Details. Paper read at The Advanced (unidirectional) Double-Hull Technical Symposium, October 25-26, 1994, at Gaithersburg, Maryland.

Kihl, D.P. 1994b. *Mean Stress Effects in Steel Weldments Subjected to Constant and Random Amplitude Fatigue Loadings*, NSWCCD-SSM-65-95/11, West Bethesda, MD: Naval Surface Warfare Center, Carderock Division.

Kopp, P. 1994. *Damage Stability Issues for Advanced Double Hull (ADH) Project*, HD-0043-01, Nov. 1994. West Bethesda, MD: Naval Surface Warfare Center, Carderock Division.

Kopp, P., and R. Bishop. 1995. *Damage Stability Model Test for the Advanced Double Hull (ADH) Program*, HD-0043-03, April 1995. West Bethesda, MD: Naval Surface Warfare Center, Carderock Division.

Kopp, P., W. McCreight, and L. Motter. 1994. Effects of Advanced Double Hull Construction on Damage Stability of Combatants, Paper No. 19. Paper read at Advanced Double-Hull Technical Symposium, 25-26 Oct. 1994, at Gaithersburg, MD.

Melton, W., J. Beach, J. Gagorik, D. Roseman, and J. Sikora. 1994. Advanced Double Hull Research and Development for Naval Commercial Ship Applications. Paper read at Proceedings of SNAME Annual Meeting, 17-18 Nov 1994, at New Orleans LA.

Michaelson, R., and D. Roseman. 1994. Concept Design of a 40,000 DWT Advanced Double Hull Tanker. Paper read at Advanced Double-Hull Technical Symposium, 25-26 October 1994, at Gaithersburg, MD.

Miner, M.A. 1945. Cumulative Damage in Fatigue. *Journal of Applied Mechanics* ASME 12(3):A159-A164.

NACE. 1991. *Surface Preparation and Cleaning of Steel and Other Hard Materials by High- and Ultrahigh-Pressure Water Jetting Prior to Recoating*, NACE No. 5/SSPC-SP 12, SSPC and NACE International, Item No. 21076, PO Box 218340, Houston TX 77218-8340: NACE International.

Nappi, N. 1985. *Preliminary Ship Structural Design Guidelines for Use of High-Strength Steel*, SD-86-173-4, Bethesda, MD: David Taylor Naval Ship Research and Development Center.

Naval Sea Systems Command. 1976. *Structural Design Manual for Naval Surface Ships*, NAVSEA 0900-LP-097-4010, Arlington, VA: Naval Sea Systems Command.

Naval Sea Systems Command. 1977. *Shock Design Criteria for Surface Ships*, NAVSEA 0908-LP-000-3010, May 1977. Washington, DC: Naval Sea Systems Command.

Naval Ship Engineering Center. 1979. *Strength of Structural Members*, Design Data Sheet 100-4, February 1, 1979. Washington Navy Yard, DC: Naval Ship Engineering Center.

NAVSEA. 1991. *Carrier Life Enhancing Repairs (CLER) Aircraft Carrier Tank and Void Inspection Manual*. Washington, DC: Naval Sea Systems Command Detachment (Pera[CV]).

NSRP. 1987. *Adaptation of Japanese Prefabrication Priming Procedure to U.S. Shipbuilding Methodology*, Report 270, KTA-Tator, August 1987. : National Shipbuilding Research Program.

Ochi, M. 1978. Wave Statistics for the Design of Ships and Ocean Structures. Paper read at 1978 Annual Meeting of SNAME, at New York, NY.

Okamoto, T., et al. 1985. Strength Evaluation of Novel Unidirectional-Girder System Product Oil Carrier by Reliability Analysis. *SNAME Transactions* Vol. 93, (No. 2.).

Palmgren, A. 1924. Die Lebensdaner Von Kugellagren. *Zeitschrift des Vereines Deutscher Ingenieure (ZVDI)* 58:339-341.

Sikora, J. 2001. *Technical Background for Advanced Double Hull Guidelines*, NSWCCD-65-TR–2001/05, January 2001. West Bethesda, MD: Naval Surface Warfare Center, Carderock Division.

Sikora, J., and E. Devine. 1997. *Construction Cost Study of an Advanced Double Hull DDG-51*, NSWCCD-65-TR-1997/32, West Bethesda, MD: Naval Surface Warfare Center, Carderock Division.

Sikora, J., A. Dinsenbacher, and J. Beach. 1983. A Method for Estimating Lifetime Loads and Fatigue Lives for SWATH and Conventional Monohull Ships. *Naval Engineers Journal* 95 (3).

Sikora, J., R. Michaelson, D. Roseman, R. Juers, and W. Melton. 1995. Double Hull Tanker Research - Further Studies. Paper read at Proceedings of SNAME Annual Meeting, 5-6 Oct 1995, at Washington, DC.

Sizemore, J., R. Roberts, V. Polito, and D. Knight. 1994. Outfitting of Advanced Double Hull Combatants, Paper No. 14. Paper read at Advanced Double Hull Technical Symposium, Oct. 25-26 1994, at Gaithersburg, MD.

Snyder, B., and P. Ostrom. 1997. *Internal Deck Options for Advanced Double Hull Ships*, NSWCCD-65-TR-1996/28, West Bethesda, MD: Naval Surface Warfare Center, Carderock Division.

Thurston, D. D. 1997. Recurring Fleet Corrosion Issues. Paper read at CORROSION 97 (NACE International) Group Committee T-9B (CINCLANTFLT Maintenance Technical Advisor), March 1997, at New Orleans, LA.

TSCF. 1995. *Guidelines for the Inspection and Maintenance of Double Hull Tanker Structures*: Tanker Structure Cooperative Forum in association with the International Association of Classification Societies.